TECHNISCHE UNIVERSITÄT WIEN

D I S S E R T A T I O N

Numerical Simulation of Heat and Mass Transfer in Building Components

ausgeführt zum Zwecke der Erlangung des akademischen Grades eines Doktors der technischen Wissenschaften

unter der Leitung von
Univ.- Prof. Dipl.-Ing. Dr.techn. Ardeshir Mahdavi
E259-3 Forschungsbereich Bauphysik und Bauökologie,
Institut für Architekturwissenschaften

eingereicht an der
Technischen Universität Wien
Fakultät für Architektur und Raumplanung

von
Shiva Najaf Khosravi MSc
Matr.Nr.: 11740239
[redacted]

Wien, November 2021

Zusammenfassung

Die thermischen Leistung von Gebäudekomponenten hat einen signifikanten Einfluss auf den Energieverbrauch der Gebäude. Aufgrund der Komplexität des Wärmeübertragungsverhaltens von Bauteilen werden zunehmend hochentwickelte thermische Modelle eingesetzt, um die Zuverlässigkeit der simulationsbasierte Analyse der Gebäude zu verbessern. Die Anwendung von Wärmeübertragungsmodellen auf Gebäudekomponenten ist jedoch mit Unsicherheiten verbunden. Um dieses Problem anzugehen, werden in dieser Dissertation acht aktuelle und thematisch zusammenhängende Beiträge zur Anwendung der numerischen Simulation in Gebäudekomponenten vorgestellt und diskutiert.

In diesem Zusammenhang wurde primär die Methode der numerischen Strömungsmechanik (CFD) angewandt, um verschiedene thermische Parameter durch parametrische Studien zu analysieren. Diese Studie liefert drei wichtige Beiträge zur Analyse der thermischen Leistung von Gebäudekomponenten:

- Eine Methodik zur Bewertung der thermischen Leistung von Fensterdetails und Kühlpaneelen.
- Eine Analyse der numerischen Simulation und der Grenzen für jede Fallstudie.
- Ein Rahmen für den Vergleich und die Bewertung der verschiedenen Simulationsansätze.

Summary

Given the impact of thermal performance of building details on energy consumption and the complex nature of heat transfer behaviour, sophisticated models of heat transfer are increasingly deployed to enhance the reliability of building performance simulation. Nevertheless, applying heat transfer model through the building details involves potentially detrimental uncertainties. To address this issue, this dissertation presents and discusses eight recent and thematically interrelated contributions toward the advancement of the numerical simulation in building details.

In this context, Computational Fluid Dynamics (CFD) method was applied to analyze different thermal parameters through parametric studies. This study presents three significant contributions to the thermal performance analysis of building details:

- A methodology for assessing the thermal performance of window detail examples and cooling panels.
- Analyzing numerical simulation and the limitations for each case study.
- A framework for comparing and evaluating the different simulation approaches.

Acknowledgments

First and foremost, I would like to thank my supervisor, Univ. Prof. Dr. Ardeshir Mahdavi for all his support and guidance during years of collaboration. I have learned and still have a lot to learn from his commitment to work and excellence.

I also want to thank Dr. Julia Bachinger of the Holzforschung Austria and Univ. Prof. Dr. Schuß and Dipl. Ing. Helene Teufl for the provision of the empirical testing data used in chapter three and five.

My sincere thanks goes out to Dr. Christian Jordan and Dr. Francesco Zonta of TU Wien, for their unfailing guidance and patience throughout my quest to fulfill my research. I am also grateful to Univ. Prof. Dr. Michael Harasek and his amazing team at the department of "Fluid Dynamic Simulation of TU Wien" for all their support.

Many Thanks goes to Mr. Josef Lechleitner, Ms. Elisabeth Finz and my dear friends Paria Saadatjoo, Anna Engedy, Eleni Marmaridou and Dr. Farhang Tahmasebi for their support.

Last but definitely not least, I would like to express my greatest gratitude to my dear parents and my lovely little sister for their support during all the years of my study.

Contents

1. Introduction

1.1. Motivation

Thermal performance simulation aims to support the design and operation of an energyefficient built environment (Mahdavi, 2003). Toward this end, energy simulation software can offer feedback on the special implications of design alternatives and allow for what-if investigation to assess the robustness of new technologies under different operating conditions (Clarke and Hensen, 2015). Nonetheless, thermal performance simulation is yet to find its place in the industry.

Heat transfer analysis is essential for any thermal system to increase its efficiency and minimizes the energy loss of the system, and it is possible by applying different analytical methods. One of the advantages of analytical methods is simplicity, potentially contributing strong physical information, without the necessity for powerful computing sources (Chen, 2019; Gilani et al. 2016). Considering, this method can be a proper option for simple heat transfer problems involving modest geometries and boundary conditions. However, in real situations, heat transfer problems include complex cases concerning both geometry and thermo-fluid boundary conditions, which cannot be resolved analytically. Furthermore, relatively limited data are usually available from experimental investigations, which are often pricey and time-consuming (Jaluria, 2013).

In such states, adequately accurate approximate solutions can be achieved by computers using numerical methods (Jaluria, 2013; Mehta et al. 2013). In this approach, the subsequent partial differential equations (continuity equation, momentum equation, and energy equation) employs for each control volume (Demirdžić et al. 1995). A numerical method can be used independently as well as in a coupled manner, for both solid-body stress analysis and fluid flow predictions (Demirdžić et al. 1995). Numerical modeling of thermal processes can provide detailed results in critical applications such as those related to energy, manufacturing, transportation, aerospace, heating, cooling, and the environment (Jaluria, 2013). Several hurdles are generally encountered in achieving reliable results from the numerical simulation. Often times, various complex physical phenomena, make the numerical simulation of thermal processes complicated (Jaluria, 2013). Numerically analyzing the thermal behavior of building

elements such as windows have received a notable observation in the literature in the past few decades (Blocken, 2014; Najaf Khosravi et al. 2016). Computational Fluid Dynamic (CFD) approach involves the numerical solution for a set of partial differential equations describing the fundamental laws of fluid motion. The commercial fluent software (Fluent 19.0, 2018) uses the numerical technique of finite volumes; it shares the domain into elementary volumes and substitutes the initial differential equations with algebraic equation of balance, one for each elementary volume.

As many studies have confirmed, The CFD simulations has the potential to yield full scale domain with complicated boundary layer such as an inner layer, including the thin viscous sublayer, the buffer layer, the logarithmic layer, and a fully turbulent outer layer (Wilcox, 1998). This approach provides detailed flow-field data in the entire computational domain and without similarity restraints. It also concedes parametric studies to be carried out smoothly and efficiently (Chen, 2009; Gilani et al. 2016; Blocken, 2014; Van Hooff and Blocken, 2010). In addition, the employment of CFD for investigating indoor air quality (Yang et al. 2001; Hooff et al. 2012) natural ventilation (Najaf Khosravi et al. 2016; Van Hooff and Blocken, 2010; Montazeri H. and Motazeri F. 2018; Van Hooff and Blocken, 2013) and stratified indoor environment (Howell and Potts, 2002) is progressing. These problems are difficult to predict with other methods, as highlighted in some recent review articles (Chen, 2009; Blocken, 2014). Nevertheless, previous studies in this area have highlighted, despite considerable advancement in the CFD-supported study of building elements, the intricate nature of heat transfer and airflow within the element is far from being fully understood, and the precision of CFD simulations remains a significant concern, particularly in the complicated models that involve complex phenomena like conduction, convection, and radiation (Blocken, 2014). Therefore, further research in this area to achieve a reliable result is needed.

This thesis presents a wide variety of challenges faced by accurate CFD-based numerical simulations of practical thermal systems (namely building elements). Since the thermal behavior, design, control, and optimization of the systems are often based on numerical simulation results, it is important to obtain accurate, realistic, and valid simulation results. As mentioned earlier, the accurate imposition of boundary conditions, combined transport mechanisms, uncertainties in the design variables, and operating conditions for optimization are well-known concerns of CFD simulation and must be addressed (Jaluria, 2013). This thesis

briefly considered the major issues that are encountered in heat transfer analysis of the building elements and the possible approaches to meet these challenges were discussed.

1.2. Objective

Given the aforementioned background, in this thesis, as a first step toward enhancing the accuracy of the numerical simulation, the results of different simulation approaches were examined and compared. In the second and third steps, the effect of other variables (such as complex boundary condition, solar radiation) on thermal performance was dissolved. As the final step, the effect of radiant panels on the flow behavior inside a test room was investigated.

1.3. Structure

In this context, the present dissertation discusses a number of recent, thematically interrelated efforts, in the area of heat transfer through the building envelop. Therby, the constituent contribution entail six selected peer reviewed publications (Najaf Khosravi et al. 2019; Pont et al. 2019; Najaf Khosravi et al. 2019; Mahdavi and Najaf Khosravi, 2020; Najaf Khosravi and Mahdavi 2021; Najaf Khosravi and Mahdavi 2021) and two submitted papers Najaf Khosravi et al.2021; Najaf Khosravi and Mahdavi, 2021). These publications were developed and written under involvement of the author of this thesis and are presented in detial in the following sections. These Sections, contain the full texts of the selected scientific publications, which constitute the core of the dissertation. As such, the bulk of the content of the following sections are identical with the original publications, however certain formatrelated adjustment have been made so as to maintain a unified appearance and enhance the readability. The sequence of the following sections is based on the model complexity that applied in each study.

This dissertation is structured in seven sections. Section one contains the introduction of the thesis. Section two (page 5) deals with an effort to model, in detail, the thermal performance of existing and retrofitted instances of casement windows. Different modeling approaches were considered, namely a conventional one (focusing predominantly on conductive heat transfer) and a more detailed one (involving coupled conduction, convection, and radiation). Then the thermal performance of a casement window was evaluated numerically toward achieving an optimum design. Chapter three focuses on the ventilated window heat transfer (page 30). The

fidelity of the CFD model and its potential toward design support was explored. Detailed boundary conditions (close to the real situation) was considered for the simulation. The simulation results were compared with the measurement data and different scenarios were considered to achieve the most energy efficient ventilated window design for winter and summer boundary condition. Section four concentrates on assessing the flow behavior in a room with a double-layered façade (page 62). The concept of age of air and flow behavior was analyzed for different configurations of double-layered facades. Finally, section five entails an empirical and computational assessment of the air flow field in the close proximity of a vertically positioned radiant cooling panel (page 71). Comparing the results simulation and experiment, allowed the evaluation of the draft discomfort risk as well as the reliability of CFD in reproduction of the measurement results. Section six discusses the research conclusions and future outlook. And finally, section seven lists the references, figures and tables.

2. Heat transfer analysis through the casement window

2.1. Back ground

It has been estimated that, the energy losses through the building envelope are responsible for the greatest percentage of energy consumption (Cuce, 2014). Besides, a notably increasing trend of global energy prices makes the application of energy-efficient rules necessary. In this respect, some standards are applied to the new buildings to improve the material efficiency, plus to enhance the thermal performance of existing buildings by the energy-efficient retrofitting (Cuce and Riffat, 2015; Baldineli and Bianchi, 2014). However, the improvement of the building envelope thermal behavior requires more and more accurate and detailed measurement techniques (Baldineli and Bianchi, 2014; Gao et al. 2014; Jim, 2014; Buratti and Moretti, 2012). Windows are indispensable components of the building envelope while they provide air ventilation, vision, day lighting, and passive solar gain. However, their high U value compared to the other components of the building envelope, make them responsible for a significant amount of energy loss in buildings (Cuce and Cuce P.2016). Regarding thermal insulation of windows, designers should consider special attention to improve the related properties of the frame and glazing (Curcija,1993). Nowadays, air or Argon filled double glazed windows are one of the common options in the fenestration market. This is mostly due to their better thermal insulation performance compared to conventional single glazing. Nevertheless, their high U-values makes them insufficient to apply as a retrofitting option for the traditional windows (Cuce et al. 2015). Therefore, accurate thermally investigation of other retrofitting options are necessary.

Improving and retrofitting the old buildings fenestration is not a simple task. Since, the status of those buildings such as heating ventilating and cooling raises complex questions and limits the possibilities. Therefore, adaptable solutions need to be investigated and applied. A large number of windows in central Europe originating from the middle of the 19th century to the middle of the 20th century are double layered, so-called box type windows (casement windows, or, in German: "Kastenfenster") (Bakonyi, 2016). The cavity of box type windows

is not sealed like in an IG (Insulating glass) unit, and it is formed not by small spacer bars but with the distance between two layers of sashes. Normally, the thickness of the air cavity is 1020 cm which provides additional thermal resistance to the window (Bakonyi and Becker, 2014).

Recent studies suggest that traditional casement windows can be thermally retrofitted by installing vacuum glazing instead of float glass in external or internal wings. Thereby, the focus of the studies has been predominantly on conductive heat transfer and applied thermal bridge analysis of the conventional and retrofitted casement windows (Proskurnina et al. 2016). Vacuum glazing is one of the most promising high-performance glazing technology developed for the low/zero carbon building concept which facilitates to minimize heat loss and high visible transmittance in slim window construction (Fang et al. 2007; Cuce. and Cuce P. 2016). Vacuum glazing technology does not have complex fabrication details. Generally speaking, it consists of two glass panes with an evacuated interstitial space. To maintain the functionality of the glazing, a vacuum-tight edge seal and a grid of distance-holding pillars are required to keep the two sheets of glass apart see in figure 1.

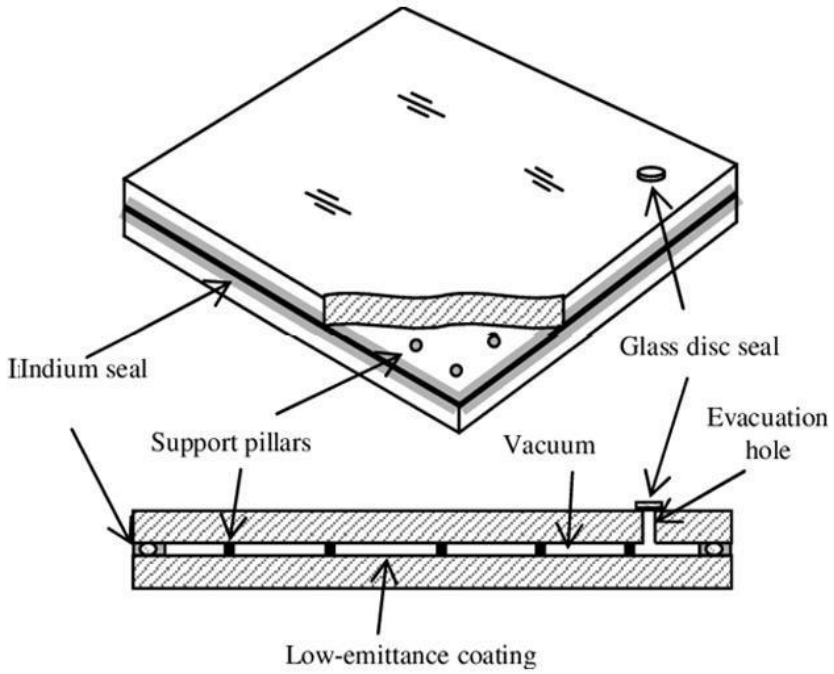

Figure 1. Schematic figure of vacuum glazing construction (EN 673:2011)

The support pillars are mostly imperceptible from a distance of about 2–3 m, hence their influence on vision is negligible (Garrison and Collins, 1995; Wilson et al. 1998). The essential function of the vacuum gap between the glass sheets is to eliminate the conduction and convection which play a significant role in the U-value of fenestration products. Vacuum glass

products feature a reduced weight and construction depth. However, as mentioned earlier, the application of any retrofit option such as vacuum glass in windows requires a critical rethinking of the current practice of window construction, especially with regard to accurate analytical heat transfer calculation, thermal bridges, minimum surface temperature and the related surface condensation risk at the glass/frame construction joints (Pont et al. 2019; Arasteh et al. 1989).

2.1.1. Overview of fenestration heat transfer modeling

The buildings' energy performance is affected by material property as well as interconnections of the components (Cappelletti et al. 2011). The accurate analysis of the external building fabric heat transfer is a critical issue of all building energy computations. The main challenges lie in the treatment of heat transfer and thermal bridges in opaque constructions such as windows, doors, rolling shutter boxes (Bakonyi, 2016; Al Senea et al. 2012; Ibrahim et al. 2014; Capozzoli et al. 2013). According to the new energy saving regulation, the level of insulation in the building has increased (Martin et al. 2011). The application of innovative high-performance materials for buildings envelopes indirectly increases the importance of local weaknesses such as geometrical and physical thermal bridges (La Rosa et al. 2014). The thermal bridge is defined as a zone whose thermal properties are significantly different from the rest of the envelope (Bianchi et al. 2014; ISO 2008). In another word, a thermal bridge is characterized as a component of the external thermal envelope where heat fluxes become multi-dimensional. Adding an insulation layer can reduce the onedimensional heat flow but does not significantly decrease the multi-dimensional one (Capozzoli et al. 2013).

Bakony has divided thermal bridges into two distinctive groups:

1) Repeating thermal bridges, which happens in inhomogeneity in the external constructions (e.g. wooden studs in lightweight walls or wall-ties in cavity walls), and

2) Non-repeating thermal bridges, which appear at the large scale details and junctures of different constructions. Specifically, when the interior and exterior surface have different dimensions or where materials with different thermal conductivities are connected (Bakonyi, 2016).

Thereby, analyzing thermal bridges is not a trivial task; it requires more complex analyses and the determination of three-dimensional heat flux (Baldinelli and Bianchi, 2014). In order to minimize thermal bridge energy losses, designing proper structural nodes, knowledge of heat

transfer as well as considering an accurate method for thermal loss calculation is necessary (Capozzoli et al. 2013; Martin et al. 2011). Some thermal bridge simulations are conduction based and they cannot predict the temperature stratification caused by convection (Proskurnina et al. 2016; Garay et al. 2014). Therefore, the simulation models should be extremely sensitive to surface convection and radiation heat transfer (Garay et al. 2014).

There are several studies in this field, mostly focus on window thermal bridges providing practical and technical solutions to reduce their effect on building thermal losses (Proskurnina et al. 2016; Pont et al. 2019).

As mentioned earlier, vacuum glazing can be considered as a retrofit option for the traditional casement window. To optimize the application of vacuum glazing, accurate heat transfer and thermal bridge analysis are necessary. Pont et al. explored the principle application possibility of vacuum glazing products in existing casement windows. According to their study, the glass edge seal is the weak spot of vacuum glass in terms of heat transfer. It requires an insulating cover which is not provided in typical insulation glass frame configurations (Pont et al. 2018).

In order to reliably estimate the heat transfer intensity through a box-type window, the consideration of the convective and radiative heat transfer in the cavity and conduction in the solid bodies of the frame is necessary (Bakonyi and Becker, 2014). To this end, first the models describing the heat transfer in enclosed cavities (fenestration heat transfer models) should be reviewed and then their accuracy for box-type windows should be analyzed.

The thermal and solar/optical properties of windows can either be defined by measurement or by calculation. The major shortcoming of the traditional experimental method is the lack of flexibility to apply parametric studies, and the limited level of details from the simple models (Ji et al. 2008). In addition, considering the cost and time for each measurement, as well as the number of procedures to provide a useful database, makes laboratory measurements impractical. Performing measurements are limited to help the development of basically different new window construction and to provide the data for validation of standard or simulation. Alternatively, numerous efforts were invested in developing databases, calculation methods, standards, and software to facilitate accurate prediction of window thermal performance. The thermal transmittance can be evaluated by different standards such as International Standard ISO 10077 (DIN 2012a). The first part of the ISO 10077specifies a

simplistic calculation scheme for a set of fenestration. The limitation of this standard is that the effects of solar radiation and the heat transfer caused by air leakage are not taken into account. Consequently, it can be applied only for a primary estimation of the thermal transmittance (DIN 2012a; Malvoni et al. 2016). The most essential standards defining "centerof-glazing heat balance calculations" are The European EN 673 (EN 673:2011) and the international ISO 10292 (Bakonyi, 2016; ISO1995). However, due to the complicated geometries of fenestration, there are some shortcomings for applying the standards.

A more precise analysis is commonly conducted through numerical evaluations (ISO 2003; ISO1995; Baldinelli and Bianchi, 2014). The thermal modeling methods for single skin windows are well documented. However, Heat transfer process in casement windows is highly complex and requires more investigation (Gustavsen et al. 2008). This is due to the interconnection of various materials with different thermal conductivity such as frames, sashes, and spacers, the transparent element as well as the presence of gas-filled cavities in their construction (Bakonyi and Dobszay, 2016). In the other word, their thermal performance depends on the thermal and geometrical properties and the interaction within its components. Therefore, to numerically calculation the heat transfer through the box-type window the model should include conduction, convection, and radiation (Siegel and Howell, 2002; Miroshnichenko and Sheremet, 2018).

Natural convection can be considered as the most important modes of fluid flow and heat transfer (Miroshnichenko and Sheremet, 2018). The simplified model for studying the natural convection heat transfer in the casement windows is a gas-filled rectangular cavity with two differentially heated (or cooled) surfaces (Bakonyi and Dobszay, 2016). This phenomenon happens in numerous conditions, such as engineering. Lately, various studies have described convective heat transfer characteristics in these enclosures (Bakonyi and Dobszay, 2016; Rabhi et al.2008; Raithby and Hollands, 1998; Ostrach, 1988; Wright et al. 1989; Hoogendoorn,1986; Zhao et al. 1999; Gustavsen and Thue, 2007; Zanghirella et al. 2011). Radiative heat transfer is another important factor affecting heat transfer through the casement window. Radiative heat transfer depends on various parameters such as the cavity geometry, surface temperature, surface emissivity, and thermophysical properties of the internal medium. Majority of studies focused on turbulent natural convection, the radiative mode of heat transfer is occasionally neglected due the required overwhelming number of computational resources. However, according to the studies, the application of thermal radiation has a significant effect on the

system, and sometimes neglecting this phenomenon can change the results of the simulation (Miroshnichenko and Sheremet, 2018; Zhao et al. 2019; Finlayson et al. 1998). Griffith et al. (1998) shows the increased accuracy in surface temperature prediction when using the radiation model (Griffith et al. 1998). Rabhi et al. investigated the effects of surface radiation and the number of partitions on the heat transfer behavior in an inclined rectangular enclosure (Rabhi et al. 2008). According to their study, higher total heat transfer within the enclosure can be achieved by considering thermal radiation in the simulation.

In this chapter, numerical simulation was applied to analyses the thermal behavior of the casement window (and the potential of their retrofit using vacuum glazing) as a case in point. The whole window temperature was analyzed to assess the effects of interactions between the glazing and the window details. The radiation model used in the simulation; the model calculates radiative heat transfer between all surface segments that can "see" each other. A surface segment "sees" another segment if there is a direct "line of sight" between them (Wright and McGowan, 2003; Kohler et al., 2001). Another goal was to document the extent to which purely conductive simulation, even if it conforms to applicable standards, may result in potential errors in the predicted values of the key performance indicators such as temperature distribution. So, toward this end, with focusing on the instance of casement windows, different simulation approaches were applied and the results were compared. The results are both relevant and important, given the possibility that a simplified or reduced modeling approach may yield an unreliable picture of a window construction's future performance.

2.2. Method

To address the aforementioned research objective (2-dimensional coupled heat transfer), a conventional casement window with an interstitial space of 150 mm and two operable wings was selected. Two dimensional model was selected for the simulation since switching from a 2D model to a 3D does not show a significant difference in the results. Therefore, considering the computational cost, it is not worthy to make a 3D model. Apart from the original construction, a retrofitted version using vacuum glazing was considered as well (Figure 2). This specific configuration matches the research specimens used in a previous study, and later the results of the temperature profiles was compared with the simulation results (Proskurnina et al. 2016). Thereby, the low-e vacuum glass is assumed to consist of two 4 mm glass panes, a 0.15 mm interstitial vacuum layer, and 8 mm edge sealing. The outside and inside radii of stainless

support pillars are 0.30 mm and 0.15 mm respectively. Support pillars were assumed to be spaced on a 40 mm grid (see (Proskurnin et al. 2016) for more details). The accurate numeric simulation of the temperature distribution through a glazing system strongly depends on the boundary condition and considering temperature-dependent material properties (Khoukhi and Maruyama, 2011). Table 1 summarizes the thermal conductivity of the constitutive elements of this construction (Proskurnin et al. 2016; Synergy, 2016). The conductivity assumption of vacuum glazing is based on the set up of the SYNERGY glass (Synergy, 2016).

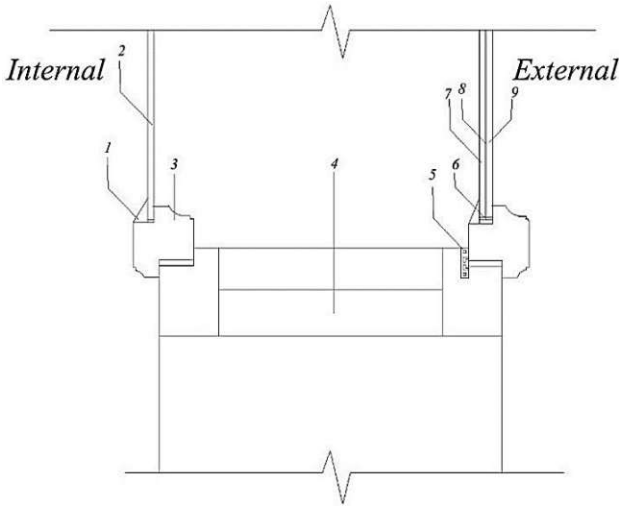

Figure 2. The schema of the casement window (retrofitted with application of vacuum glazing at the external wing)

Table 1. Thermal conductivity assumptions regarding the constitutive elements of the selected casement window (see Figure 2)

	1. Window putty	2. Lime glass	3. Wooden frame	4. Mineral insulation	5. Window seal	6. Silicon	7. Glass	8. Vacuum layer	9. Edge seal
Thermal conductivity	0.375	1	0.11	0.045	0.3	0.24	1	0.0000975	1

This study applies a numerical approach to the solution of the complex system of differential equations with corresponding initial and boundary conditions. The boundary condition was assumed as night time winter temperature (with indoor and outdoor temperature 20˚C and -10˚C respectively). Convection heat transfer was assumed on two sides and zero heat flux at the bottom and top of the window construction. we used default surface heat transfer coefficients based on EN ISO 10077-1 (EN 10077:2003). The internal and external heat transfer coefficient values were assumed to be 7.7 and 25 $W.m^{-2}.K^{-1}$ respectively. Adiabatic boundary conditions were applied at the bottom and top surfaces. No-slip velocity boundary conditions were defined at all the solid surfaces. The density of the fluid is treated with the

ideal gas law. Specific heat of air is assumed to constant (1006 J/kg K). Viscosity and thermal conductivity (k) of air were considered as a function of temperature.

The accuracy and persistence of CFD simulation results are closely connected with the geometry of the case and the appropriate grid structure (Zanghirella et al.2011; Gavan, 2009). The parameter y+ is a critical value to the correct application of turbulence models (Pasut and Carli, 2012). An important feature of the mesh is that the y+ value must be less than, or close to 1 for the first grid close to the walls. This value permits the use of k-epsilon with enhanced wall treatment, or k-omega as turbulent models (Pasut and Carli, 2012). Niu and van der Kooi (Niu and van der Kooi, 1992) have confirmed that the position of the first grid point from the surface significantly influences the heat transfer from a window (Awbi, 1998). This strategy considerably reduce the total amount of cells without affecting accuracy of the results (Awbi, 1998; Blocken et al. 2007). In the following study, a sensitivity grid analysis were performed and low dimensionless wall distance (y^+) were obtained on the cells adjacent to the slats surface ($y^+ = 0.63$). Due to the rather detailed geometric representation the targeted combined airflow and heat transfer modelling, a very fine grid had to be formed. The total number of grid element was 34453. Figure 3 illustrates the computational domain.

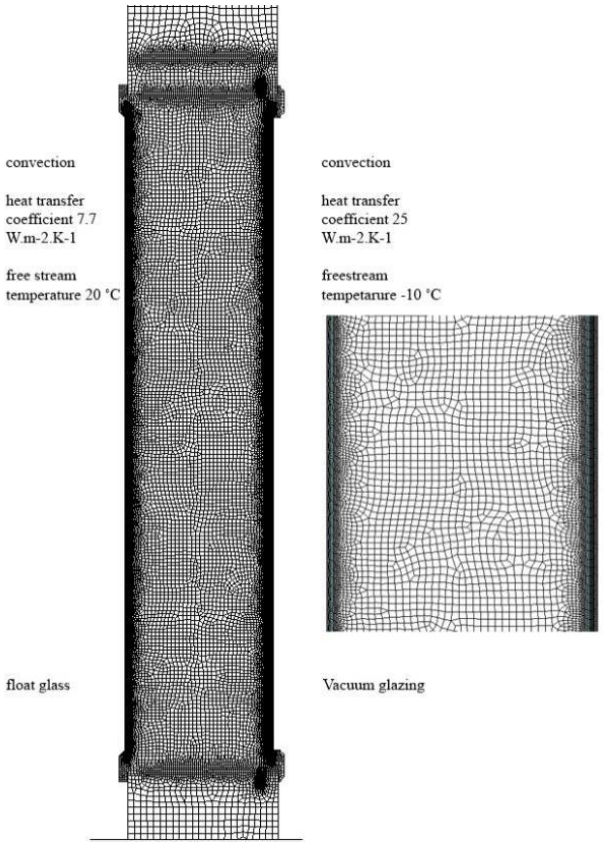

Figure 3. Boundary condition and computational grid

The deployed CFD code uses a finite control-volume method to solve the governing equations. These governing equations consist of continuity equation, momentum balance and energy balance equations (Gustavsen et al. 2005). The computational approach involved twodimensional, steady-state, double precision calculation with temperature dependent thermosphysical properties for the fluid (air), constant properties for solid materials, incompressible ideal gas model for the buoyancy forces, the SIMPLE (Semi-Implicit Model for PressureLinked Equations) pressure based solver, the Pressure Staggering Option (PRESTO) scheme

(to find the pressure values at the cell faces), the Quadratic Upstream Interpolation for Convective Kinetics (QUICK) scheme for the momentum. Shear Stress Transitional (SST) k–ω turbulence model is suggested to simulate turbulent natural convection in a differentially heated 2D cavity (Menter, 1994; Omri and Galanis, 2007). k–ω model, also provides the most reliable results compared to the measurement data from Betts and Bokhari (Betts and Bokhari, 2000). Discrete ordinates method (DOM) was applied as it is reported to provide accurate radiative energy transfer modeling in CFD simulations (Selcuk and Kayakol, 1997). In this study, the internal emissivity of the glass is assumed to be 0.94. Solar heat gain, energy loss by air infiltration and heat loss through the frame are not considered in the heat transfer calculations. As seen in figure 4 there are three major heat transfer mechanisms involved in this problem: conduction, convection, and radiation. Conduction dominates when the fluid movement adjacent to the window surface and between the glazings is pretty week.

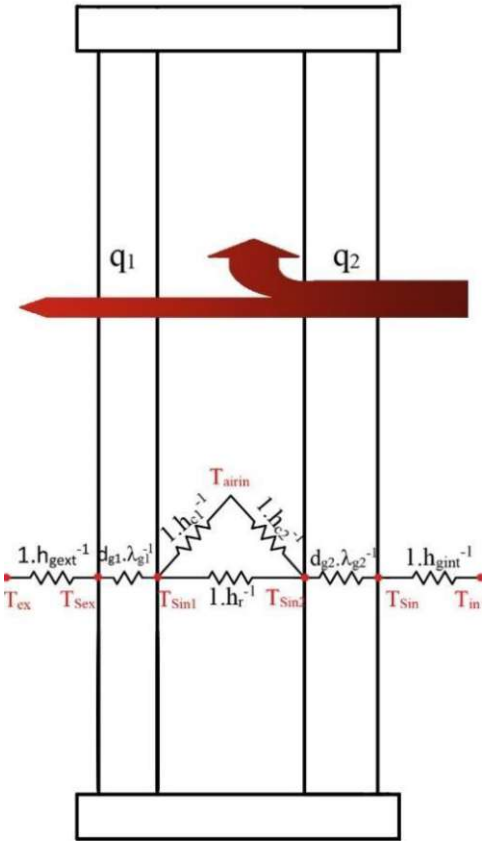

Figure 4. Schematic diagram with electrical analogy; λg = thermal conductivity of the glass; Tex= outdoor temperature; Tse= outdoor surface temperature of glass; Tsin= indoor surface temperature of glass; hr = radiative heat transfer coefficient; hgext = heat tr

2.3. Results and discussion

2.3.1. Thermal behavior of the window at the winter time

As mentioned earlier, the window glazing and frame have a considerable effect on the temperature distribution and also on the *U*-value of the window. For most of the simulation results presented in this study, the radiative heat transfer model was enabled.

Figure 5 compares the computed temperature distribution patterns for the aforementioned simulated scenarios. The temperature fields of the enclosure with and without a retrofit option.

When looking at Figure 4, there is clearly an improvement in the temperature distribution of the externally retrofitting window.

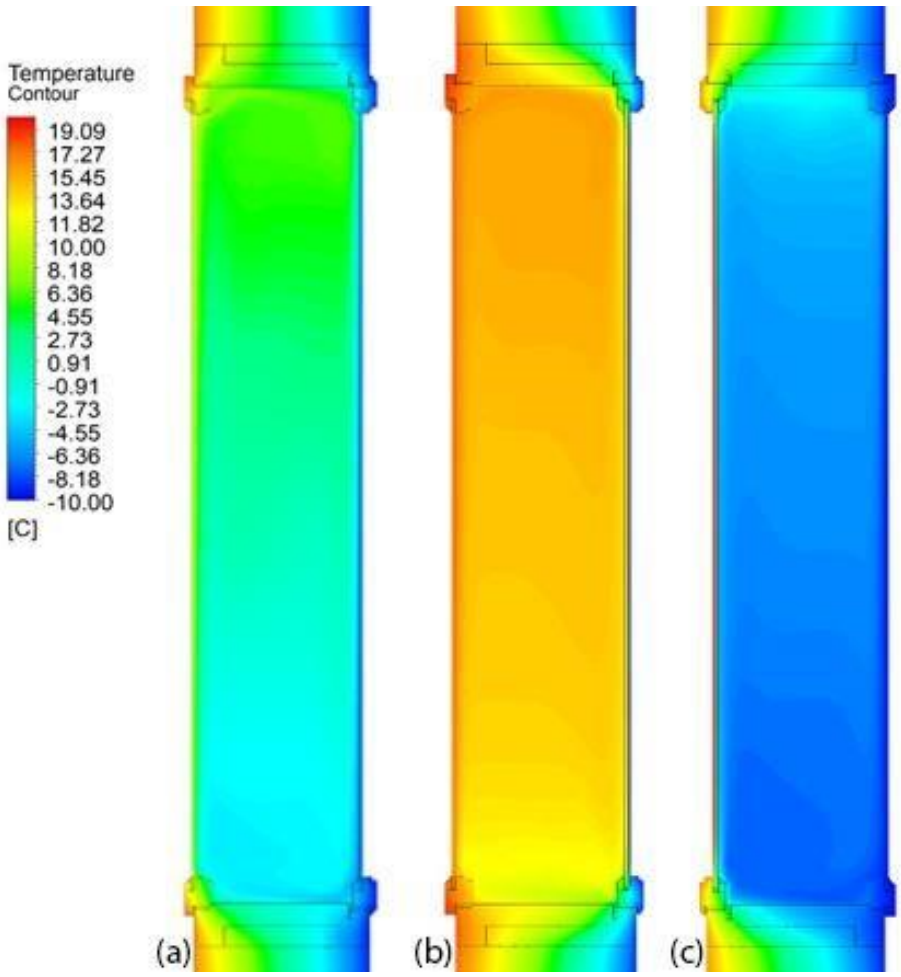

Figure 5. Temperature distribution in the casement window: (a) original construction; (b) retrofitted external wing; (c) retrofitted internal wing.

For the sake of comparison, Figures 6-8 demonstrates the temperature distribution in three different cross-sections of the conventional and retrofitted casement windows. It is emphasized that in the regions of solid–fluid contact there is a sudden change of temperature in most cases. This is due to the thermal boundary layer that occurs close to the walls so that the particles of fluid that come into contact with these walls reach thermal equilibrium.

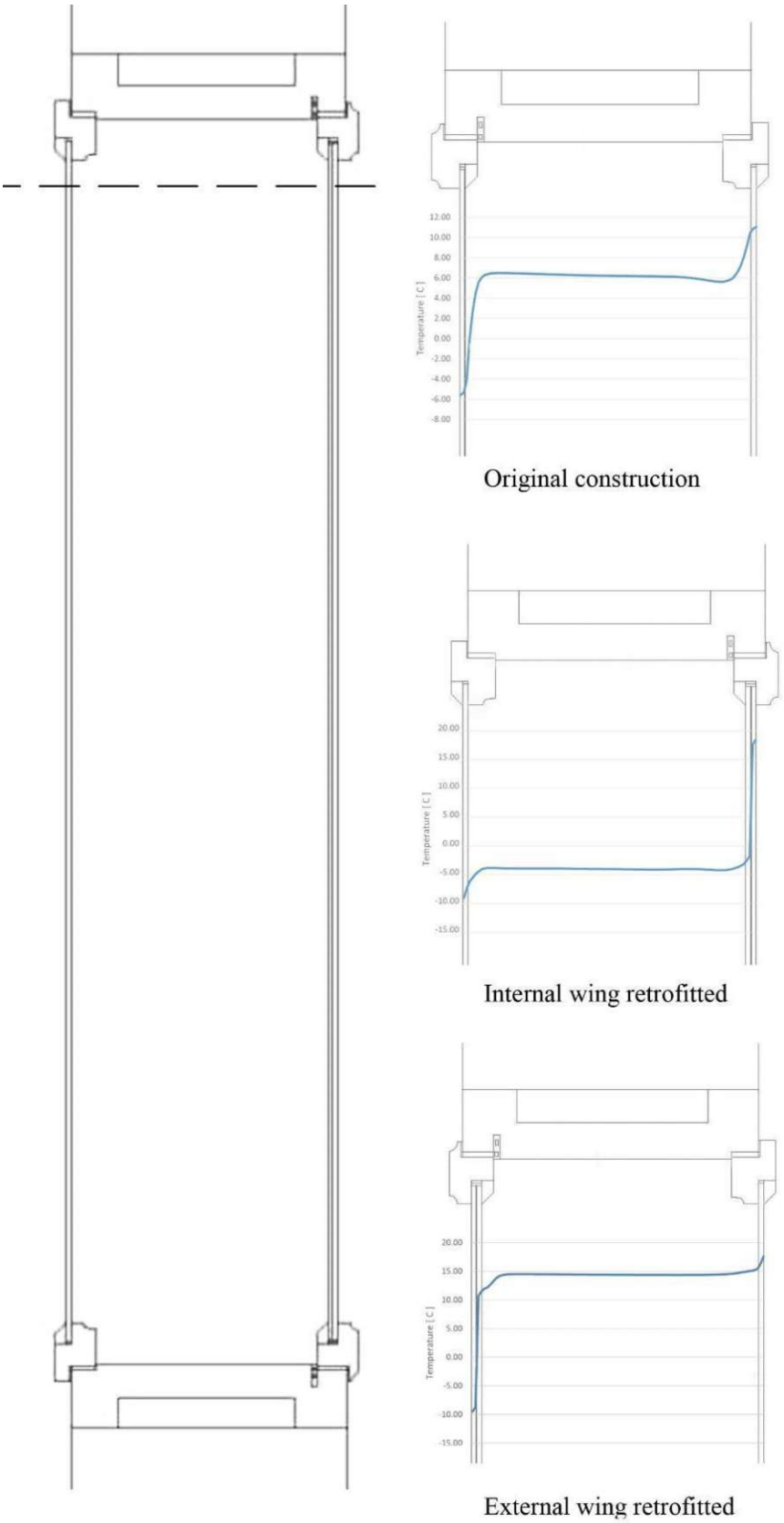

Figure 6. Comparison of the temperature distributions in top cross-sections along the casement window.

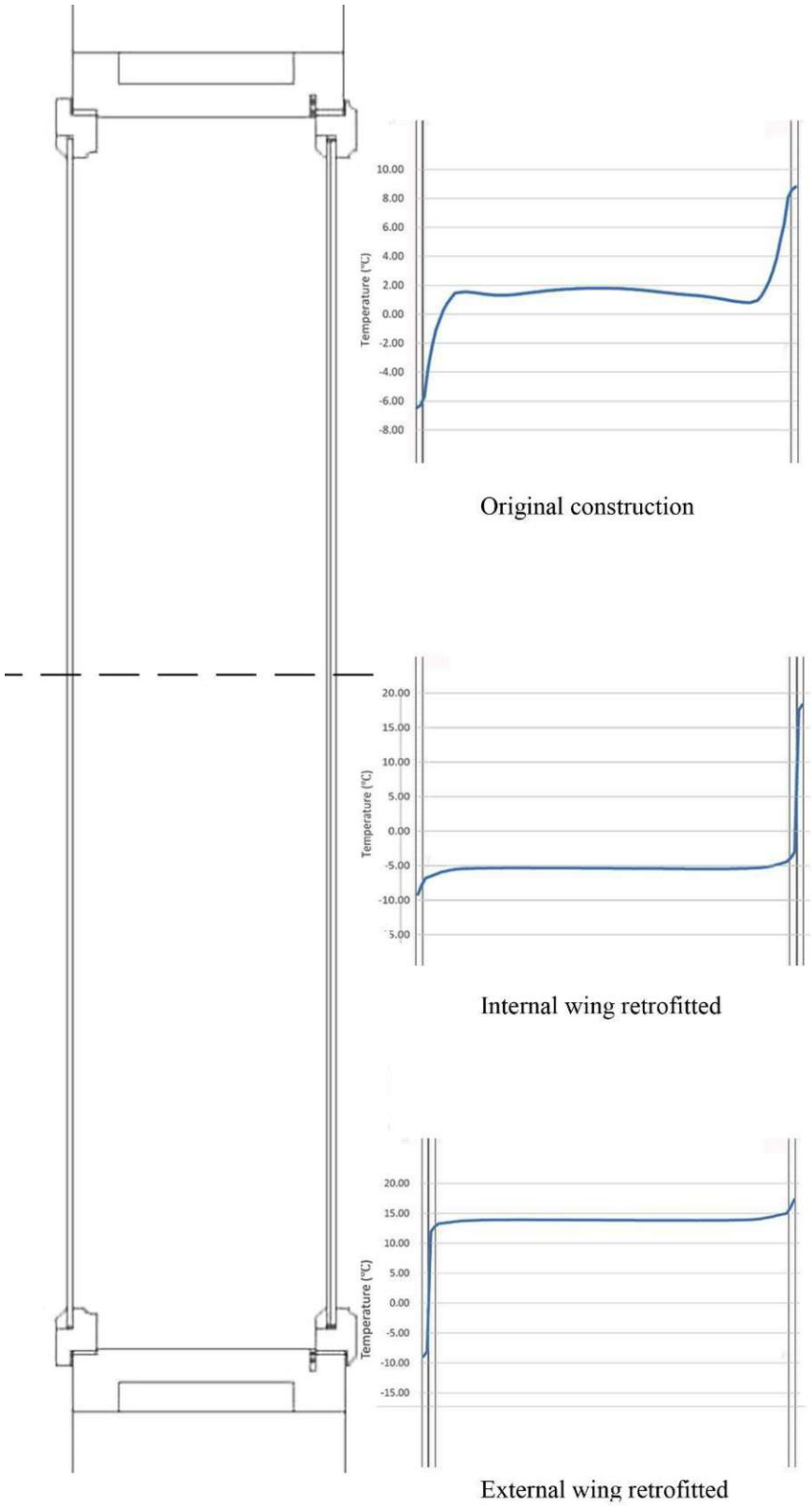

Figure 7. Comparison of the temperature distributions in the cross-sections along the center casement window.

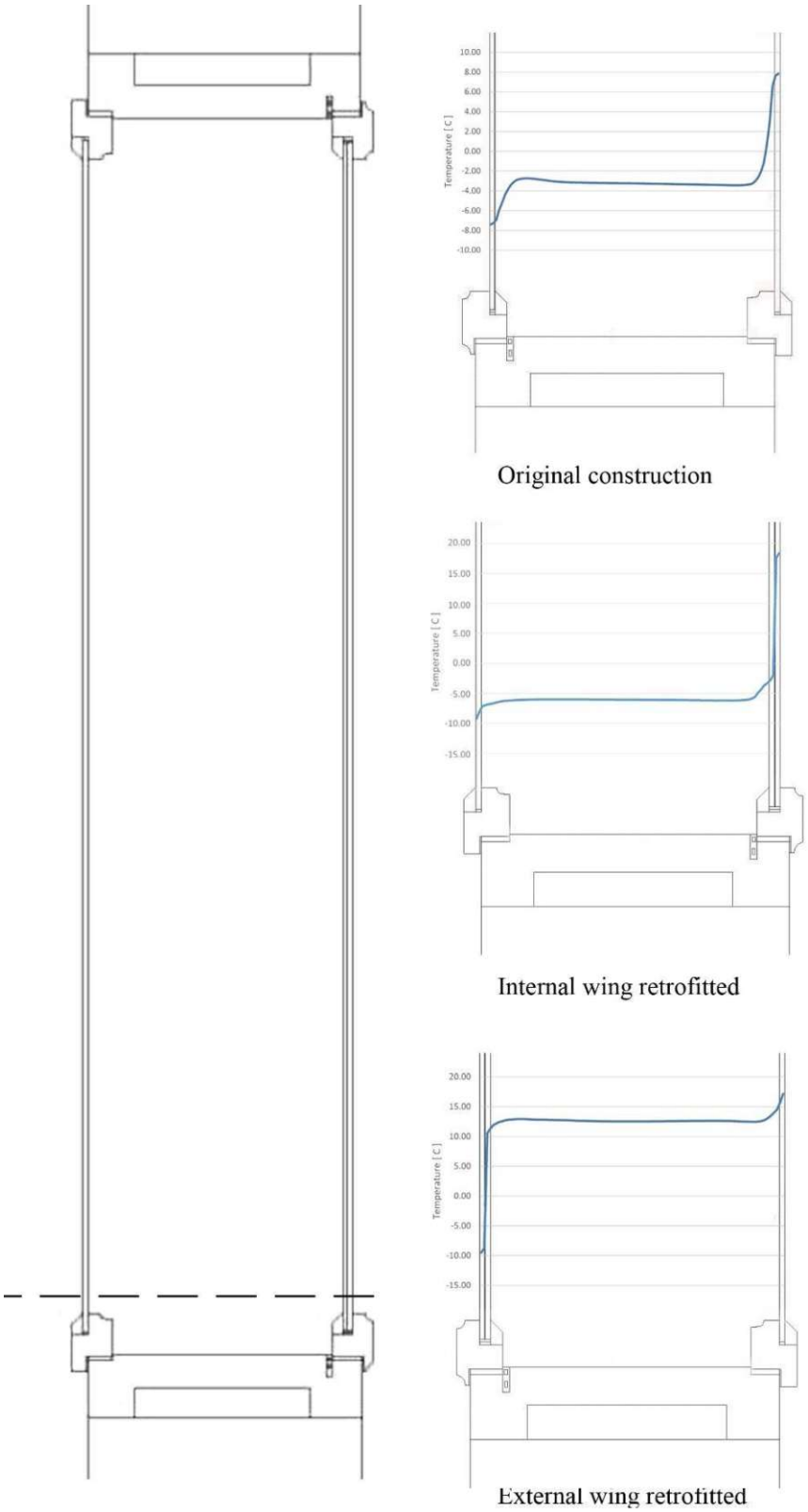

Figure 8. Comparison of the temperature distributions in the bottom cross-sections along the casement window.

The internal glass surface temperature can be maximum 12.5 C in the conventional window. This value in the retrofitted cases is more than 18.50 C. As it is shown in the Figure 9 this value in the middle of the casement window is 8.20 for the original construction, internal retrofitted 17.43 retrofitted externally 17.85. All the results indicates that the application of vacuum glazing can significantly reduce the heat transfer rates. Specifically, the external wing retrofit option appears to be the most suitable retrofit option given higher surface temperatures and the associated reduction of condensation risk.

To emphasize the effect of the retrofit option on temperature and flow distribution, the temperature distribution on the inner glass surface is also shown at the graphical chart (Figure 9). Table 2 summarized computed surface temperatures at selected locations (see Figure 9) on the surface of the inner glass of the inner wing of the casement window for two scenarios

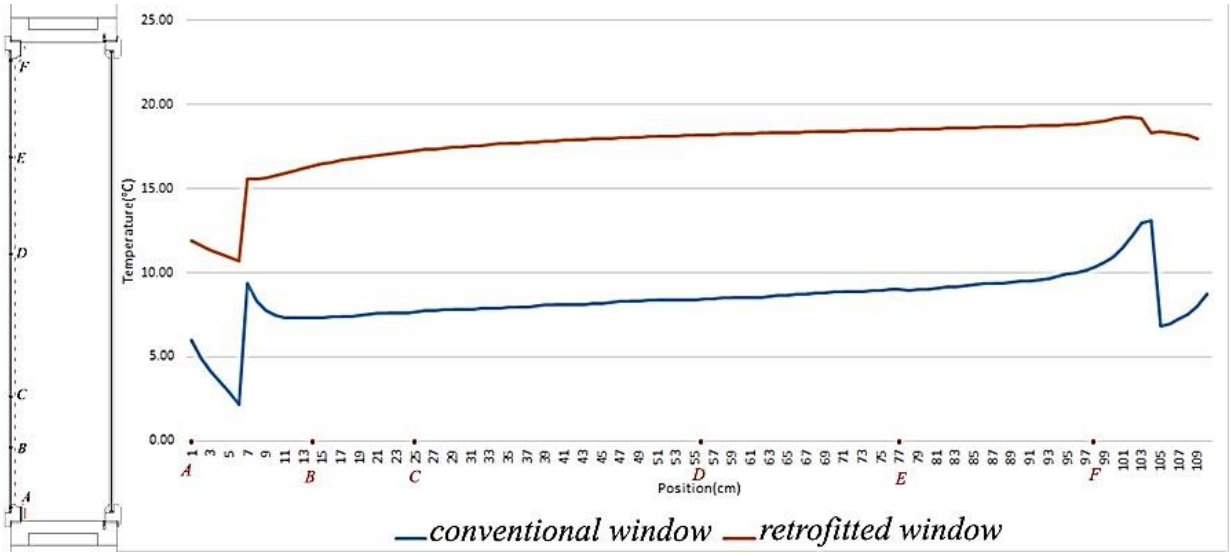

Figure 9. Temperature profile across the cavity-side surface of the inner glass layer

Table 2. Computed surface temperatures (°C) at selected locations on the surface of the inner glass of the inner wing of the casement window for two scenarios.

Points	Retrofitted window	Conventional window
A	10.71	2.32
B	16.87	7.61
C	17.50	7.96
D	18.26	8.69
E	18.57	9.23
F	19.22	12.34

The temperature distribution on the surface of the inner glass layer (before and after application of vacuum glazing as a retrofit option) indicates application of vacuum glazing at

the external wing has a notable impact on the temperature distribution inside of the cavity as well as the inner glass surface.

Figure 10 displays the airflow velocity distribution for two simulation scenarios (original construction and external wing retrofit). Table 3 provides numeric information regarding the cavity mean temperature and air flow velocity for the same scenarios. As it can be seen from Figure 10 and Table 3, application of vacuum glazing to the external wing significantly reduced the mean air flow velocity in the cavity thus suppress the convection current as well as the overall heat loss rate through the construction.

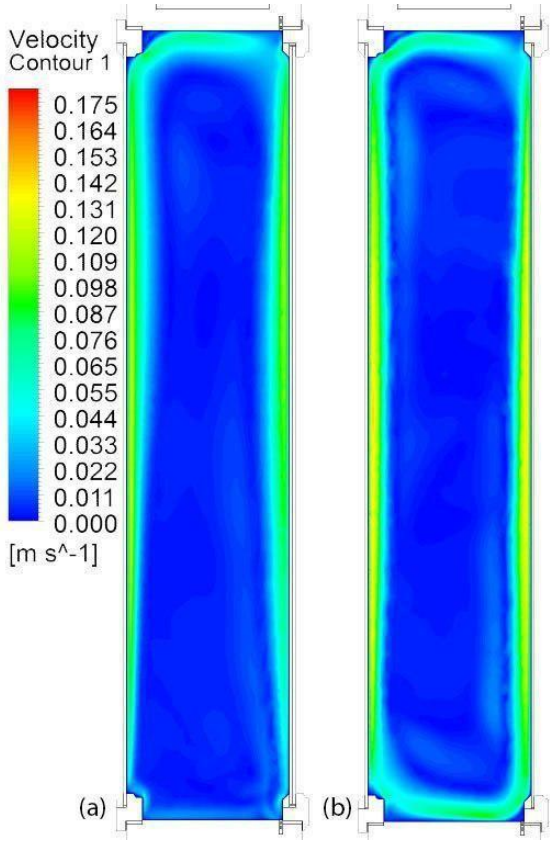

Figure 10. Velocity contour inside the casement window cavity: (a) external wing retrofitted; (b) original construction.

Table 3. Mean airflow velocity and temperature at the interstitial space between two wings

Scenario	Mean temperature (°C)	Mean Velocity ($m.s^{-1}$)
Conventional window	1.03	0.043
Retrofitted window (external wing)	14.64	0.030

In order to show the effect of retrofit option on the flow field, streamlines for the conventional and retrofitted window are showing in Figure 11. As seen in Figure11, the fluid (air) rises along the hot side and falls down along the cold side of the interstitial space which

creates a primary circulation. Additionally, multicellular secondary circulations are seen in the cavities of the casement windows which cause short cuts between hot and cold surfaces thus increases heat transfer. Combination of primary and secondary circulations establishes convection currents mentioned in Figure 11a. Nevertheless, these currents has reduced significantly with application of the retrofit option.

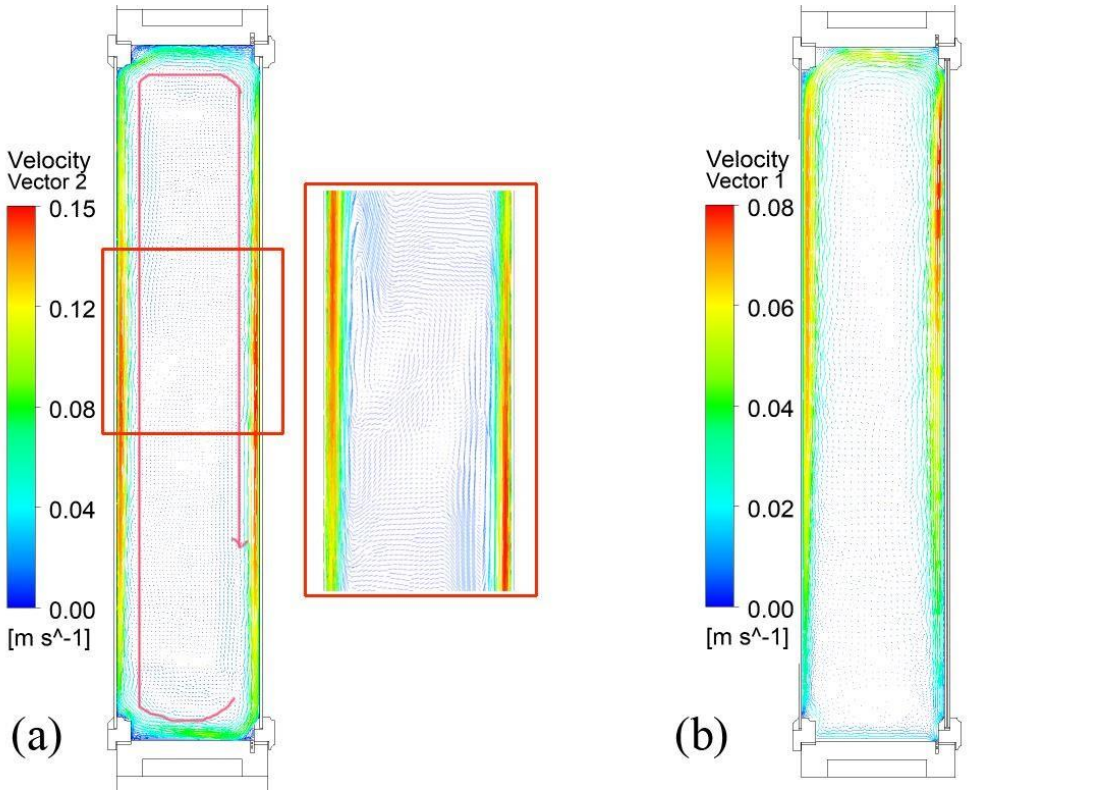

Figure 11. Streamlines a: the conventional, b: retrofitted window

2.3.2. Condensation

The window's condensation resistance is an important issue, since accumulated water (and possibly frost or ice) may cause damage, additionally, condensation is the visible evidence of its poor thermal performance (Wright and MacGowan, 2003). The evaluation of condensation risk in case of complex fenestration systems is a non-trivial challenge. A first, rather basic possibility to query this issue would be to consider the profile of the surface temperature on the inner layer of the window element. Therefore, there has been a significant concern on the temperature distributions of the indoor surfaces of windows that are subjected to night-time

winter conditions (Wright and MacGowan, 2003). Based on simulated minimum surface temperature values, the dimensionless temperature factor at outer glass panes of ventilated window ($fRsi$) can be derived as per the following equation (ISO 2007):

$$fRsi = (\theta si -).(\theta i - \theta e)^{-1} \quad (1)$$

θsi = temperature at the internal surface at the point with the lowest temperature

θi = the internal temperature,

θe = the external temperature

Table 6 summarized the computed minimum inside surface temperatures, associated temperature factor and the heat flux values for the three considered scenarios. These results suggest that the retrofitted casement window exceeds the minimum temperature factor value ($fRsi$= 0.71) according to the applicable regulation in Austria (OENORM B8110-2 2020). However, application of vacuum glazing to the internal wing is not recommended as it results with very low cavity temperatures and increases condensation risk.

Table 4. Comparing minimum inside temperatures and temperature factors for different types of the window

Window type	Minimum inside surface temperature (°C)	fRsi	Heat flux(W.m^{-2})
Conventional casement window	7.67	0.59	110.40
Window with retrofitted internal wing	13.34	0.77	20.25
Window with retrofitted external wing	16.16	0.87	20.67

Besides, the results show that the application of vacuum glazing has improved the thermal performance of the casement window as the heat flux has reduced significantly.

2.3.3. Different aspect ratio

As mentioned earlier the width of the buffer zone can affect the natural convection currents. Although the flow inside the box-type window cavity is always in the turbulent regime, various width of the cavity can cause different temperature and velocity fields as well as cavity stratifications. According to the previous studies, smaller cavity width can cause a linear temperature profile between the coldest and hottest surface temperatures, while cavities

with higher thickness create a distinct S shape in the temperature profile (Gan, 2001; Bakonyi, 2016). The effect of width of the interstitial space on the overall thermal performance is more noticeable in the windows with small cavities between 15-30 mm. According to their findings, increasing the thickness of the cavity in box-type cavities can slightly reduce the thermal transmittance and improves the insulation effect (Gan, 2001; Bakonyi, 2016).

To evaluate the optimum design of the casement windows three externally retrofitted cases with different cavity thicknesses were simulated (A: the retrofitted window with 20cm cavity thickness. B: the retrofitted window with 15cm cavity thickness. C: the retrofitted window with 10cm cavity thickness.) The height of the window in all the cases is identical (1m). To decrease the number of influencing parameters, the dimensionless aspect ratio and dimensionless temperature was applied. Aspect ratio describes as the ratio within the entire cavity height and the cavity depth (Bakonyi, 2016):

$$A=H.L^{-1} \qquad (2)$$

Here, A represents the aspect ratio, H is the height of the cavity, and L represents the thickness or depth of the cavity.

Figure 15 clarifies the effect of cavity width on the temperature distribution in the retrofitted casement window. Table 8. Compares the numerical values for the aforementioned simulation scenarios.

Table 5. The numerical values for the aforementioned simulation scenarios

Simulated scenarios	**Aspect ration**	**Minimum surface temperature** (℃)	**Mean temperature**(℃)
A	5	16.98	13.82
B	6.67	16.9	13.99
C	10	16.77	14.22

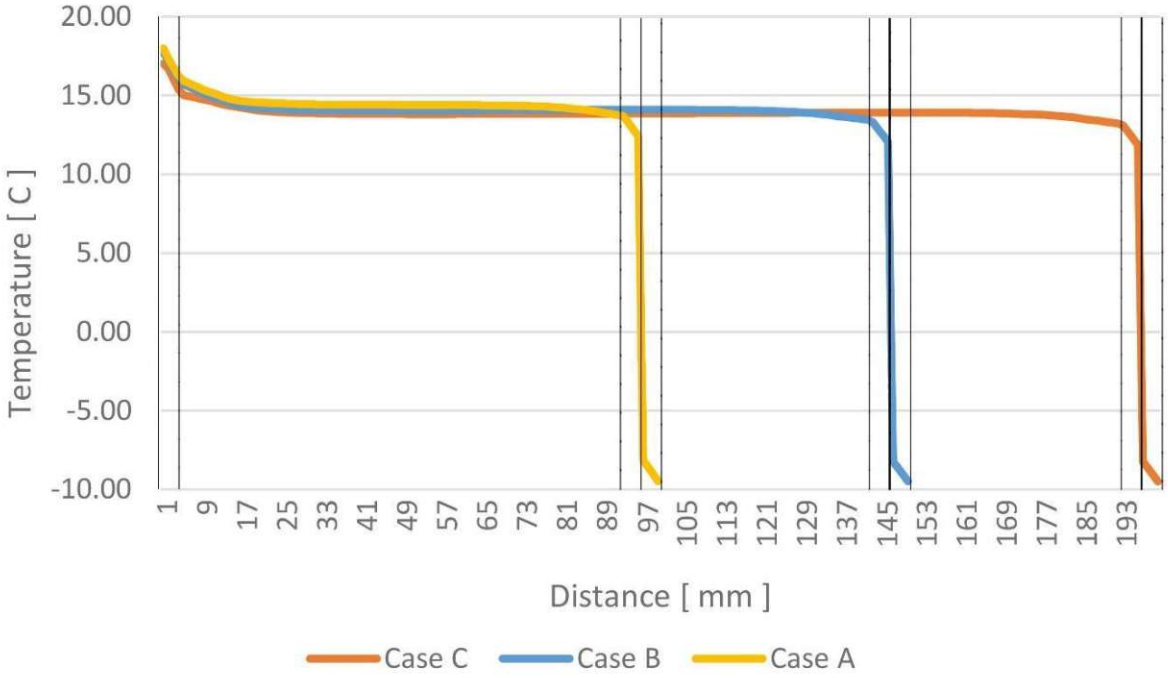

Figure 12. Compares the temperature distribution for the aforementioned scenarios.

These simulations were intended to clarify the effect of cavity width. By increasing the depth of the cavity the average velocity of the flow decreased. It can be seen that the temperature rise is roughly the same for the two scenarios and it is confined to an area close to the warm surface. As expected, natural buoyancy becomes more dominating as the depth increase and the velocity of the flow reduces. However, the velocities result in the areas close to the warm surface were almost identical for both cases. Still, comparing the simulated cases, case C with 10 cm thickness and a higher aspect ratio of the cavity shows slightly better performance.

2.3.4. Different simulation approaches

As discussed earlier, heat transfer process in casement windows are highly complex, as they involve combined conduction, convection, and radiation (Gustavsen et al, 2008). At the next step of the study, different approaches for the simulation was considered. Comparing the results indicates the importance of application conductive, convective, and radiative heat transfer in the model.

First, an accurate correlations for natural convection effects inside two panes of the casement window was developed. To this aim, we compared the results of two-dimension

coupled conduction and convection simulation with results of the previous study which conducted conductive thermal bridge analyses of the retrofitted casement window with application of vacuum glazing at the external wing (Proskurnina, 2016). Table 4 summarizes the temperature of the selected locations at the boundary of interstitial space and the solid element as well as minimum inside surface temperature and temperature factor. The location of the points is illustrated at Figure 12a in addition, Figure 12b, and 12c shows the temperature counters of the selected section of the window.

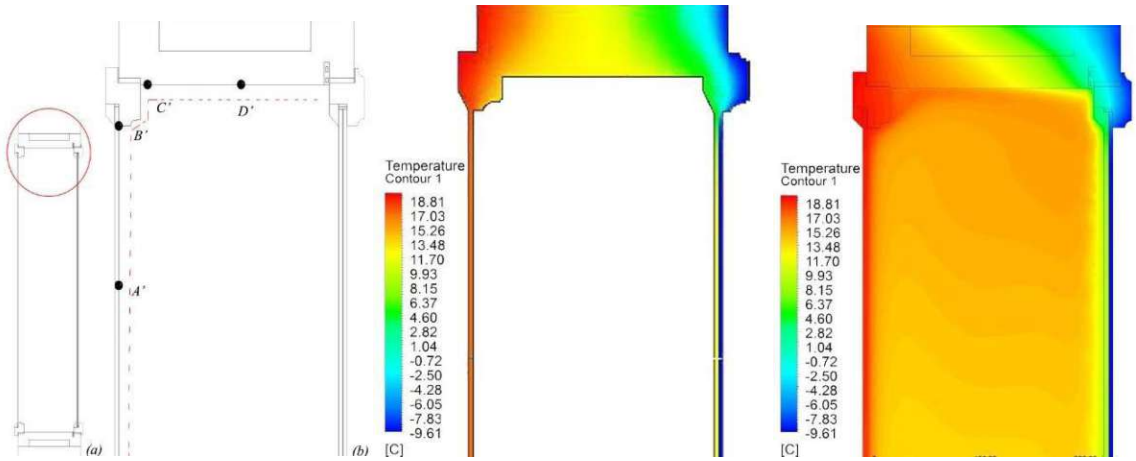

Figure 13. (a) Scheme of the retrofitted window (b) location of selected points. Figure left. Temperature distribution in the section of casement window (consideration of conduction heat transfer).Figure right. Temperature distribution in the section of casement

Table 6. The temperature (°C) of the selected locations (see Figure12), minimum inside surface temperature and temperature factor

	Conduction based model	**Convection + conduction**
A	16.93	18.78
B	17.00	19.20
C	14.79	17.38
D	12.75	13.68
Minimum inside temperature *(°C)*	16.61	16.91
Temperature factor	0.89	0.90

According to the outcomes of the simulation the temperature at these selected points, minim internal as surface temperature well as associated temperature factor values are higher when the convection effect is considered.

Majority of the conduction-based software have the limitation on calculating airflow behaviors such as velocity and temperature distribution; so, they usually under- or over-predict the effect of thermal bridges in the overall thermal transmittance.On the other hand, the

simulation method which considers conductive and convective and radiative model can provide more accurate results of window surface temperatures. Because, these models permit the software to account for localized heat-transfer effects and interactions that cannot be addressed in the basic conductive models. In this step of the study, to indicate the effect of radiative heat transfer model in the simulation, two simulation results were compared (convection, conduction vs. convection, conduction and radiation) for the retrofit versions with installed vacuum glazing in the exterior window wing. Figure 13 compares the temperature distribution on the inner glass surface of the internal wing for the retrofitted external wing. Table 5. Computed surface temperatures at selected locations on the surface of the inner glass of the inner wing of the casement window for two scenarios. Results are also included for the latter case without consideration of radiative heat transfer.

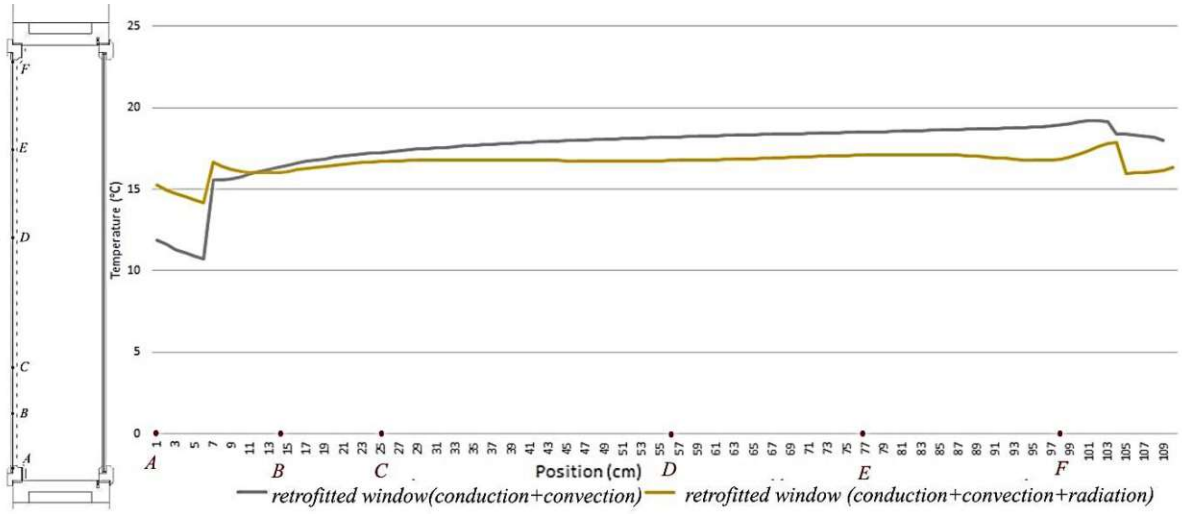

Figure 14. Temperature distribution on the surface of the inner glass layer of the internal wing for retrofitted (external wing) scenarios with different simulation approaches.

Table 7. Summarized computed surface temperatures (°C) at selected locations (see Figure 13) on the surface of the inner glass of the inner wing of the casement window for two scenarios.

Points	Retrofitted window(conduction+convection)	Retrofitted window(conduction+convection+radiation)
A	10.55	13.73
B	16.63	16.37
C	17.28	16.69
D	18.34	17.11
E	18.73	17.04
F	19.32	17.33

As figure 13 and table 5 clearly illustrate that both models (with and without consideration of radiation) imply the presence of thermal stratification in the cavity due to natural convection. However, considering radiation in the heat transfer simulation results in a more uniform temperature distribution in the whole cavity. As such, the computed minimum indoor surface temperature was higher when the radiation effect was considered, whereas the maximum indoor surface temperature was lower.

2.3.5. Thermal behavior of the window at the summer time

As mentioned earlier one of the goals of the study is to optimize the thermal performance of the retrofitted casement window. To this end the thermal performance of the casement window was analyzed for the summer case. The boundary condition was assumed as night time summer temperature (with indoor and outdoor temperature 30˚C and 20˚C). The internal and external heat transfer coefficient values were assumed to be 7.7 and 25 $W.m^{-2}.K^{-1}$ respectively. Table 7 summarizes the average, minimum and maximum temperature of the indoor glazing for all the aforementioned simulation cases. Figure 14 displays the temperature distribution for the case studies in the summer boundary condition.

Table 8. Summarizes the numerical results of simulation for the summer case.

Simulated cases	Average Temperature(℃)	Maximum Temperature(℃)	Minimum Temperature(℃)
Vacuum in	20.56	20.87	20.53
Vacuum out	20.83	21.01	20.47
Without vacuum	23.89	24.19	22.64

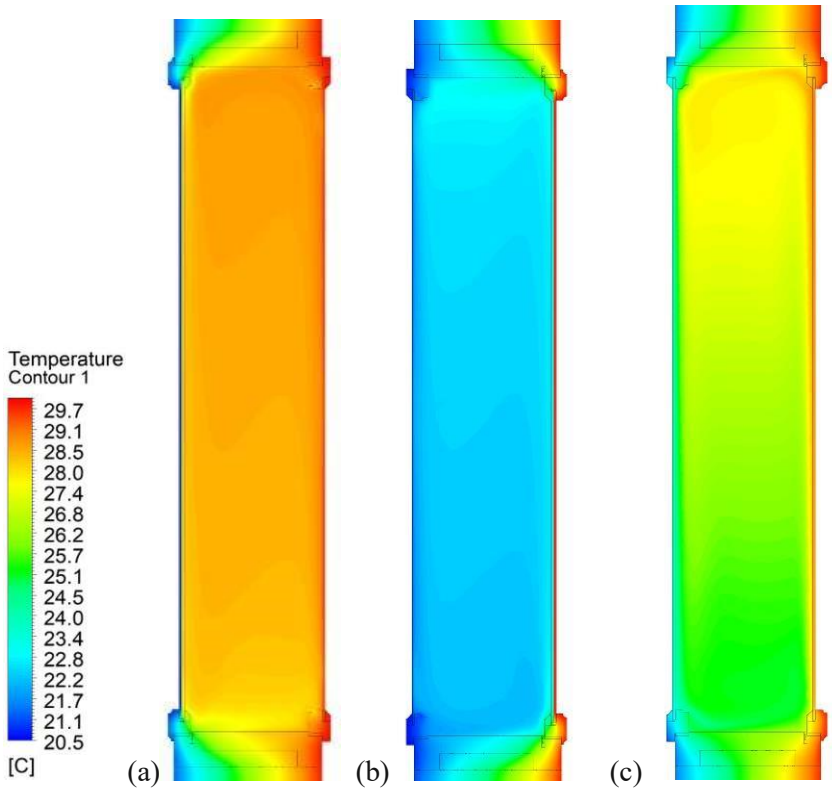

Figure 15. (a):Window with retrofitted internal wing, (b):Window with retrofitted external wing, (c) :Conventional casement window

The casement window can improve thermal comfort conditions by decreasing the temperature difference between the room air and the surface of the interior glass. According to the results with help of the retrofit option the surface temperature of the interior glass being decreased, consequently, the radiation exchange between this surface and the occupant can be decreased. This effect can be seen in both retrofit options. The result shows that the thermal performance of the internally retrofitted option is slightly better for the summer case. However, the difference is negligible and according to the results of the winter case, the external vacuum layer is suggested.

2.3.6. Conclusion

Windows are typically characterized as thermally weak points in building envelopes. Improving their thermal behavior can reduce buildings' energy demand. To analyze the heat flow through the casement window and retrofit options, numerical computations were carried out for different outdoor temperatures (summer and winter time). By testing under defined boundary conditions, the investigation described that vacuum glazing in the external wing of a

casement window can significantly influence the temperature and air distribution inside of the construction's cavity. Moreover, such a retrofit can reduce heat loss through the window construction. The benefit of retrofitted casement windows is more profound in cold regions, since the heat loss through the windows can be reduced significantly by application of vacuum glazing. The results of the simulation for the summer time indicated that application of both retrofitting options (vacuum glazing at the external side, vacuum glazing at the internal side), can decrease the surface temperature of the interior glass significantly. Consequently, the radiation exchange between this surface and the occupant can also decreased. The study also highlights the difference in results due to different modelling approaches. Specifically, purely conductive simulations of the thermal behavior of the casement window leads to results different from those obtained via coupled conductive and convective heat transfer simulation. As such, a more reliable modelling approach requires the consideration of convective processes associated with air flow within the cavity space of a casement window. In addition, this study highlighted the non-negligible implication of including radiative effects in the simulation. Hence, to obtain more consistent and reliable results, a comprehensive mode of computation may be necessary, involving conductive, convective, and radiative heat transfer processes.

3. Heat transfer analysis through the ventilated window

3.1. Background

Windows represent essential elements of buildings' envelope. Given their higher thermal transmittance, improving their thermal behavior has been a persistent subject of interest (Gloriant et al. 2015). Different approaches to energy-efficient glazing systems are still debated among scientists (Ma et al. 2015; Kull et al. 2015). Optimum glazing is expected to allow for high solar gains and low heat loss in winter. Windows are also expected to facilitate sufficient air change rates (Feist et al. 2005). To achieve these attributes, various transparent buildings components have been developed, including the ventilated windows (Danza et al. 2016). These type of windows have received increasing attention since their introduction in northern Europe (Poirazis, 2006). As the name implies, the main difference between conventional windows and ventilated windows is the existence of free or forced convection in the interstitial cavity between the window's layers. In certain instances, operable vents located at the top and bottom of the frames enable, depending on the operation mode, the flow of air in the cavity (Appelfeld and Svendsen, 2011).

The five main operation modes of a ventilated window are schematically illustrated in Figure 16. These are referred to here as supply (i), exhaust (ii), indoor air curtain (iii), outdoor air curtain (iv) and insulation mode (vi) (Gosselin and Chen, 2008; Wang et al. 2017). The appropriate ventilated window configuration depends on the method of operation as well as the climatic circumstances. For instance, a high supply air temperature to the indoor space in the cold season would be desirable (Gosselin and Chen, 2008). Ventilated windows, which could be in principle deployed both in new and old buildings, have the potential to provide preheated ventilation air during the wintertime (Carlos et al. 2010; Southall and McEvoy, 2000; McEvoy et al. 2003). The supply air window is a modification of the multiple pane windows in which air is pulled in from outside and is heated through conduction, convection, and radiation in the cavity (Southall and McEvoy, 2000; Bhamjee et al. 2013). Solar radiation, absorbed by the louvers and glazing layers turns into heat, which is transferred both to the exterior and interior space via long-wave radiation, convection, and conduction. Moreover, convection due to wind and buoyancy contributes to heat transfer between glazing panes (Torre et al. 2009). The design

and operation of ventilated windows must take a number of challenges into consideration. Open cavities raise issues such as security, acoustics, air quality, cleaning and maintenance, and condensation (Hasse and Wigenstad, 2012). If falling below the dew point temperature, low surface temperature of glass panes may trigger condensation risk (Gosselin and Chen, 2008).

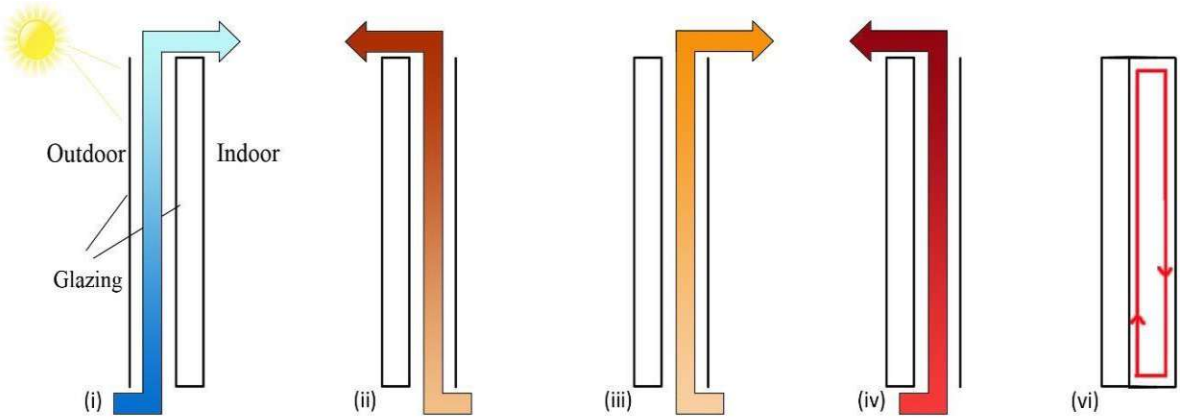

Figure 16. Schematic illustration of the principle operation modes of a ventilated window. Adopted from (Gosselin and Chen, 2008; Wang et al. 2017)

According to the previous studies, condensation occurs on the outer glass pane at the cavity side when the vents operate in reverse (i.e., when indoor air enters into the cavity). In general, this phenomenon occurs when the oscillating pattern of airflow through the vents is not sufficient to dispel the condensation from the surfaces (Baker and McEvoy, 2000). The result of an experiment by Baker and Mcevoy (2000) indicates that when the doors of the test room (including the exhaust vents) are closed, the airflow velocity reduction inside the cavity can lead to condensation (Baker and McEvoy, 2000). Other studies suggest that the application of single-layer glass as an outer pane can result in lower surface temperatures and condensation (Laverge et al. 2010).

To achieve the optimum configuration of the ventilated windows, analyzing their thermal performance is essential. Hence, the thermal behavior of ventilated windows, or supply air windows, have received significant attention in the literature in the last few decades (Bhamjee, 2011; Safer et al. 2005; Saelens et al. 2004; Tanimoto and Kimura, 1997; Bhamjee et al. 2013; Gosselin and Chen, 2008). The thermal performance of the ventilated window has been investigated via experimental methods (Gosselin and Chen, 2008; Strachan and Vandaele, 2008; Xu and Yang, 2008). Oftentimes, experiments were conducted to validate CFD or energy balance models or to assess the risk of condensation (Gosselin and Chen, 2008; Baker and McEvoy, 2000; Xu and Yang, 2008; Jiru and Haghighat, 2008). Experimental studies are of course highly

instructive, but also rather expensive and time-consuming. This makes them less effective for parametric studies. Deployed carefully, CFD-based numeric simulations can provide alternative or at least complementary means of investigation (Ji et al. 2008). As such, there have been advances in CFD application regarding ventilated windows. Some of the related studies have focused on the CFD simulation of the flow in the cavity (Gosselin and Chen, 2008; Safer et al. 2005; Jiru and Haghighat, 2008; Manz, 2004; Gratia and DeHerde, 2004; Popa et al.2012; Zeng et al. 2012; Iyi et al. 2016), some have concentrated on the overall energy performance (Xu and Yang, 2008; Manz and Frank, 2005; Pappas and Zhai, 2008; Fuliotto et al. 2010; Carlos, 2014), and some compared supply air window with the other alternatives (Yilmaz and Cetintas, 2005; Joe et al. 2013; Tanaka et al. 2009; Chen et al. 2009; Choi et al. 2012; Hamza, 2008; Hoseggen et al. 2008). As many studies have confirmed, Computational fluid dynamics (CFD) has the potential to yield high-resolution information about the flow field nature. Needless to say, the resources needed for detailed 3D simulations are considerable (Xu and Yang, 2008; Ji et al. 2008).

The study of the literature in this area reveals many different approaches to numerical simulation. This is due to the variety of possible geometric configurations and to the diversity of the heat transfer modes (natural or forced convection, with or without consideration of radiation). In this context, Table 9 summarizes the results of a detailed review of the topically relevant CFD applications. It entails information on the studies' turbulence modeling approach, the type of solar radiation modeling, the main objective of the study and considered parameters, the type of the window, and if coupled (outdoor wind flow and indoor airflow), decoupled (only indoor airflow), two-dimensional or three-dimensional simulations were performed.

Table 9. Overview of CFD-supported thermal performance studies of ventilated windows

Ref.	Window Type	Dimension/coupling/steady or transient	Main objective of the study	Turbulence and radiation modeling
(Gosselin and Chen,2008)	SM, EM	3D/S/ DC	Suggesting a new method to apply both in CFD and radiation calculations to determine airflow and heat transfer through the window	K– ε RNG/S2S
(Safer et al.2005)	DSF (OAC)	3D/S/DC	The impact of angle, blind position, and air outlet position on the airflow development of the window was numerically analyzed.	K– ε realizable/NS
(Haneul et al. 2019)	OAC	3D/S/C	The main objective was to evaluate the effect of colored or low-emissivity glass as an outer pane to improve cooling performance.	K– ε RNG/ S2S
(Southall and McEvoy 2000)	SM	2D/S/ DC	Different glass types, configurations, and ventilation were considered to evaluate the thermal performance of the window in summer time.	K– ε/NS
(Ghadimi et al. 2012)	IAC	2D/S/ DC	Overall forced convective heat transfer in an airflow window was calculated.	K– ε RNG/NS
(Torre et al. 2009)	OAC	2D/T/ DC	The main objective of this study was to investigate the influence of solar radiation on the airflow pattern and temperature distribution on a glass facade with external louvers.	K– ε RANS/DO

(Marjanovic et al. 2005)	IM	3D/S/DC	The heat transfer rate from a window surface was evaluated for different aluminum blade angles for both summer and winter conditions.	K– ε /NS
(Huifen et al. 2013)	EM	3D/T/C	Different building envelopes and building orientations and their effect on DSF thermal performance were examined numerically.	K– ε RNG/ DO
(Zeng et al. 2012)	OAC	2D/S/C	To numerically evaluate the buoyancy force and address the high computational cost, the porous model was suggested and the accuracy of the model was investigated.	standard K-ε /HS
(Fuliotto et al. 2010)	DSF(SM)	3D/S/DC	Introducing a simple analytical method to the contribution of the solar radiation in the DSF's energy balance.	K-ε RANS /HS
(Pappas and Zhai, 2008)	SM	3D/S/C	Integrated CFD and building energy simulation was applied to assess the Double Skin Facade energy performance.	K-ε RANS/NS
(Wang rt al. 2017)	SM, EM, OAC, IAC	2D/S/DC	The effect of different glazing, opening, and airflow size on the thermal performance of the airflow window was investigated for both summer and winter time.	standard K-ε /NS
(Cho et al. 2018)	OAC, IM	3D/S/C	Solar heat gain coefficients (SHGC) and the cavity air temperatures were analyzed to the open and close conditions of the window's external opening.	Realizable K- ε RANS/S2S
(Demanega et al. 2018)	IM	2D/S/DC	CFD+RayTracing method was applied to both Standard and Complex Fenestration Systems with integrated blinds the results compared with the ISO 15099 standard.	k-ε RNG /S2S
(Skaff and Gosselin, 2014)	EM, OAC	2D/S/DC	Total heat gain reduction provided by ventilated glazing units was compared to insulated units under summer conditions. A different operating design, as well as optimum cavity space were investigated.	laminar flow/S2S
(Manz, 2004)	OAC	2D/ T/DC	The influence of the glazing layer sequence and ventilation properties on the total solar energy transmittance and thermal behavior of double façades was evaluated.	standard k-ε /HS
(Ji et al.2008)	DSF(OAC)	2D/S/DC	A numerical method was applied to evaluate the thermal behavior of the ventilated faced with different angles of the Venetian blind.	k-ω model. MC model
(Li et al. 2017)	DSF (OAC)	2D/T/DC	Evaluating the heat transfer in an integrated double skin facade and phase change material (PCM) blind system.	K-ε RNG/ DO
(Dama et al. 2017)	OAC	2D/T /O	The CFD and BS models were combined to obtain a realistic picture of the DSF thermal performance.	SST K –ω RANS/NS
(Gloriant et al. 2015)	SM	2D/S/ DC	CFD simulation was applied to recalculate windows simulation parameters and apply them in a simplified building simulation model.	Laminar, Tr on the surfaces
(Bhamjee et al. 2013)	SM	3D/S/DC	The thermal behavior of the supply air window was compared for the natural and forced flow cases.	SST-K ω, DO
(El Ahmar et al. 2019)	DSF (OAC)	3D/S/DC	To analyze the ability of two simulation applications, the thermal performance of DSF was evaluated with Energy Plus and Open FOAM CFD. The results compared with experimental outcomes.	standard k-ε/NS
(Parra et al. 2015)	DSF (OAC)	3D/T/ DC	The influence of several optical, construction, and operation parameters of a DSF in terms of energy savings, was estimated in terms of the reduction of the solar load entering the building.	RNG k- ε, P1 radiation model
(Souza et al. 2018)	DSF (OAC)	3D/T/DC	The airflow and heat convection within the cavity was investigated and the results compared with the measurement outcomes.	k- ε model, NS
(He et al. 2011)	IM, OAC, IAC	2D/S/C	The airflow and heat convection within the cavity was investigated, IM mode showed more efficient performance during the winter for the summer case OAC mode has an advantage.	RNG k- ε,/HS
(Noh-Pat et al.2020)	ODGU	2D/S/DC	The numerical analysis on two configurations of ODGU indicated application of (clear glass + air + clear glass) can be the most energy-efficient option for the hot climate.	Laminar, RIM

IM: Insulation Mode; SM: Supply Mode; EM: Exhaust Mode; IAC: Indoor Air Curtain; OAC: Outdoor Air Curtain; IM: insulation mode; DSF: Double Skin Façade; ; 3D: three-dimensional; 2D: two-dimensional; C: coupled outdoor-indoor simulations; DC: decoupled outdoor-indoor simulations; I: indoor; O: outdoor; S: steady; T: transient; S2S: surface-to surface radiation model; DO: discrete ordinates radiation model; NS: no solar radiation; HS: heat sources instead of solar radiation model; ODGU: Open DoubleGlazing Unit.

As such the review supports a number of observations:

- The majority of CFD studies focus on (i) the heat gain capacity of the window, (ii) buoyancy-driven ventilation or (iii) overall heat transfer through the window.
- The conclusions on which turbulence models perform best are not always compatible. For instance, the higher performance of the standard k-□ or the RNG k-□ turbulence model widely implemented for CFD simulations of ventilated window (Ji et al. 2008; Gosselin and Chen, 2008; Torre et al. 2009; Safer et al. 2005; Manz, 2004; Zeng et al. 2012; Pappas and Zhai, 2008; Fuliotto et al. 2010; Haneul et al. 2019; Ghadimi et al. 2012; Marjanovic et al. 2005; Huifen et al. 2013; Cho et al. 2018; Li et al. 2017; El Ahmar et al. 2019; Parra et al. 2015; Southall and McEvoy, 2006) while SST-K ω model has been pointed out in some studies (Dama et al. 2007; Bhamjee et al. 2013). In addition some studies applied Laminar flow model (Gloriant et al. 2015; Skaff and Gosselin, 2014). This disparity can be linked to the physical features of the case studies, however also different computational parameters and settings applied in different studies.
- A large number of CFD investigations focus on DSF, whereas few address supply air windows (Gloriant et al. 2015; Gosselin and Chen, 2008; Wang et al. 2017; Southall and McEvoy, 2000; Pappas and Zhai, 2008; Fuliotto et al. 2010).
- The majority of the conducted studies are limited to 2D models and in many of these studies the solar radiation and outdoor windflaw and indoor airflow were not considered. In some cases heat sources were applied instead of solar radiation (Manz, 2004; Zeng et al. 2012; Fuliotto et al. 2010).
- Some studies do not consider the dependency of material-related properties on temperature (Gosselin and Chen, 2008; Southall and McEvoy, 2000; Safer et al. 2005, Xu and Yang, 2008). Most CFD model the thermal performance of window under the assumption of a constant outdoor temperature and do not consider the wind impact. These factors are, however, important, when assessing the thermal performance of the ventilated windows.
- To reduce the resolution of the mesh and hence the simulation time, the majority of studies do not consider indoor or outdoor conditions. In some cases (Gloriant et al. 2015; Wang et al. 2017; Bhamjee et al. 2013; Demanega et al. 2018; Skaff and Gosselin, 2014; Parra et al. 2015), heat transfer coefficients for indoor and outdoor surfaces are considered. In one case, the radiative temperature on the glazing surfaces was considered (Gloriant et al. 2015).

These observations suggest that, despite considerable progress in the CFD-supported study of ventilated windows, the complex nature of airflow and heat transfer in a ventilated window is far from being fully understood. Therefore, further research in this area is needed.

Predicting the thermal performance of a ventilated window is not a trivial task. The cavity flow patterns are the consequence of several flows and simultaneous thermal and optical processes.

These processes are highly dynamic and in constant interaction with each other. This feature makes them depend on the geometric, thermo-physical, optical, and aerodynamic characteristics of the different window elements. Moreover, the dynamics of indoor and outdoor temperatures, outdoors wind speed and direction, and radiation intensities influence the windows' behavior (Gosselin and Chen, 2008; Torre et al. 2009; Jiru and Haghaghat 2008; Parra et al. 2015; Hensen et al. 2007). Hence, to consider a ventilated window in building physic simulations, various phenomena have to be considered (Figure 17):

- Conductive heat transfer within the panes in the glazing layers;
- Convection and long wave radiation between the inner glass and the inside environment, between the outer glass and outside environment, and also between the glazing panes;
- Convective heat transfer between the panes of glass caused by airflow (unknown convective coefficients in the windows interstitial cavity makes the modelling challenging).
- Absorbed solar radiation by the glass panes (Gloriant et al. 2015).

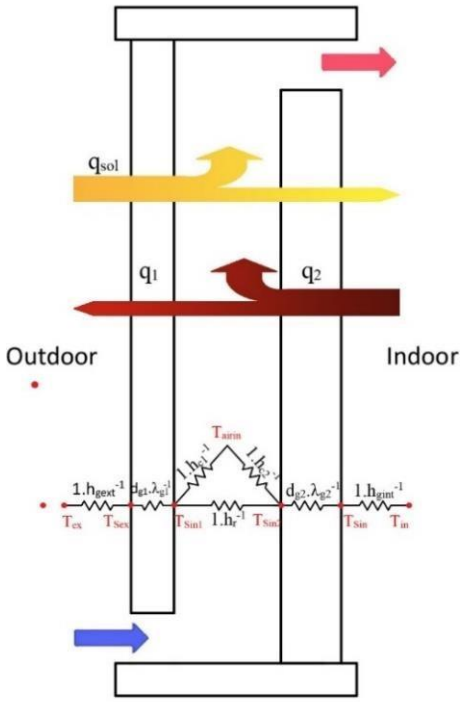

Figure 17. Schematic diagram with electrical analogy; λg = thermal conductivity of the glass; Tex= outdoor temperature; Tse= outdoor surface temperature of glass; Tsin= indoor surface temperature of glass; hr = radiative heat transfer coefficient; hgext = heat tr

Given the complexity of the physical processes involved, a candidate simulation model should ideally incorporate full three-dimensional processes, appropriate turbulence models, realistic boundary conditions, solar radiation effects, and temperature-dependent material properties (Bhamjee et al. 2013). The simulation models should be also tested and – to the extent possible – calibrated against measurement data.

In this context, the present study concerns the investigation of the ventilated window for summer and winter condition in terms of its emergent field characteristics (velocity and temperature distribution) and thermal performance. First, Different variables were considered to achieve the optimal design for the supply air ventilated window for the winter boundary condition. At the following sections, we numerically analyzed and compared the thermal behavior of the two modes of ventilation window operation (exhaust and outdoor curtain mode) under summer conditions.

Winter condition (Supply air ventilated window)

To assess the thermal performance of the supply air ventilated window the following variables were considered:

(1) Environmental conditions:

- Outdoor air temperature;
- Insolation (double layered glazing)

(2) Cavity geometries

- Depth: 50 mm, 25 mm;
- Height: 2.0 m , 1.0 m;
- Opening width: 24 mm, 12 mm.

The values of these variables were computed by numerically modelling the fluid dynamic, heat transfer in the window and solving the model in a commercially available CFD code. Furthermore, available measured data obtained from an empirical set-up was applied to evaluate the CFD model and examine the heat gain ability of the window as well as the influence of solar radiation on temperature distribution and ventilation behavior. The CFD model was subsequently utilized to compute air temperature, and air velocity distributions. A CFD-based approach can support the detailed study of the complex flow and thermal characteristics of a ventilated windows (Fuliotto et al. 2010). Our main objective here was to explore the optimization potential of the window design with regard to the geometry of the cavity (height, depth, opening size) as well as the position of the double layered glazing (inside versus outside). Condensation risk of the outer glass pane at the cavity side was evaluated for each case.

3.2. Modeling the ventilated window

3.2.1. The CFD model

As mentioned earlier, in this study the thermal behaviors of ventilated window cavities with buoyancy-driven airflow was investigated through the CFD simulation. The simulation includes buoyancy-driven air flows resulting from solar and thermal radiation and conduction within the ventilated window system.

The results of CFD simulations are highly sensitive to the boundary condition assumptions (Pappas and Zhai, 2008). The total solar energy transmittance depends on outdoor conditions (air temperature, radiant temperatures, solar radiation, wind), indoor conditions (air and radiant temperatures, air velocity), façade geometry, optical (solar reflectance and transmittances) and thermal properties (emissivity, thermal conductivities) of all layers and fluid-dynamic

properties (Manz, 2004). Previous study indicates that the accuracy can be improved by modelling ambient outdoor conditions (Pasut and De Carli, 2012) . Hence, in order to simulate the thermal behavior of the ventilated window, the analysis applies highresolution coupled (outdoor wind flow and indoor space) 3D steady Reynolds-Averaged Navier-Stokes RANS) computational fluid dynamics (CFD).

The finite volume code applied is ANSYS FLUENT 19.0 (Fluent 19.0, 2018). Ansys design modeler and Ansys meshing were applied as a pre-processor to create the geometry, mesh, and the computational domain. Figure 18 represents the computational domain.

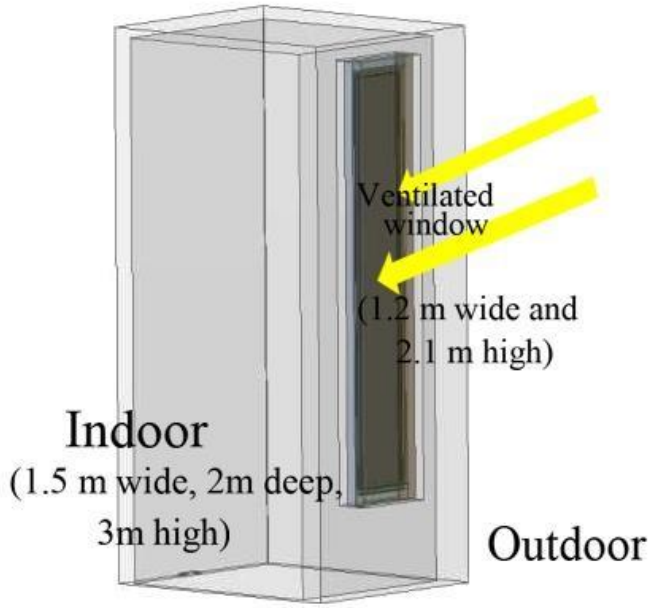

Figure 18. Computational domain

In this model, a mesh with hexahedral element was generated. A finer mesh was applied between the glass sheets to achieve higher resolution concerning the air movement in the cavity. The mesh and the relative number of cells is a critical parameter that strongly influences the computational time (Pasut and De Carli, 2012). In the present case, the grid cell size within the cavity was kept to a maximum of 2 mm, as larger dimensions would significantly alter the results. A grid independence study was performed to assure the sufficiency of the mesh density. To check the grid independency, different mesh sizes were applied to the cavity. The mean temperature and mean velocity of the cavity were monitored and the results are presented at the table 10.

Table 10. Grid test.

Grid size of the cavity (mm)	Mean temperature °C	Mean velocity ($m.s^{-1}$)
4×4	8.718	0.315
3×3	8.723	0.312
2×2	8.728	0.303

For different element sizes, almost the same temperature and velocity value were obtained. Based on these results, the mesh size of 4×4 mm was selected for the cavity. The total number of the mesh for the whole domain was 2939898. Figure 19 displays a vertical section of the cavity grid generation.

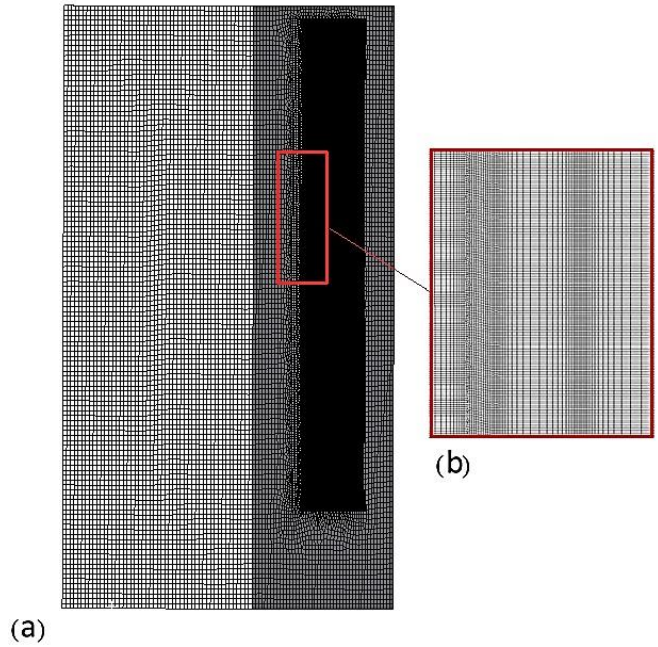

Figure 19. a) .Grid generation in the indoor space b) vertical cross section of the cavity

The inflow section of the outdoor space was set as a velocity inlet boundary and the parameters were set according to local meteorological parameters and the generalized logarithmic law of gradient wind (see figure 20).

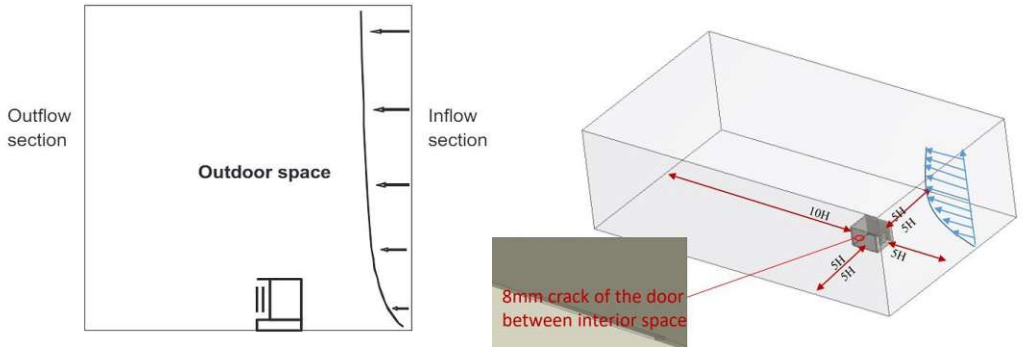

Figure 20. Computation domain

The outflow section of the outdoor space was set as a pressure outlet boundary and the lateral section was set as a symmetric boundary. As can be seen in figure 21. 8mm crack of the door was considered as an exhaust vent. The main reason for creating an exhaust vent is to get convergence in the continuity equation. Figure 21 displays the mesh creation for the exhaust vent.

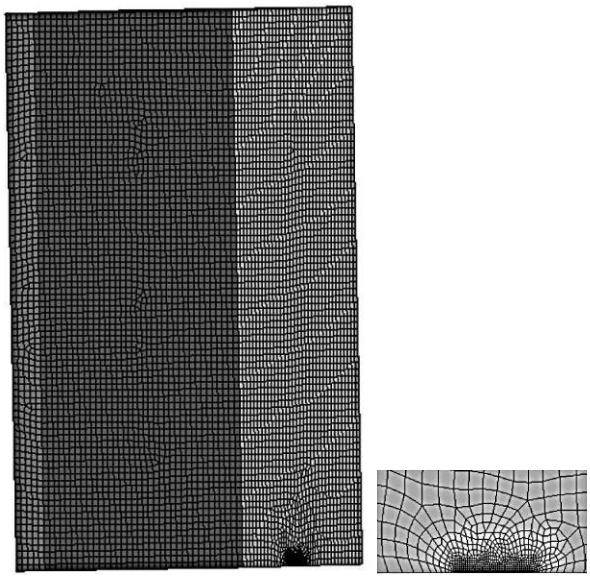

Figure 21. Exhaust vent

A constant value of 8.7 ($W.m^{-2}.k^{-1}$) was assumed for the heat transfer coefficient between the inner pane of the internal façade and the indoor air, and the indoor air temperature was set 20 °C corresponding to the experimental conditions, described later in the paper (Nusser et al. 2016).

Due to the transient variations of solar radiation and outdoor air temperature, the thermal behavior of the window units is rather dynamic. However, due to their relatively small thermal

mass, the glazing units react relatively swiftly to the dynamics of prevailing thermal conditions. Based on this observation, and given considerations pertaining to computational efficiency, thermal processes in the ventilated window were modelled assuming a steady-state mode (Skaff and Gosselin, 2014).

3.2.2. CFD setup

As mentioned above, the present study applies a three-dimensional domain in a steadystate mode. The conservation equation for mass, momentum, and thermal energy, which is known as Reynolds-averaged Navier–Stokes equation was solved to predict the field variables temperature and velocity. The subsequent partial differential equations (1): continuity equation; (2): momentum equation; (3): energy equation) were utilized as a governing equation concluded from the mass conservation law, and conservation law of momentum (Cho et al. 2018).

$$\int_{V} \frac{\partial}{\partial t}(\rho dV) + \oint_{A} \rho V^{r} . da = 0 \quad (3)$$

$$\int_{V} \frac{\partial}{\partial t}(\rho dV) + \oint_{A} \rho v_r \otimes v . da = -\oint_{A} pI . da + \oint_{\partial tV} f_b \, dV \quad (4)$$

$$\frac{\partial}{\partial t}\int_{V} \rho E dV + \oint_{A} [\rho H V_r + S_E \, dV] + v_g p] . \mathrm{da} = -\oint_{A} q" . da + \oint_{A} T . v dA + \oint_{V} f_b . v dV + \oint_{V} \quad (5)$$

Where v presents continuum velocity, v_r is the relative velocity; V is volume; a is the area; p is the pressure; I is the unit vector; T presents the viscous stress tensor; E is the total energy; H is the enthalpy; q" is the heat flux vector; $\otimes$ is kronecker product; S_E radiation energy source

Buoyancy due to density change was applied in the energy equation. The discrete ordinates (DO) model was applied as the radiation model (Torre et al. 2009; Choudhary and Malkawi, 2001). This model is capable of modelling glass, a semi-transparent media (Gosselin and Chen, 2008). Three radiative processes are mainly relevant for the window system, namely the incident solar radiation, radiation exchange between glass panes, and inward thermal radiation. The widely deployed K-ε realizable turbulence model was applied (Pasut and Carli, 2012; Launder and Spalding, 1974). The pressure based solver was used (Bhamjee, 2011). For

pressure–velocity coupling, the SIMPLE segregated solver was applied (Bhamjee, 2011). The discretization scheme used for the momentum, energy, turbulent kinetic energy, and specific dissipation rate was the second order upwind scheme. Pressure Staggering Option (PRESTO) was used for the pressure discretization scheme. Gradient reconstruction was done using The Least Squares Cell-based method (Bhamjee, 2011). The acceptable residual limits were set at $<10^{-3}$ for continuity, x, y and z momentum, turbulent kinetic energy and turbulent specific dissipation, whereas this limit for energy was $<10^{-6}$ (Bhamjee, 2011). Monitors for area weighted static temperature on the supply vent, maximum velocity in the cavity area, and supply vent mass flow rate were setup. When the changes in the monitor variables were less than one percent, the monitors where considered as stable. Three types of materials were applied in each simulation, namely transparent fluid (air), semi-transparent solids (glazing), and opaque solids (frames and walls) (ASHRAE, 2005)[146]. Table 11 summarizes the assumed thermal conductivity and solar (infrared) property of the layers.

To evaluate the CFD model's reliability, a reference case which corresponds to the actually implemented experimental setup was considered (Nusser et al. 2016). Figure 22 schematically illustrates the vertical section of the ventilated window with free convection that was applied as a reference case. To generate information relevant to design considerations, first the effect of height of the cavity was evaluated. Second, the influence of the cavity depth, and then the width of the opening and the position of the double layered glazing were analyzed.

Table 11. Assumed properties of simulated glazing units

Material	**Single glazing** (6 mm)	**Low-Emissivity double glazing** (4+12+4 mm)
Transmittance	0.752	0.305
Reflectance	0.143	0.402
Absorbance	0.105	0.250
Emissivity	0.84	0.148
Thermal conductivity	1	0.043

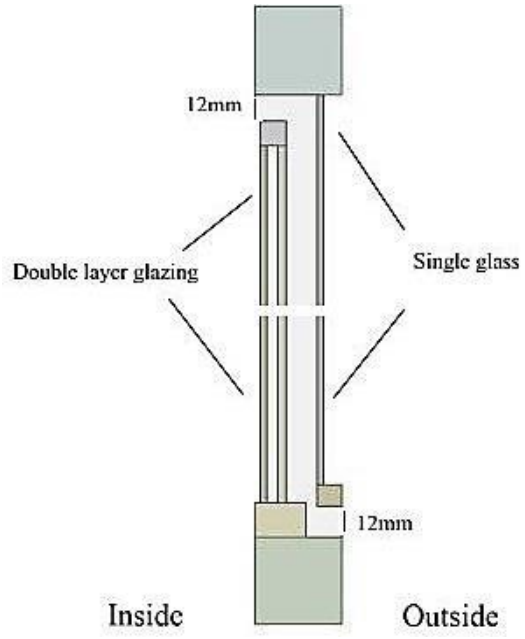

Figure 22. Schematic illustration of the supply air ventilated window

3.3. Comparison with measurement

3.3.1. Laboratory test

The Ventilated windows under optimum flow conditions can operate as a heat gain device. Escaping indoor space heat through the inner pane enters the window cavity and returns into the room (Southall and McEvoy, 2006; Calos and Corvacho, 2013). These features enable the window to function as a passive solar element. The window's ventilation ability, as well as heat loss recovery, was examined in the laboratory tests (see figure 23), and subsequently, the effect of solar radiation was analyzed in the field trials by "Holzforschung Austria" (Nusser et al. 2016).

Figure 23. Holzforschung test facility *(Nusser et al. 2016)*

To examine the performance of the CFD model, the simulation results were compared with measurement data from both trials (laboratory and field test). The aim of the laboratory test was to estimate the capability of ventilated window to preheat the supply air. To this end, a mock up ventilated window (1.2 m wide and 2.1 m high) was installed in a window test facility. Outside and inside air temperature was set to -1 °C and 20 °C respectively**.** A pressure difference of 5 Pa between indoor and outdoor was generated in the test facility. During the laboratory test, thermocouples with a measurement accuracy of ± 1.5 K were installed to measure air and surface temperature (Nusser et al. 2016). The CFD simulation model replicated the experimental configuration, also in terms of the boundary conditions. Figure 24 illustrates the temperature distribution profile (along the depicted path) obtained from the CFD simulation together with the measured temperature at two sensor locations in the window specimen. For visualizing the flow pattern, temperature and velocity profiles are made (see Figure 25).

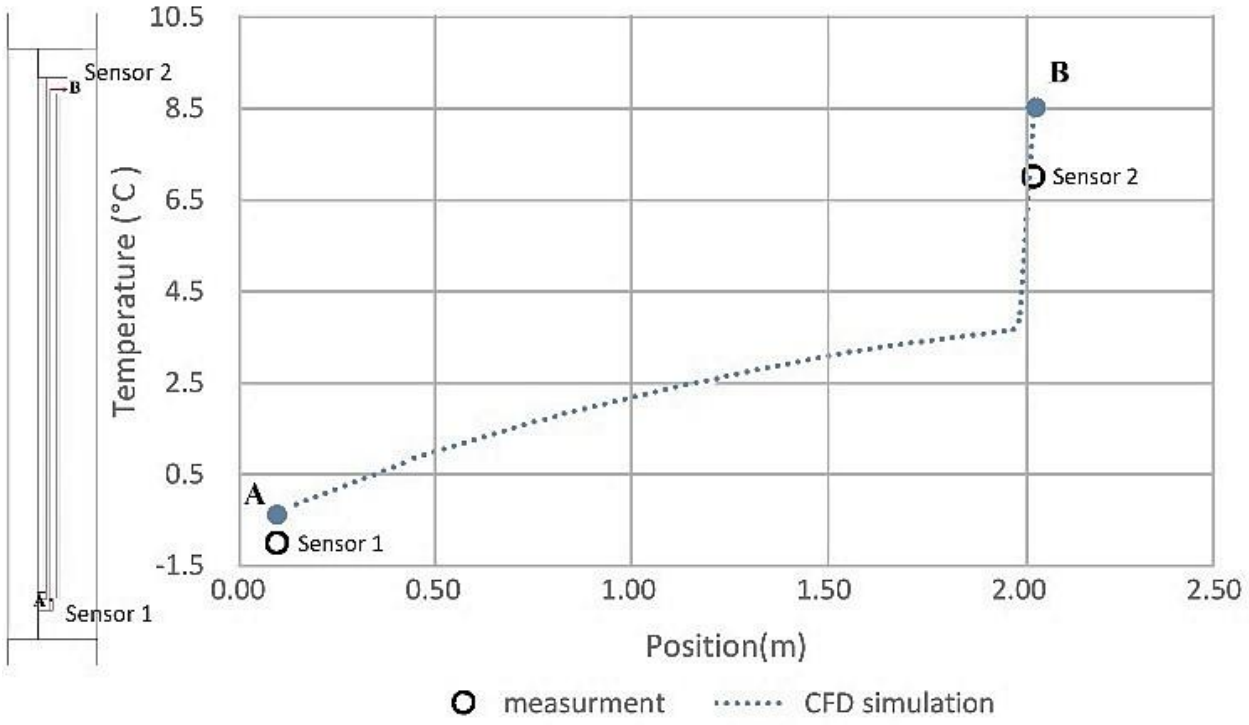

Figure 24. Left: schematic section through the examined ventilated window with the position of the two temperature probes (A to B); Right: Measured (sensors A and B) and simulated temperature profile. The distance information (xaxis) denotes the relative distances.

The measurement results document the capacity of the ventilated window to pre-heat the incoming air for ventilation during the cold season. Simulation results may be suggested to agree in tendency with the measurements. The larger disagreement between simulated and measured value in case of sensor 2 may be partially to the difficulty to superimpose the position of this sensor in reality and in the simulation model.

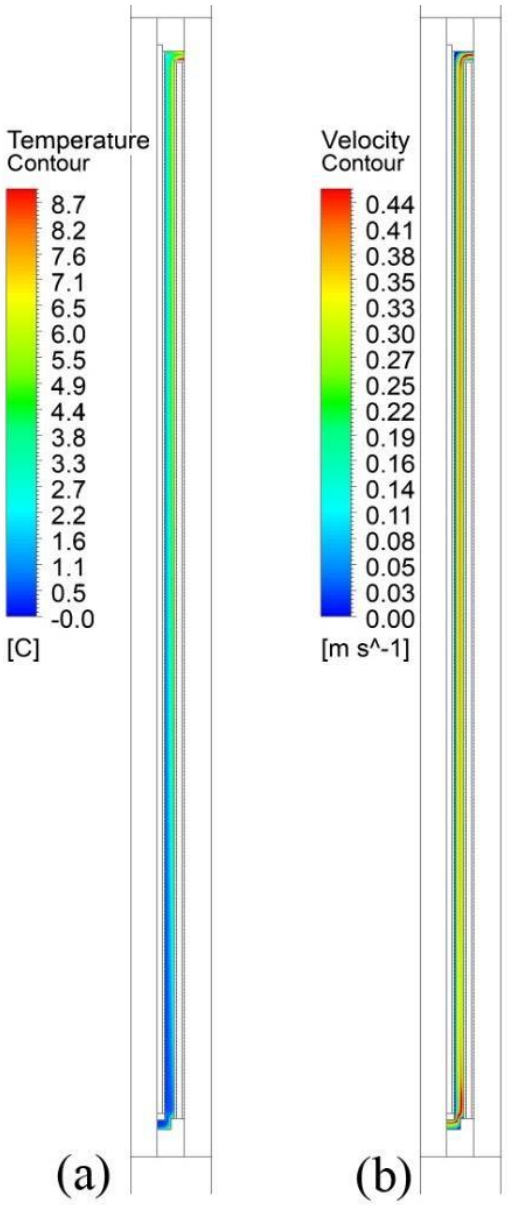

Figure 25. Temperature and velocity distribution in the window cavity (laboratory test)

3.3.2. Field trial

As stated earlier, the results obtained from the numeric model were compared to the results of field trial measurements. The aim of the field trial was analyzing the thermal performance of the ventilated window and the effect of solar radiation under real outdoor climate conditions (Nusser et al. 2016). The location of the field trial was Stetten, Austria (Latitude: 48°14'N; Longitude: 16°21'E). A 1.2 m wide and 2.1 m high ventilated window was installed in the

Holzforschung test facility (see figure26) (Nusser et al. 2016). The west side of the façades was exposed to real weather conditions, the other side faced the thermally conditioned room.

Figure 26. Holzforschung test facility *(Nusser et al. 2016)*

The tested window had a sealed double glazing on the interior side and a single uncoated glass pane on the exterior. All glass panes were 4 mm thick, the air gap was 50 mm, and the argon filled cavity in the double sealed glazing was 12 mm. The inlet valve-in was positioned in the bottom frame and the air was sucked under the external sash. Measurements of the temperature were made along the window air gap. The solar irradiance on the west-facing vertical surface, the air speed and the indoor and outdoor temperatures were recorded every 10 minutes over five winter days (11-16 January 2016). During the experiment indoor temperature was kept at an almost constant level (around 20 °C). Standard equipment was installed to monitor and record temperature, global and diffuse solar irradiation, wind speed, and humidity. The measurement accuracy of the air temperature sensors and thermocouples were ±0.1 K and ±1.5 K respectively (Nusser et al. 2016).

The experimental results did not reveal any significant relationship between wind speed and the air temperature in the ventilated window's cavity. On the other hand, the solar radiation was shown to have a strong influence on the air temperatures in the buffer space. Generally, the measured temperature of the air supplied to the space was found to be between 10 to 20 K higher than the outdoor air entering the window's inlet(Nusser et al. 2016). A one-hour long segment of measured data from the first day of measurements could be identified as involving relatively small fluctuations of the boundary conditions. We thus could treat this period as quasi

steady-state. The registered mean values of the boundary condition during this one-hour period (13:00, January 11th, 2016) were treated as the applicable boundary conditions for the CFD simulation model (see Table 12).

Also in this case, the simulation model overestimates the temperatures at positions A (3.9 °C instead of 3.5 °C) and B (17.48 °C instead of 16.7 °C). However, the simulated air temperature increase (13.6 K) in the cavity matches fairly well with the measured value (13.2 K). Figure 28 displays the visualized flow pattern within the in cavity.

Given steady-state boundary conditions, the effective capacity of ventilated windows in terms of preheating magnitude of the outdoor air may be expressed in relative terms as follows:

$$\square = (\theta_s - \theta_e).(\theta_i - \theta_e)^{-1} \qquad (6)$$

In this equation, $\square$ denotes a measure of window's preheating capacity under specified boundary conditions, and $\square_s$, $\square_e$, and $\square_i$ denote supply air temperature, outdoor temperature, and indoor temperature respectively. As applied to previously described experiments, the $\square$-value can be shown to be 0.49 for the laboratory experiment and 0.84 for the field trial. This difference can be readily explained given the presence of solar radiation and the associated warming effect in case of the field trial.

Figure 27 illustrates the temperature distribution in the window's cavity as computed by CFD simulation together with the measurements obtained from the two sensors.

Table 12. Boundary conditions for the CFD simulation model (winter case)

Variable	Value	Unit
Wind speed	3.5	$m.s^{-1}$
Outdoor temperature	3	°C
Indoor temperature	20	°C
Irradiance	180	$W \cdot m^{-2}$

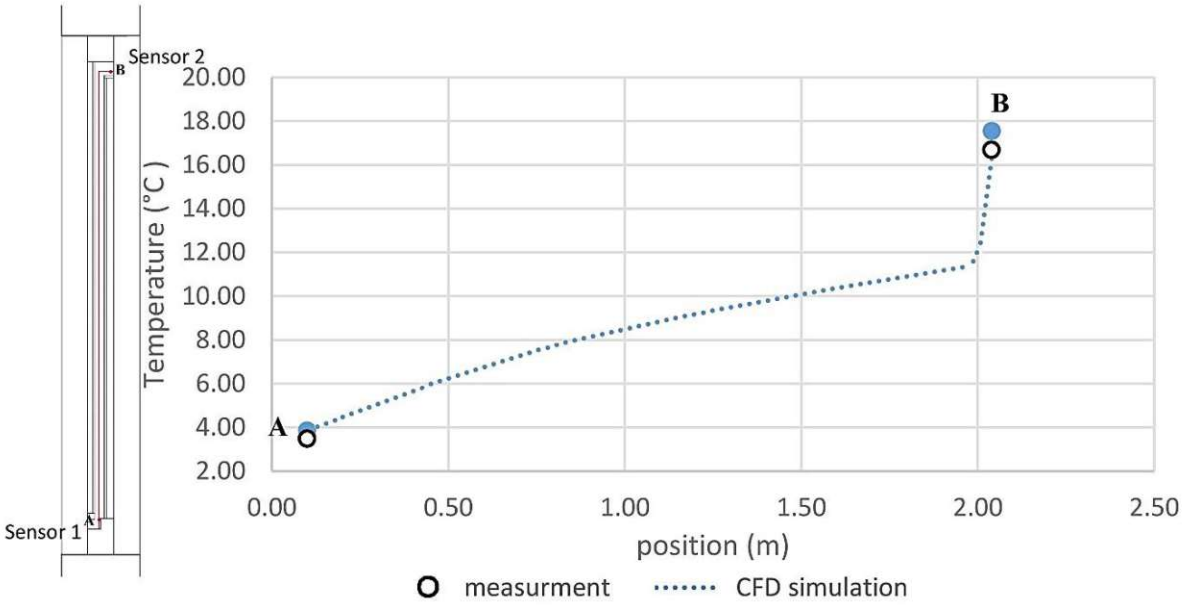

Figure 27. Left: schematic section through the examined ventilated window with the position of the two temperature probes (used in the course of field measurements); Right: Measured (sensors A and B) and simulated temperature profiles.

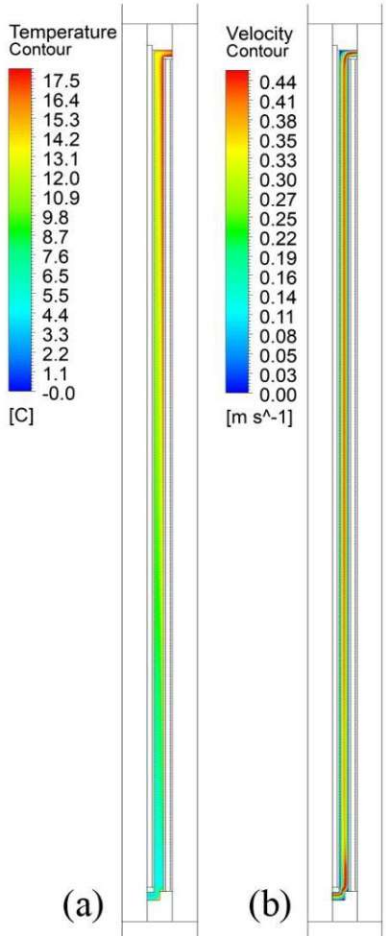

Figure 28. Temperature and velocity distribution in the window cavity (laboratory test)

3.4. Comparison of ventilated window configurations

3.4.1. Thermal Performance

As mentioned before, the main objective of the present contribution was to computationally investigate the effects of the height and depth of the cavity, width of the supply air opening and the position of the double layered glazing (inside versus outside) on the performance of the ventilated window. Note that the assumed boundary conditions match the previously mentioned assumptions in the case of the field trials, namely 20 ℃ and 3 ℃ for indoor and outdoor temperature respectively (see Table 12). The solver settings are identical to those used for comparison with the experiment. Generally, the thermal performance of a ventilated window can be assessed by four criteria, namely *i)* airflow rate through cavity openings; *ii)* average cavity air temperature; *iii)* incoming air temperature; *iv)* heat flux through interior glazing (Greffet et al. 2013; Pappas and Zhai, 2008) . To decrease the number of influencing parameters, the dimensionless aspect ratio was applied. Aspect ratio describes as the ratio within the entire cavity height and the cavity depth [26]:

$$A=H.L^{-1} \quad (7)$$

Here, A represents the aspect ratio, H is the height of the cavity, and L represents the thickness or depth of the cavity.

3.4.2. Cavity height

The complex convection fluid flow induced by solar radiation in the interstitial space depends strongly on the height of the cavity (Fuliotto et al. 2010; Ji et al. 2008). A taller cavity is more exposed to the solar radiation and consequently, provides a more effective buoyancy force (Pappas and Zhai, 2008). To evaluate the effect of cavity height, the thermal behavior of two ventilated windows under the identical boundary conditions and different height (1 m and 2 m high) were estimated. Table 13 includes the simulation results for the aforementioned cases. The table includes also the computed air flow rates as well as the values of the aforementioned heating capacity indicator □. The temperature difference between the buffer area and outdoor zone is a significant factor in creating airflow rate.

The results suggest that the window with the higher vertical dimension, and aspect ratio provides higher incoming temperature. The height of the window determines how long it takes for the air to flow through the cavity. The higher the cavity the higher the potential preheating of the air, as larger part of the glazing is exposed to the solar radiation.

Table 13. Supply air temperature (°C), heat flux (W.m^{-2}), effectiveness, volumetric flow rate, and mean cavity temperature (°C) for the ventilated windows with two cavity height assumptions.

Cavity height	Supply air temperature	Heat flux	Effectiveness (□-value)	V	Aspect ratio	Mean cavity temperature
1m	16.66	1.25	0.8	2.11	20	8.70
2m	17.48	1.29	0.85	2.03	40	9.01

3.4.3. Cavity depth

Most studies have determined that in the case of double skin façades, the cavity widths does not have a large effect on the overall thermal performance. Hence, the decision on the sufficient depth of the cavity is based on the following parameters: *a)* Considering ventilation requirement; *b)* Providing adequate space for the shading device; *c)* cleaning and maintenance (Pappas and Zhai, 2008). To investigate the effect of cavity depth on the thermal performance of the ventilated window, two cases with different cavity depths (25 mm and 50 mm) was evaluated. Table 14 provides the numerical results of the simulation.

Table 14. Supply air temperature (°C), heat flux (W.m^{-2}), effectiveness, volumetric flow rate, and mean cavity temperature (°C) for the ventilated windows with two cavity depth assumptions.

Cavity depth	Supply air temperature	Heat flux	Effectiveness (□-value)	V	Aspect ratio	Mean cavity temperature
25mm	16.85	0.85	0.81	2.10	40	8.9
50mm	16.66	1.25	0.8	2.11	20	8.70

According to these results, the supply air temperature is slightly higher in the ventilated window with a smaller cavity depth and higher aspect ratio. However, ventilated window with a 50 mm cavity depth can provide sufficient space to accommodate adequate shading elements. By increasing the depth of the cavity the average velocity of the flow decreased and consequently, the airflow through the cavity takes a longer time. Surprisingly, the results reveal that this phenomenon does not cause an increased preheating air. It can be noticed that the air temperature rise is approximately the same for both scenarios and it is confined to an area close to the warm surface. As expected natural buoyancy becomes more dominant as the depth

increases and the velocity of the flow decreases. Though the simulation results indicate the air velocity in the areas close to the warm surface is almost equal for both cases.

3.4.4. The effect of opening size and the type of the glazing

As mentioned earlier, another aim of the investigation was to computationally investigate the effects of the width of the supply air opening and the position of the double layered glazing (inside versus outside) on the performance of the ventilated window. The incoming airflow behavior depends strongly on the opening geometry and thermal property of the glazing (Carlos, 2014). The temperature of supply air depends on absorbed solar radiation by glazing and the heat lost from the indoor space to the cavity (Carlos and Corvacho, 2015). The total solar heat gain depends on the incident solar radiation on the outer glazing unit and the portion that could reach the inner glazing. As the cavity between glazing units is ventilated and the airflow heats by convection, the absorbed solar radiation by both glazing units influence the heat exchange between the surfaces and the airflow. With higher absorbance values of the inner pane more solar energy can is transferred into the cavity (Carlos and Corvacho, 2015). Single layered glazing in the inside wing transfers more solar radiation to the indoor space.

To assess the effect of opening size and the position of double layered glazing, four cases were considered as per the Table 15. The assumed window dimensions are identical in all four cases (1 m wide and 1 m high).

Table 15. Summary of the simulated configurations (width of the inlet opening was assumed to be 12 mm in all cases)

Case	Width of the supply air opening	Position of the double-layered element
A	12	inside
B	12	outside
C	24	inside
D	24	outside

Table 16 summarizes the simulation results for the four cases in terms of the temperature of the supply air entering into the room. The effect of the aforementioned variables can be clearly seen in Figure 29, which illustrates the computed temperature profile along the depicted path in the window cavity.

Table 16. Supply air temperature, volumetric flow rate for the simulated scenarios.

Cavity depth	Supply air temperature	Effectiveness (□-value)	*V*	Mean cavity temperature

A	16.66	0.8	2.11	8.70
B	17.86	0.87	2.23	10.95
C	16.26	0.78	2.10	8.63
D	17.23	0.83	2.20	10.90

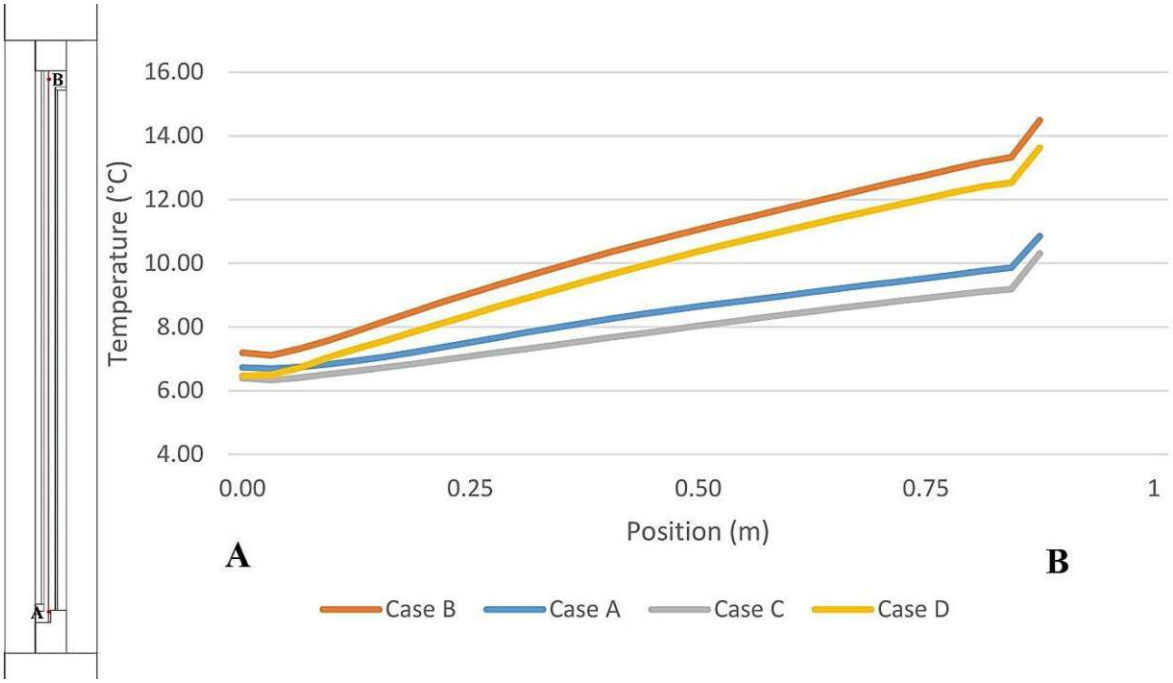

Figure 29. Simulated temperature distribution in the windows' cavity space

According to the results, a significant temperature rise within the cavity is noticeable in all cases. Two sources of thermal energy can be assumed to contribute to the preheating of the air flowing through the cavity, namely incident solar radiation and conductive heat transfer from inside the room through the inner glass pane to the cavity. Cases B and D display a significantly higher average temperature in the buffer space as compared to the other two cases. This indicates the effect of conductive heat transfer from indoor space to the cavity via the single pane of glass. Consequently, reduced heat transfer from indoor space to the cavity in cases A and C can be suggested to be responsible for the lower values of the computed supply air temperature.

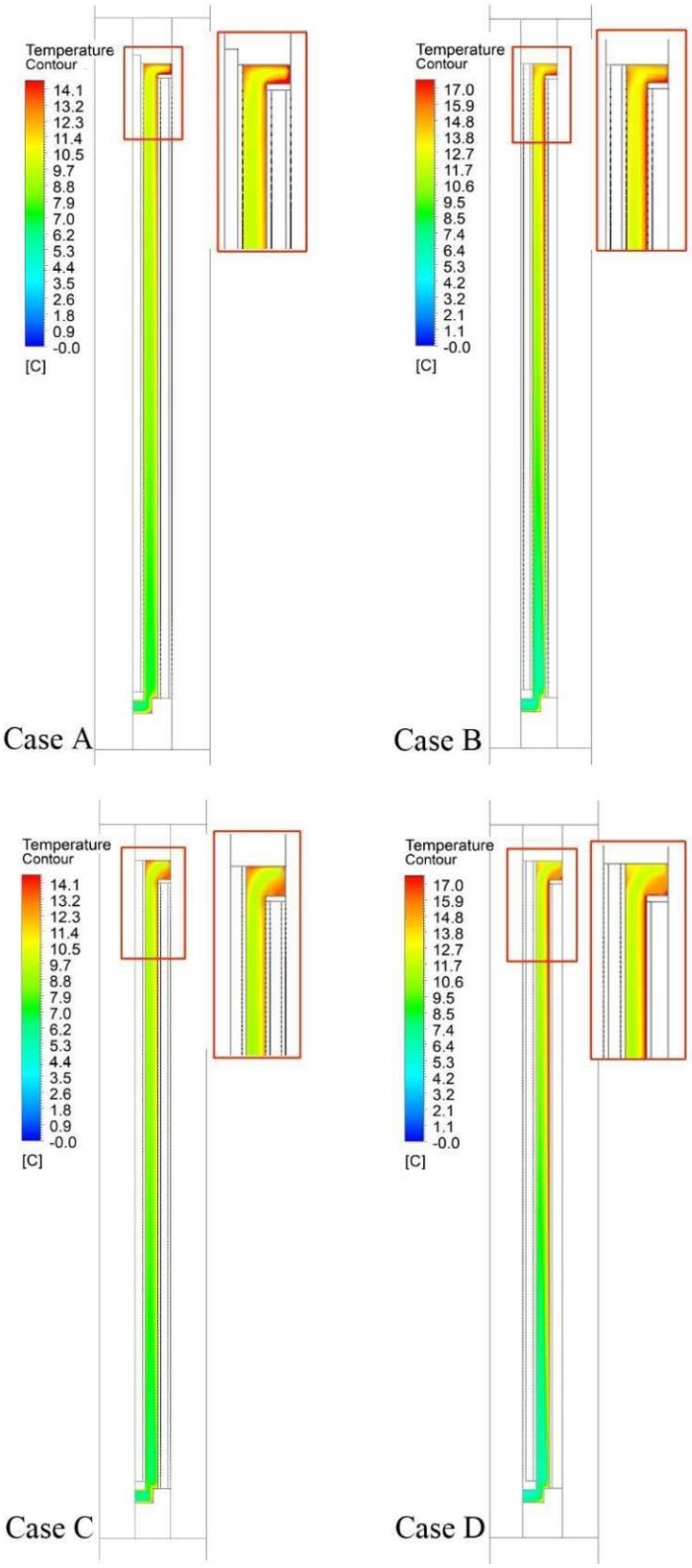

Figure 30. Temperature distribution in the cavity for the case studies

3.4.5. Condensation issues

As stated earlier, one of the challenges regarding ventilated windows pertains to the risk of condensation on the outer glass pane at the cavity side. The evaluation of condensation risk in case of complex fenestration systems is a non-trivial challenge. A first, rather basic possibility to query this issue would be to consider the profile of the surface temperature on the inner layer of the window element. Based on simulated minimum surface temperature values, the dimensionless temperature factor at outer glazing panes of ventilated window (f_{Rsi}) (ISO, 2007) can be derived as per the following equation:

$$f_{Rsi}(\theta_{si} - \theta_e).\ (\theta_i - \theta_e)^{-1} \qquad (8)$$

Herein, θ_{si} denotes the temperature at the internal surface at the point with the lowest temperature, θ_i indoor temperature, and θ_e outdoor temperature.

Table 17 provides numeric information regarding the minimum inside surface temperature of the outer glass layer as the dimensionless temperature factor for the aforementioned scenarios. As it could be expected, when the double layered glazing is applied to the outside window wing (i.e., cases B and D), the temperature factor value (f_{Rsi}) clearly exceeds the minimum recommended value of 0.7 according to the applicable regulation in Austria (OENORM B8110-2 2020). In Case A, the smaller size of the width of the supply air opening can be assumed to have contributed to somewhat higher cavity temperature.

Table 17. Minimum surface temperature obtained from CFD simulation together with calculated fRsi values

Simulated scenarios	**Minimum surface temperature**	f_{Rsi}
Case A	8.70	0.76
Case B	10.97	0.88
Case C	8.69	0.70
Case D	10.90	0.82

3.5. Summer condition (exhaust and outdoor curtain mode)

As mentioned earlier, ventilated window functions as a solar collector under incident solar radiation. The solar energy passing through the outer glazing warms up the interstitial space and eventually internal glazing surfaces. Re-emitting the trapped heat from these surfaces increases the indoor air temperature. Hence, the thermal behavior of ventilated windows strongly affects the indoor temperature and consequently energy consumption of a building.

In the course of this study, we numerically analyzed the thermal performance of the two modes of ventilation window operation (exhaust and outdoor curtain mode) under summer conditions. Figure 31schematically illustrates the vertical section of the ventilated window for the summer case.

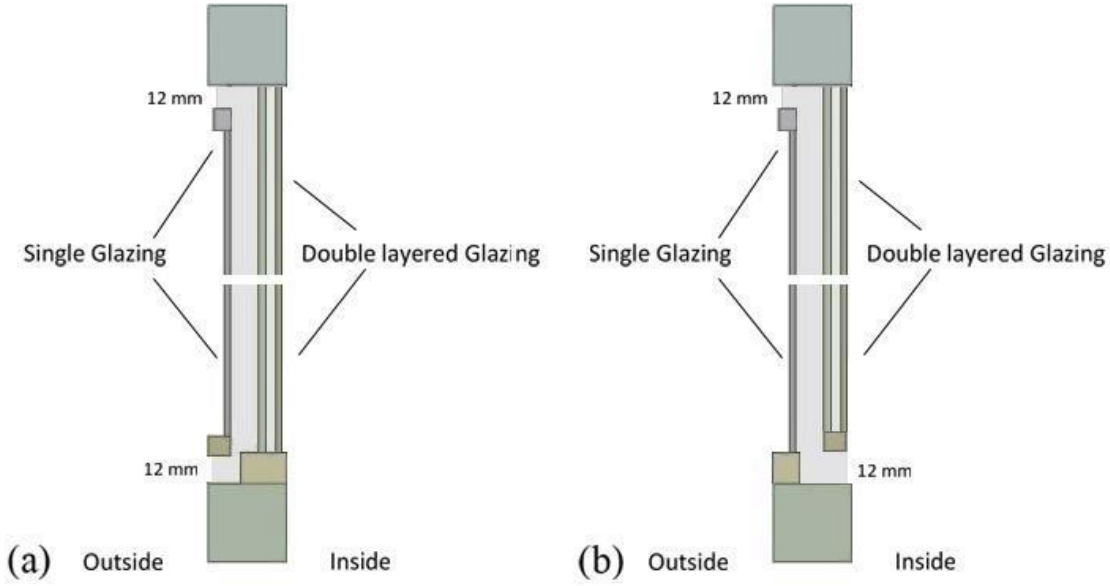

Figure 31: Schematic illustration of ventilated window for the summer case; a: outdoor curtain mode, b: exhaust

To evaluate the CFD model's reliability, a reference case (outdoor curtain mode) which corresponds to the actually implemented experimental setup was considered (Nusser et al. 2016). The location of the field trial and dimension of the window was identical to the winter case (see at the section 3.3.2) (Nusser et al. 2016). The solver setting and material property were indistinguishable with the winter case (see table 11 and section3.2.2)

According to the experimental results, the wind effect was not noteworthy. On the other hand, the solar radiation showed a visible difference in the temperature conditions in the buffer area. During the night, the temperature at the lower measuring position was derived by the outside air temperature. The air temperature at the upper opening was about 5 K higher than at the lower measuring point. On the other hand, during the daytime, the effect of solar radiations was more obvious since the maximum temperature difference between top and bottom opening was about 20-30 K. In this study, a one-hour long segment of measured data from the third day of measurements could be identified as involving relatively small fluctuations of the boundary conditions. We thus could treat this period as quasi steady-state. The registered mean values of

the boundary condition during this one-hour period (10:00 AM, July 16th, 2016) were treated as the applicable boundary conditions for the CFD simulation model. Table 18 shows the boundary condition for the summer case.

Table 18: Boundary condition for the CFD simulation (summer mode)

Variable	Value	Unit
Irradiance	650	$W.m^{-2}$
Wind speed	2	$m.s^{-1}$
Outdoor temperature	22	°C
Indoor temperature	25	°C

Figure 32 illustrates the temperature distribution profile (along the depicted path) obtained from the CFD simulation together with the measured temperature at two sensor locations in the window specimen.

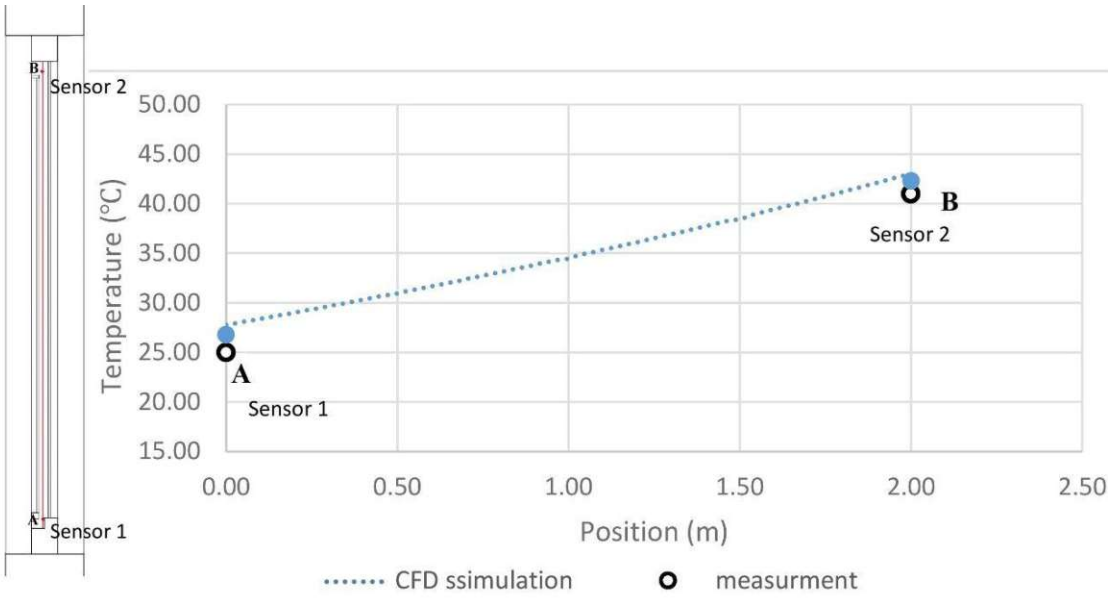

Figure 32: Left: schematic section through the examined ventilated window with the position of the two temperature probes (A to B); Right: Measured (sensors A and B) and simulated temperature profile. The distance information (xaxis) denotes the relative distance

The measurement results documented the effect of solar radiation on warming the air temperature of the interstitial space during the warm season. The CFD simulation slightly overestimates the temperature values. However, simulation results may be suggested to agree in tendency with the measurements.

3.5.1. Analyzing thermal behavior of exhaust and outdoor curtain ventilated window

As mentioned earlier, one of the goals of this study was to computationally investigate the thermal behavior of ventilated window (exhaust and outdoor curtain mode) during the warm season.

To this end, the thermal behavior of two modes of ventilated windows under the identical boundary conditions and identical dimensions in both cases (1 m wide and 1 m high) were estimated. According to the results, in both cases, the temperature difference among openings at the top and bottom is between 12-20 K. For the sake of comparison, figure 33 demonstrates temperature and velocity counters for exhaust (a,b) and outdoor curtain air (c,d) ventilated windows.

In the exhaust air ventilated window the mean air temperature and consequently the air velocity is higher. In this type of the ventilated window the buffer space is connected to the indoor air temperature. The solar radiation heats the outside surface of the glass to induce airflow exhausted from indoor space. The generated negative pressure makes the outdoor fresh air enter from other openings of the room. The system is appropriate when the outdoor temperature is not so high.

On the other hand, the Curtain air window expels the accumulated warm air from buffer space. The solar radiation induces airflow in the interstitial space and consequently reduces heat flux into the room through the glass. This type of the window is a proper option for the warm season.

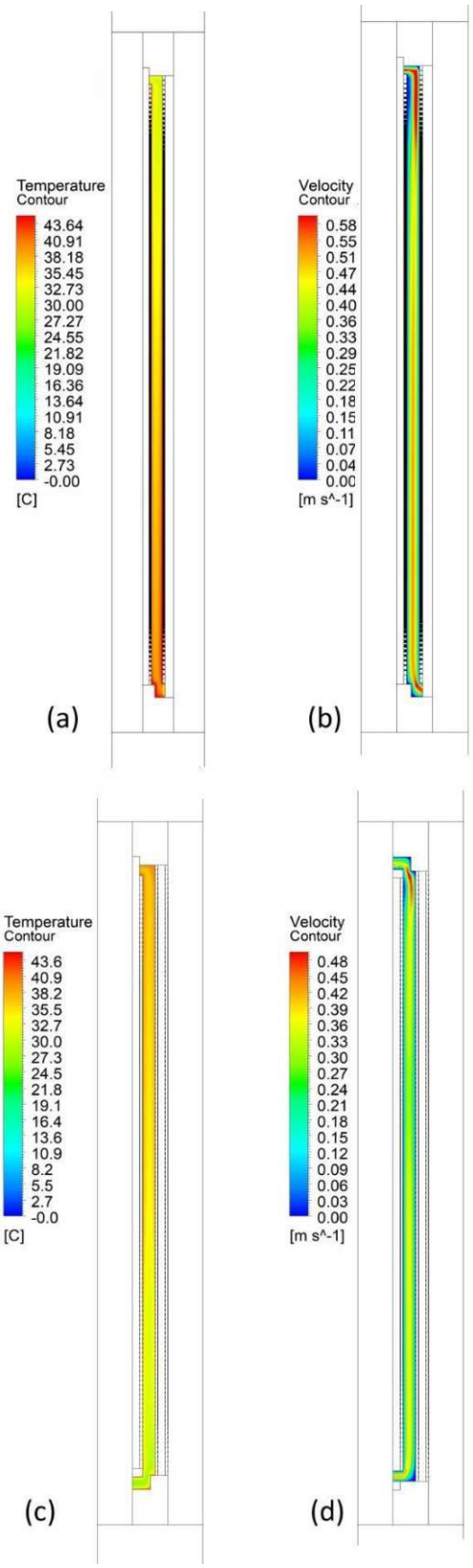

Figure 33: Temperature and velocity distribution in the window cavity, a,b: exhaust and b,c curtain air ventilated window

To assess the effect of double-layered glazing location, four cases were considered as per Table 19. The assumed window dimensions are identical in all four cases (1 m wide and 1 m high).

Table 19: Summary of the simulated configurations (width of the inlet and outlet opening was assumed to be 12 mm in all cases)

Case	Ventilated window type	Position of the double-layered element
A	outdoor curtain	inside
B	outdoor curtain	outside
C	exhaust	inside
D	exhaust	outside

In order to reduce energy consumption and improve the indoor thermal environment of the buildings, the ventilation rate should be considered to estimate the inner pane temperature. Table 20 summarizes the simulation results for the four cases in terms of the mean temperature of the inner layer glazing and buffer space.

Table 20: temperature difference, mean air velocity and man surface temperature for the simulated scenarios

Case	Mean temperature(°C)	Mean velocity($m.s^{-1}$)	Inner layer glazing temperature (°C)
A	33.98	0.30138465	38.32
B	32.87	0.30339436	32.46
C	36.17	0.43248557	41.40
D	34.43	0.41398697	36.82

The results of the CFD-based investigation suggest that the application of low-emissivity glazing as the exterior glass pane can improve the cooling effect in both cases. According to the results, with help of low-emissivity glazing as the exterior pane, the surface temperature of the interior glass drops, and consequently, the radiation exchange between this surface and the occupants can be decreased. In addition, the outdoor curtain air mode of the ventilated window reveals a slightly better performance under summer boundary conditions by reducing the temperature difference between the room air and the surface of the interior glass.

3.6. Conclusion

The results of the present study are compatible with general assumptions concerning the functionality of ventilated windows. The most distinctive characteristic of the ventilated windows is the potential to contribute to indoor air quality and higher energy efficiency. In general, this window serves as a solar collector under inward flow conditions and incident solar

radiation. The solar radiation absorbed by the layers of the window as well as heat losses from the indoor environment preheats the air within the gap and creates buoyancy forces that induce an upward flow of air. The temperature inside the ventilated window is expected to be higher than the outdoor temperature during most of the day. This results in lower conductive heat losses depending on ambient temperature and solar radiation level.

Our study covered a thermal analysis of several ventilated window configurations. The thermal performance of these models was evaluated numerically by a commercially available CFD under winter conditions. As noted at the outset of this dissertation, deployment of numerical method in heat transfer simulation of building detail requires a rigorous concerning the details of the model, mesh generation, etc. To gain confidence concerning the model's reliability, its performance was first compared with laboratory and field measurements before its deployment toward the aforementioned parametric analysis.

The results point to the ventilated windows' potential to deliver preheated fresh air to indoor spaces. A temperature rise in the order of 3 to 18 K was computationally observed in the windows' cavity under the specified boundary conditions. The field studies proved the strong effect of solar radiation on the thermal behavior of the ventilated window, nevertheless did not display a clear influence of the wind velocity. Rather, the thermally driven buoyancy force in the cavity seems to be the principal driver behind the airflow. Amongst the simulated alternatives, analyzing the geometry of the cavity shows that taller cavities and smaller cavity depth can provide higher incoming air temperature. Evaluating the width of the inlet opening and position of double-layered glazing indicates that Case B with 12mm opening width displayed better results in terms of higher cavity temperatures and higher minimum surface temperatures (inner glass surface of the outer wing), resulting also in a lower risk of condensation in the cavity. However, Case A has the advantage of higher energy efficiency given the lower rate of heat transfer from the indoor space to the cavity.

Analyzing the summer performance of two type of ventilated window (exhaust and outdoor curtain mode), reveals that the application of low-emissivity glazing as the exterior glass pane can improve the cooling effect in both cases. In addition, the outdoor curtain air mode of the ventilated window shows a better performance under summer boundary conditions.

4. The effect of double skin façade on indoor flow behavior

4.1. Background

Natural ventilation has become an increasingly widespread approach to reduce energy consumption and expense. Providing efficient natural ventilation in the buildings has been a constant subject of interest for building designers and the researchers (Lomas, 2007; Chen, 2009). The fresh air supply from natural ventilation produces a sustainable alternative for higher energy-intensive types of mechanical ventilation (Hasse and Amato, 2009). Additionally, it is an efficient strategy to improve thermal comfort by providing the ventilated cooling air in the indoor environment (Artmann et al. 2007; Montazeri H. and Montazeri F., 2018).

Natural ventilation efficiency is affected not only by the ventilation flow rate but also to a great extent by the airflow pattern in the room. The importance of the airflow pattern on the air quality was recorded by (Montazeri et al. 2010; Mundt et al. 2004). The application of natural ventilation schemes in buildings is limited, essentially due to inadequate outdoor climatic conditions, air pollution, or noise pollution. Noise negatively affects the inhabitants, especially in dense urban areas and near main transportation routes. Despite multiple noise control efforts, complaints from environmental noise clarify a rising trend in recent years. Consequently, the sound insulation feature of the building envelope is highly important. Thereby, natural ventilation and noise reduction must be addressed in tandem. Previous researches have discussed some of the subjects involved (see, for example, (Nunes et al. 2010; Mahdavi, 1993) several studies have analyzed the sound insulation properties of the open windows (Nunes et al. 2010; Buratti, 2002). Various approaches for noise control in buildings with natural ventilation have been investigated (De Salis et al. 2002; Migneron and Potvin, 2010). The Department of Building Physics and Building Ecology at the Technical University of Vienna has commenced studies focusing on a system of double-leaf façades (DLF) that can provide natural ventilation while facilitating sufficient sound insulation (Bajraktari, 2015).

Recently, double-leaf facades have received ever-greater importance in modern building fashion especially in the office buildings. Enhanced sound insulation and greater user satisfaction are the main advantages of the double- leaf façade (Gratia and De Herde, 2004).

The second skin in this type of facades, is located in front of the inner layer to reduce wind pressure and control the noise (Gratia and De Herde, 2004). Different parameters impact the ventilation capacity of these façades which can strongly influence the ventilation performance and the indoor air quality.

While natural ventilation is conceptually simple, its detailed analysis can be a challenge. The ventilation performance is influenced by the buildings' form, its surroundings, and climate situation (Karava et al. 2007; Mochida et al. 2005). For instance, different window configurations create different ventilation effectiveness, indoor air quality (IAQ), and consequently impact on comfort conditions in the occupied zone (Karava et al. 2007). Earlier researches on wind-driven ventilation has revealed the significant influence of the size and position of the inlet and outlet openings of the double leaf facade on the flow inside the building (Montazeri H. and Montazeri F., 2018; Gratia and De Herde, 2004). This complexity of winddriven ventilation, can make the development of a successful design complicated (Karava et al. 2007, Mochida et al. 2005). Hence, Prediction of the airflow through large openings (partly open windows) remains significant source of uncertainty in building simulation (Karava et al.
2007, Furbringer, 1999).

4.2. Method

This chapter concentrates on a double-leaf façade solution, which offers sufficient sound insulation while facilitating natural ventilation. The impact of various variables on such a system (e.g., the size of the opening, location of the openings, the relative displacement of the openings in the two layers, the cavity sound absorption) were examined via parametric laboratory sound transmission measurements during the previous research project. Additionally in the current study, the natural ventilation efficiency of the related facade was analyzed via CFD simulation. To this end, first, the experimental wall was installed in the opening (dimension: 3.1 by 3.1 m) connecting two reverberant chambers of the acoustic laboratory of TU Wien (see Figure 33).

Figure 34. View (left) and schematic illustration (right) of the experimental modular double wall.

The experimental double wall consisted of two layers of chipboard elements. The distance between the two layers was 43 cm. As displayed in figure 33, these layers were structurally decoupled. In a five by five grid structure, each layer had 25 dismountable square elements (50 x 50 cm). Different numbers of elements can be opened in each layer, leading to different effective opening areas. Moreover, a number of elements embody smaller openings (50% and 25% of the regular element's area). Given the flexibility of the grid structure, the distance (d) between openings (see Figure 34) and thus the respective view factor and angle of sound diffraction can be varied. Likewise, the amount and location of cavity absorption can be changed via installation of modular sound absorption elements. The CFD simulation model replicated the experimental configuration. Table 21 shows a sample of these configurations applied in CFD simulation.

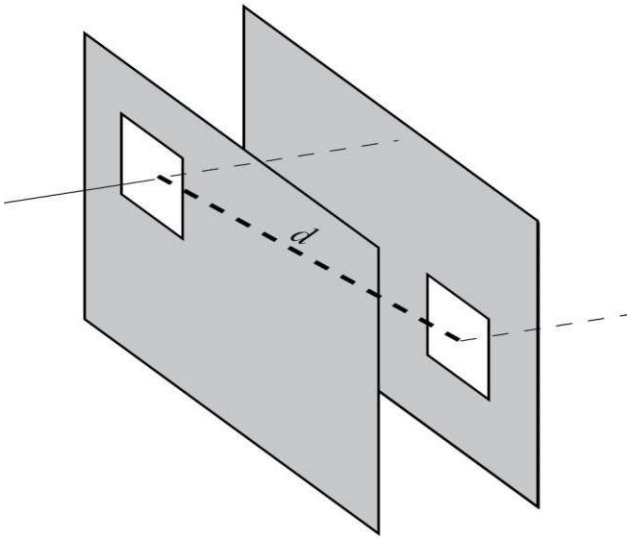

Figure 35 . Illustration of distance (d) between openings

Table 21. Selected instances from the list of configurations of the experimental DSF (the codes of the openable elements are shown in Figure 33). Distance d is shown in Figure 34.

Config. number	Code of the open element in layer facing the source room	Code of the open element in layer facing the receiver room	Distance d (m)
1	1	1	0.43
2	1	13	1.48
3	1	25	2.86
4	6, 16	6, 16	0.43
5	6, 16	8, 18	1.09
6	6, 16	10, 20	2.05
7	1, 6, 11, 16, 21	1, 6, 11, 16, 21	0.43
8	1, 6, 11, 16, 21	3, 8, 13, 18, 23	1.09
9	1, 6, 11, 16, 21	5, 10, 15, 20, 25	2.05

An empirically-based equation and a simple analytical one were developed for the prediction of the sound insulation of double-leaf facades with openings for natural ventilation (Bajraktari et al. 2015).

To evaluate the natural ventilation performance, high-resolution coupled (outdoor wind flow and indoor airflow) 3D steady RANS CFD simulations of single sided-ventilation were performed for 9 configurations of double-leaf façade (different sizes and positions of the openings). The results of these computational estimations were compared with the measurement results to discuss the potential and limitations of their predictive performance.

4.2.1. Wind tunnel experiments

Air flow simulations were performed for a single-zone isolated building with an integrated double-leaf façade.

To this goal, a coupled indoor-outdoor computational domain was constructed with a high level of detail. The computational model consisted of the building model, the upstream and downstream domain lengths are 5H and 10H respectively (H is the height of the building), based on the best practice guidelines by Franke et al.(Karava et al. 2011; Franke and Baklanov 2007) and Tominaga et al.(Tominaga et al. 2008). Accordingly, the simulated space was 4 m wide, 5 m deep, and 3 m high. The modelled double façade configuration was consistent with the laboratory setting deployed for the aforementioned acoustical measurements and it was facing the approach flow (Figure 35). Ansys design modeler and Ansys meshing were applied as a pre-processor to create the geometry, mesh, and the computational domain.

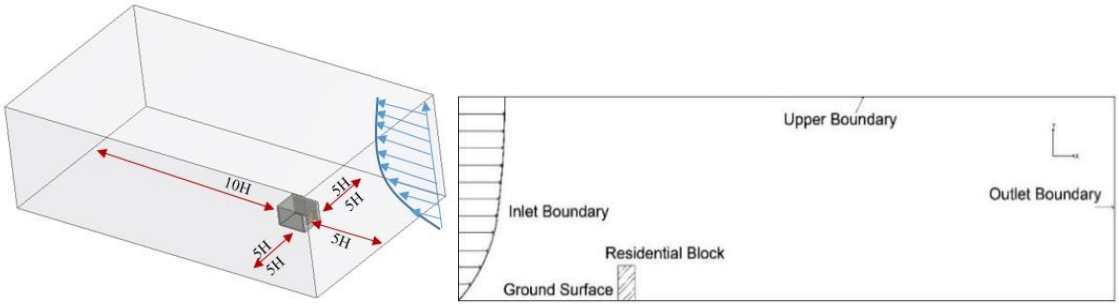

Figure 36. Calculation Domain. (a) Perspective (b) Section of the domain.

The boundary conditions are summarized in table 22. At the inlet of the domain, neutral atmospheric boundary layer inflow profiles of mean wind speed U (m/s), turbulent kinetic energy k (m^2/s^2) and turbulence dissipation rate ε (m^2/s^3) were imposed. It was assumed that the building was situated on urban area. Note that, Friction at the ground level reduces the airspeed thereby wind velocity changes with height above ground level (see figure 36).

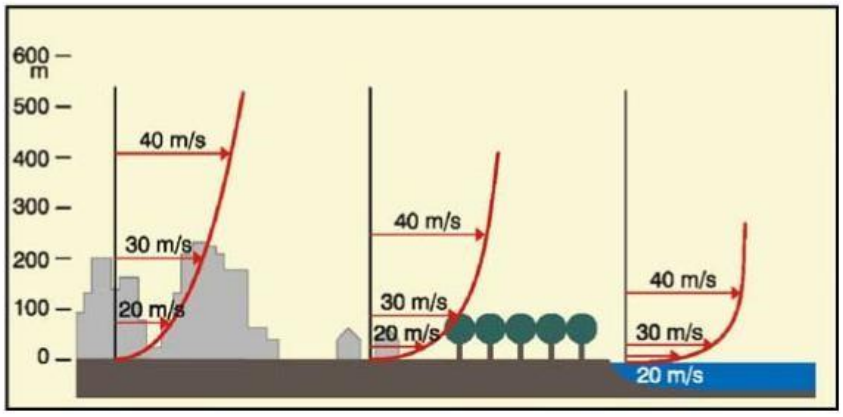

Figure 37. Wind speed related with location

Table 22: Boundary conditions for the analysis domain.

Inlet	*See Eq. 9*
outlet	Zero static gauge pressure
Upper and side boundary	Symmetry
Ground and building surface	No-slip walls

In order to define the external boundary condition in CFD, the airflow needed to be calculated for the external wind. In designing a naturally ventilated building, the site-condition effects such as adjacent buildings, walls, and vegetation on wind velocity needs to be studied. In built-up areas, this boundary layer influence is more conspicuous because of the rough surface created by large buildings. Therefore, considering a proper surface roughness to obtain an accurate results is necessary (Gratia and De Herde, 2004). In the present study, the wind profile was obtained using the following equation:

$$V_z.V_{10\text{-}1} = (Z.10\text{-}1)_a \qquad (9)$$

Here, V_z denotes air speed at height Z and V_{10} air speed at the height of 10 m, and the exponent *a* surface roughness (0.36 for urban area) (Blocken and Carmeliet 2004). The walls of the computational domain were modelled as no-slip walls with zero roughness. The standard wall functions were applied. Zero static gauge pressure is applied at the outlet openings. The SIMPLE algorithm was used for pressure-velocity coupling, pressure interpolation was second order and second-order discretization schemes were used for both the convection terms and the viscous terms of the governing equations.

4.3. Results and discussion

Acoustical calculations and air flow simulations were conducted for the 9 double-façade configurations described in Table 21. As the key acoustical performance indicator, ΔR_w (see Eq. 4) denotes the reduction of weighted sound reduction index of a configuration as compared to the base case with both layers fully closed (see Table 22). As such, this reduction term denotes the difference between the weighted insulation index of the fully closed configuration ($R_{w,max}$) and that of a specific configuration that includes openings (R_w)(Mahdavi and Khosravi, 2020; Mundt et al. 2004).

$$\Delta R_w = R_{w,max} - R_w \qquad (10)$$

The CFD simulation results were processed in terms of the mean air flow velocity and the mean age of air τ_p in the test space. The local mean age of air (Cuce and Riffat, 2015; Bakonyi, 2016) is the average time for the air to travel from an inlet opening to any point of the room; so it is a rather significant indicator of the freshness of room air. The actual air change time is the period it takes to replace the air in the room. It has been confirmed that this is twice the mean age of air in the room (Montazeri H and Montazeri F, 2018). The local mean age of air was estimated by solving a user-defined scalar (UDS) transport equation. The diffusivity for the UDS transport equation was computed using the following equation:

$$\tau_p = (2.88 \cdot 10^{-5})\, \rho + \mu_{eff} \cdot Sc_t^{-1} \qquad (11)$$

Here, ρ denotes the density of the air, μ_{eff} the effective viscosity of the air, and SC_t the turbulent Schmidt number (SC_t = 1.2 for natural ventilation) (Awbi, 1998).

The boundary conditions for the UDS is set to 0 at the inlet and outlet openings of the domain. Second-order discretization is used for the convection and diffusion terms of the scalar transport equation. Table 23 entails a summary of the CFD simulation results for the aforementioned 9 configurations. Consideration of the computed age of air and air velocity data does not reveal a linear relationship, but is consistent (higher mean air velocity values correspond to lower mean age of air values).

Table 23. Ventilation performance indicators for 9 configurations.

Config.	Mean Age of air inside the room	Mean velocity inside the room	ΔRw

1	3.6	3.3	29
2	10.8	0.9	20
3	14.0	0.8	18
4	2.7	4.7	33
5	22.1	0.7	27
6	35.1	0.5	25
7	1.3	9.7	38
8	8	1.7	33
9	11	1.2	30

According to the simulation results, the size and position of the opening on each leaf can significantly influence the induced airflow and indoor air quality. Based on the simulated mean velocity on the opening surface as well as the area of each opening, by enlarging the openings on the front and back leaf the induced flow rate increases. The highest value achieved when four elements are opened on each leaf and openings on the front and back leaf are located in front of each other (configuration 7). In configuration 8 and 9, the location of the front leaf opening as well as the numbers of open elements are the same. However, the position of the back leaf opening is different. In the configuration 8, the back leaf opening is closer to the front leaf opening so the amount of airflow is higher and the air inside the zone has a better quality. In addition, in the other configurations with smaller size of openings, by placing the open elements in front of each other the airflow value has higher value than the similar cases. Consequently, the mean velocity inside the room has a higher value.

Simulation results indicates that the mean age of air value was considerably low in configuration 7. However, Due to the position of the openings which is causing shortcircuiting, the indoor air quality has reduced significantly in configurations 5-6. The results prove that using two openings rather adjacent to each other will not enhance the induced airflow. In addition, it leads to a considerable reduction in the indoor air quality inside the room. The negative impact of short-circuiting is expected to happen (Mundt et al. 2004).

Figure 37 further concerns the relationship between the pertinent acoustical parameter (ΔR_w) and the selected air flow parameter (τ_p). However, in this figure, age of air is expressed

logarithmically, so as to be consistent with the likewise logarithmic nature of sound insulation reduction values.

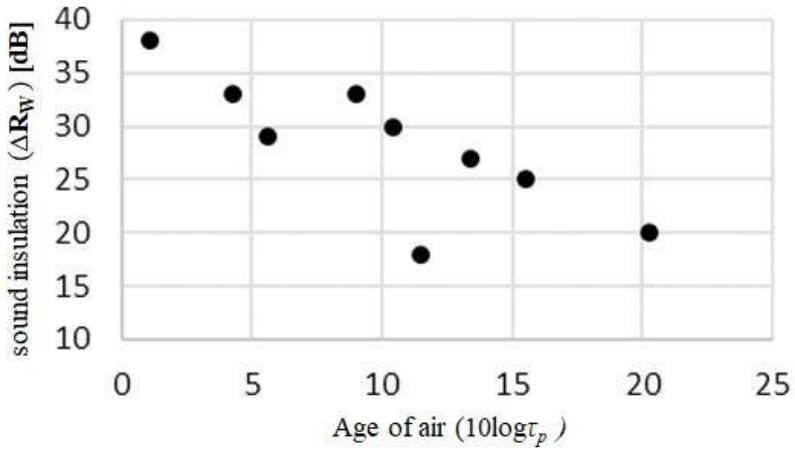

Figure 38: The relationship between measured ΔRw and computed age of air for the selected 9 double-façade configurations.

The data summarized in this Figure appears to be plausible: Higher degrees of acoustical insulation correspond to lower levels of air freshness. However, the relationship between the measured ΔR_w and computed age of air values cannot be characterized in terms of a strong correlation. In other words, we cannot simply assume that a configuration with higher levels of sound insulation automatically translates in proportionally higher levels of air change. Specifically, configurations 3 appears to be somewhat of an outlier. In this particular configuration, the relatively large displacement might be responsible for a better than average acoustical performance.

To summarize, the acoustical measurements suggest that reasonable levels of sound insulation may be obtained from double-façade configurations, even if they involve openings for natural ventilation. Moreover, the derived grey box models allow for a fairly reliable estimation of the sound insulation levels based on a number of input variables related to the configuration at hand (e.g., opening area, opening displacement). However, the quantitative prediction of the levels of air change is non-trivial.

5. CFD analysis of a local radiant cooling solution

5.1. Background

It has been suggested that climate change due to greenhouse gas (GHG) emissions is one of the most significant challenges facing humanity (Gustavsson et al. 2015). Specifically, the global reliance on non-renewable energy sources leads to an increasing concentration of greenhouse gases in the atmosphere and thus contributes to climate change. In this respect, particular attention should be given to the household sector as a major consumer of energy (Olonscheck, et al. 2011). The move from uniformly conditioned indoor environments to smaller, individually controlled zones, can be advantageous in view of thermal comfort and energy efficiency (Lio et al. 2019). Limitations of traditional cooling systems, such as noise, draft, vertical thermal gradients, and high energy demand necessitate the investigation of alternative cooling systems. In this context, the application of water in chilled radiant panels can be of interest (Nio et al. 1995). These panels can be broadly classified based on their installation location. The most common form is the ceiling-mounted cooling panel.

Radiant cooling ceiling systems were investigated, among others, in the laboratories in European countries in the early 1990s (Stetiu, 1999). They have been shown to have the potential to provide adequate thermal conditions (Wilkins and Kosonen, 1992). In some systems, the pipes are inserted in the surface layer of a wall, ceiling, or floor (Chiang et al. 2012). Lately, the integration of radiant cooling into furniture (e.g., in desks) has received attention (Rhree et al. 2017). Thereby, the chilled water could circulate through the table top to remove the sensible heat, while latent heat is removed by an all-air cooling system (Wilkins and Kosonen, 1992). As compared to conventional cooling systems, radiant cooling panels have the potential to offer smaller vertical temperature gradients, lower air movement velocity, and reduced local discomfort (Yingdong et al. 2017). Whereas conventional air-conditioning systems are mainly based on convection, radiant panels utilize a combination of radiation and convection (Gan, 1994).

The thermal performance of the cooling panels has been investigated via both experimental and computational methods. The thermal comfort of five human subjects in a laboratory test room equipped with cooling ceilings was analysed by Nagano and Mochida (Nagano and Mochida, 2004). In their experiment, the temperature difference between the ceiling and the room air was less than 5 K. According to their findings, the mean radiant temperature for a supine human body should be applied in the design of ceiling radiant cooling. Another study

compared the radiant cooling systems with air-conditioning systems in terms of thermal comfort, energy consumption, and cost. The results suggested that the radiant ceiling panel system is capable of creating a smaller vertical variation of air temperature and a more comfortable environment (Imanari et al. 1999).

Experimental studies are of course highly instructive, but also rather expensive and timeconsuming. If carefully applied, CFD-based numeric simulation can provide alternative or at least complementary means of investigation. Computational fluid dynamics has become an important tool in the prediction of thermal comfort in occupied spaces (Nilsson, 2007). Compared to the experimental techniques, CFD simulations can provide detailed values regarding the flow distribution and concentration fields in the whole domain, rather than just targeted points for data collection (Chen et al. 2010, Hayashi et al. 2002, Liu et al. 2013). Nevertheless, proper CFD application necessitates sufficient grid resolution, accurate choice of numerical models, estimation of numerical errors, and control over other numerical parameters for precise verification and validation (Roache, 1997, Oberkampf and Trucano, 2002, Stamou and Katsiris, 2006). Despite the dramatic progress in its application, CFD has not replaced experimental and theoretical analyses, but represents a highly useful complementary tool (Li and Nielsen, 2011, Liu et al. 2015, Srebric et al. 2015). As such, experimental studies have been conducted to probe the precision of numerical simulation of the indoor thermal environment (Murakami et al. 1991).

Myhren et al. (Myhren and Holmberg, 2008) applied CFD simulations for two office rooms equipped with separate heating and ventilation systems, to investigate potential cold draught problems, the differences in vertical temperature gradients, and air speed levels. Another study compared the energy efficiency of the cooling panel with the all-air cooling system via CFD simulation and experimental method. Thereby, the cooling panel was found to be more energy efficient (kim et al. 2005). Predicting thermal comfort by applying virtual human manikins in the CFD simulation has been reported by numerous studies (Nilsson, 2007). According to our observation, there are no relevant standards in CFD simulations for the sizes, shapes, and postures of human model, and their application mostly depends on the purposes of the research works (Gao and Niu, 2004; Cheong and Huang, 2013; Gao and Nio, 2005; Kong et al. 2017). Because of the excessive simulation time, the majority of CFD studies have applied simple (e.g., rectangular) shapes. In some cases, the nature of the study necessitated a complex human model (Yang and Sekhar, 2013).

Within the framework of a recently completed research project, the potential of vertical radiant panels in the proximity of users was investigated and related technological requirements regarding envelope tightness and ventilation systems as well as water vapor condensation risk were evaluated (Cheong and Huang, 2013). In the present contribution, we explore the potential of CFD simulations to analyse the airflow patterns and the velocity fields inside a test room with a vertical radiant panel positioned in the close proximity of a workstation. Simulated results were compared with previously obtained measurements. The objective of the numeric analysis was to capture the air flow patterns and local discomfort risk.
The study included also the air velocity field around a simplified human model.

5.2. Method

Predicting the thermal performance of a cooling panel is not a trivial task. In general, this system represents a mixed convection heat-transfer mode, including human body buoyancydriven thermal plumes, and radiation through the panel and wall surface. To this end, a prototypical local radiant cooling panel was installed in a mock-up office room of a laboratory (see Figure 39).

Figure 39: Test room equipped with a cooling panel

During the laboratory experiments, the ambient air temperature and relative humidity in the room were kept at 30±0.5°C and 40±3%, respectively. The target panel surface temperature was 10°C. The air flow speed was measured and simulated at several heights (10, 35, 60, 85,

and 110 cm above the floor) and distances (1, 1.5, 2, 3, 4, 5, 10, 15, 20, 30, 40, and 50 cm from the radiant panel) (see Figure 40).

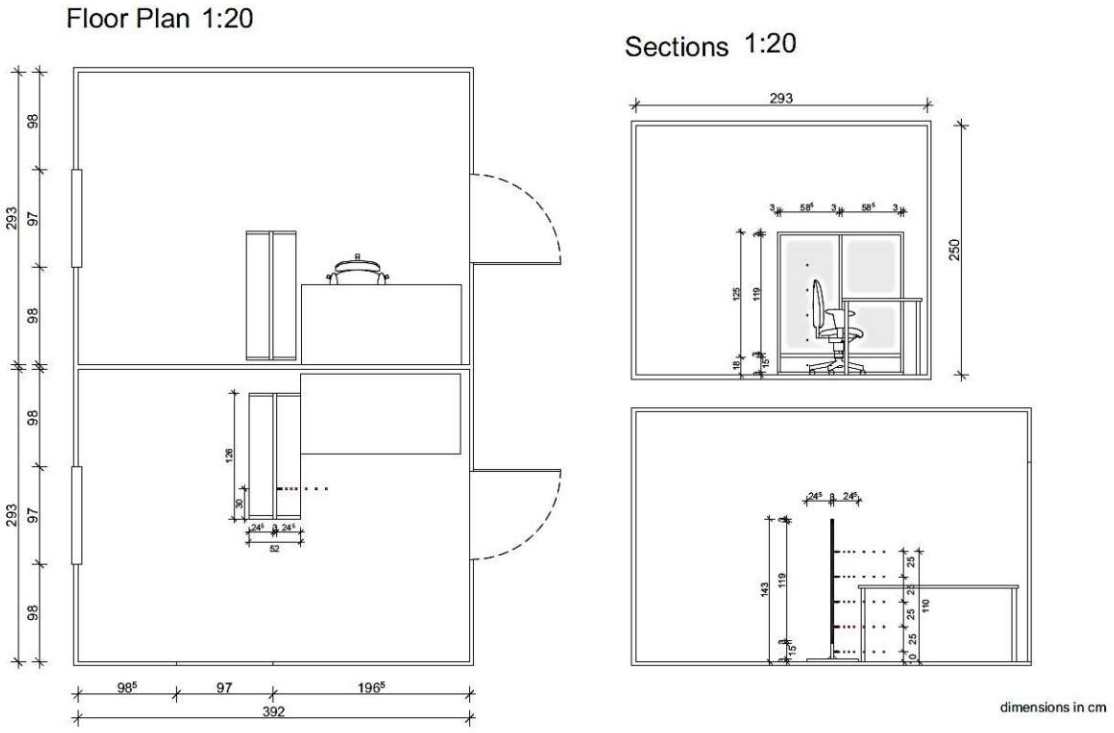

Figure 40: Floor plan and sensors locations at the test room

The CFD model's boundary conditions were adapted from the thermal conditions of the laboratory. Note that during the experiment the surface temperature of the panel's frame was higher than the chilled part of the panel. Within the CFD model, the cooling element was simplified and no distinctions were made between the surface temperature of the frame and the chilled part of the panel. As a result, for the CFD simulations the whole panel temperature was considered to be 11°C.

CFD model was implemented in the finite volume code ANSYS FLUENT 19.0. The model involves the vertical cooling panel mounted in the test space and a simplified human model for some simulation cases. Ansys design modeler and Ansys meshing were applied as a pre-processor to create the geometry, mesh, and the computational domain. In this model, a mesh with hexahedral element was generated. Buoyancy due to density change was applied in the energy equation. The discrete ordinates (DO) model was applied as the radiation model. The pressure-based solver was applied. The SIMPLE segregated solver was used for pressure–velocity coupling.

Various studies have assessed the performance of turbulence models. For RANS-based models, selecting a proper turbulence model is essential for heat transfer analysis. The answers to the question of the best-performing turbulence models are not always consistent. For instance, the standard k-□ or the RNG k-□ turbulence models are widely implemented for CFD simulations of cooling panel, while SST-K ω model has been applied in other studies. In addition, some studies applied a Laminar flow model. The results of the literature review revealed that the k-ε family of turbulence models presented similar results consistent with laboratory data (Yakht and Orszag, 1986; Shih et al. 1995; Jones and Launder, 1972). The SKW and SST turbulence models showed a lesser performance level in predicting air velocity (Menter, 2012; Chen and Xu, 1998). This disparity can be due to the physical features of the case studies, as well as different computational parameters and settings applied in different studies. Hence, for each specific simulation study, the selection of the turbulence model may have to be reassessed. In the present study, CFD simulations were carried out using the same geometry but with different turbulence models (RNG k-□ and SST-K ω). To check the reliability of the turbulence model, the simulation results were compared with experimental. Note that we used the discretization scheme employed for the energy, momentum, turbulent kinetic energy, and specific dissipation rate was the second order upwind scheme. Pressure Staggering Option (PRESTO) was used for the pressure discretization scheme.

5.3. Results and discussion

The air velocity could be an influential parameter for the thermal comfort: Increased airspeed can aid the evaporation of sweat thus leading to a cooling effect, particularly if loose clothing is worn. Nevertheless, too high air velocity may cause discomfort and a draughtiness sensation. Average air speed is typically recommended not to exceed 0.15 $m.s^{-1}$ in the occupied zone to prevent discomfort (ASHRAE, 1992). The CFD method can complement the experimental results by allowing the detailed examination of the velocity field at different spots. Given the complexity of the physical processes involved, a candidate simulation model should ideally incorporate complete three-dimensional processes, suitable turbulence models, realistic boundary conditions, and temperature-dependent material properties. In this study, to gain confidence concerning the model's reliability and the employed turbulence model, we first compared the computational results with the laboratory measurements. Subsequently, the study covered the human model analysis.

5.3.1. Turbulence model

Two different turbulence models (k-ε and k-ω) were applied for the CFD simulation. During the experiments, air velocity was measured at 75 locations. Figure 41 illustrates the velocity distribution profile (on the sensors location) obtained from the CFD simulation for two different turbulence models, together with the measured velocity values in the test room. The effect of turbulence models on the air velocity distribution can be seen in This Figure. As such, the k-ε and the k-ω family of turbulence models overestimated the values by up to 0.05 and 0.1 $m.s^{-1}$ respectively. In this study, the CFD simulation results obtained while using the k-ε family of turbulence models were found to more closely correspond to the experimental results.

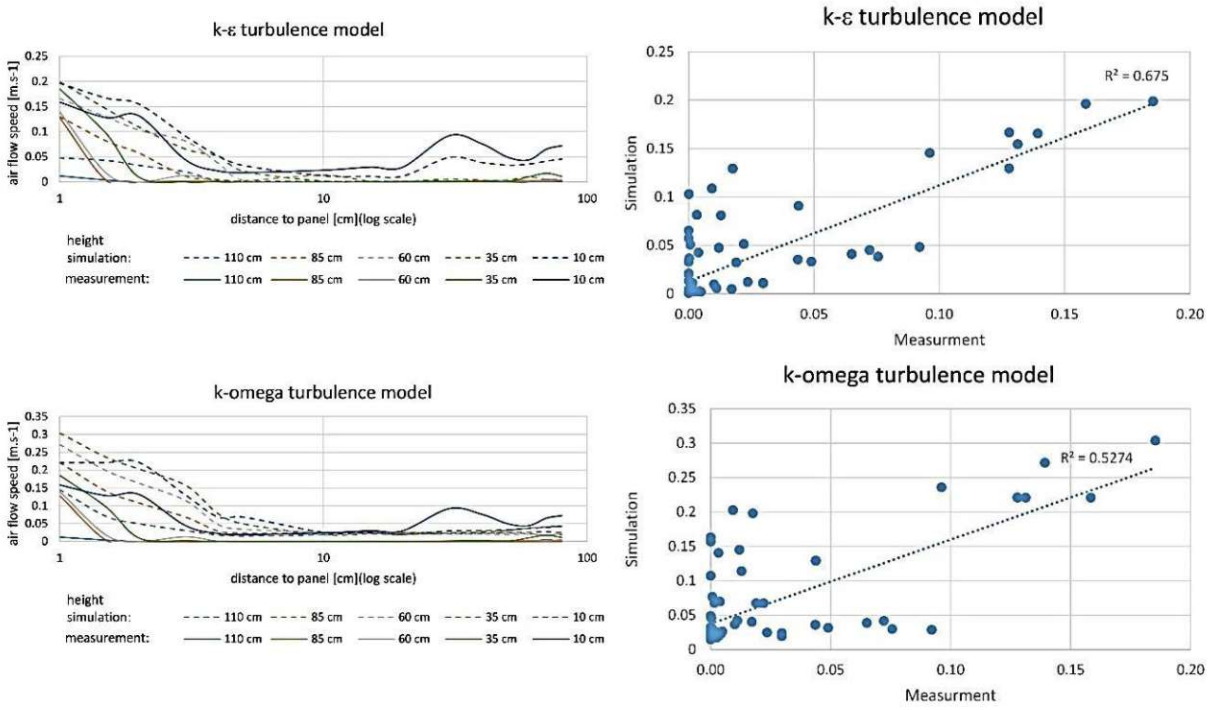

Figure 41: Measured and simulated velocity profile for two different turbulence models (Left: velocity as a function of distance from the panel; Right: Simulated velocities plotted against corresponding measurements)

Aside from the values of air velocity at the feet/ankle zone (slightly higher than 0.2 $m.s^{-1}$ in), the values were still below the limits of the standards in most parts of the occupied zones (ASHRAE, 1992): The mean air velocity across the zone was found to be less than 0.15 $m.s^{-1}$).

As mentioned earlier, in this study we considered a highly simplified human model (body temperature 35) in three distances from the cooling panel (20 cm, 35 cm and 55 cm). The cooling was provided by radiant panels and the manikin acted as the source of heat generation in the room. The flow in the room is dominated by buoyancy. The solver settings were identical to those used for the aforementioned comparison with the experimental results. The main objective of this query was to explore the potential influence of the human presence on the air flow pattern around the radiant cooling panel.

Figure 42 illustrates the simulated velocity contours for the aforementioned simulation scenarios. The results indicate that the velocity in the vicinity of manikin lies in the range of 0.10 $m.s^{-1}$ to 0.28 $m.s^{-1}$. The velocity range in the zone can be suggested to be within the recommended maximum velocity range to avoid draft (Berglund and Fobelets, 1987). With increasing distance from the cooling panel, its effect on the velocity field clearly diminishes.

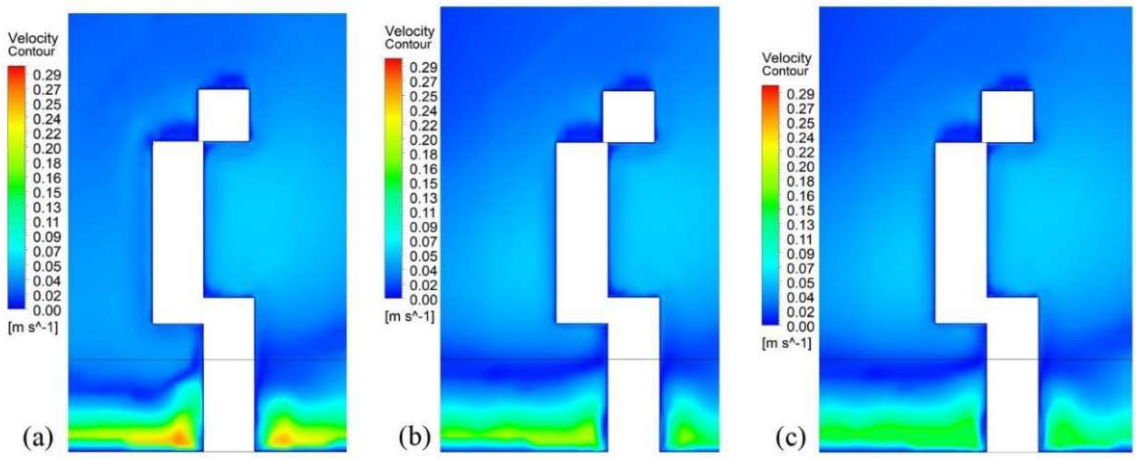

Figure 42: Simulated velocity contours around a human model at three distances from the radiant panel, namely distance of human model from panel, namely 20 cm (a), b: 35 cm (b), and 55 cm (c)

5.4. Conclusion

Using local radiant cooling panels has been suggested to be a potentially promising alternative to traditional air-conditioning system. Our study involved the thermal analysis of a prototypical local cooling panel installed in a laboratory test room. The thermal performance of the model was evaluated numerically by a commercially available CFD. To gain confidence

concerning the model's reliability, its performance was first compared with laboratory measurements. The air velocity fields obtained from the CFD study point to a slight potential for local discomfort at the feet/ankle zone, but the overall velocity field in the test room was found to be acceptable. In addition, the simulated flow around a virtual manikin (simplified human model) at three different locations yielded ranges of velocities than can be suggested to be below the recommended maximum velocity in the test zone.

6. Conclusion

As noted at the outset of this dissertation deployment of heat transfer model in building elements such as windows requires rigorous standards concerning the model's thermal performance.

According to the literature review majority of the standard fenestration, heat transfer models do not take into account the three-dimensional nature of the flow and the radiative heat transfer or the temperature stratification of certain flow regimes when calculating the overall window thermal transmittance. Nevertheless, the simplified heat transfer calculation in the common building energy simulation method can under or over-predict the effect of thermal bridges in the overall thermal transmittance of external walls. The results of the extensive sensitivity analysis show even disregarding the possible errors in the physical models the uncertainty of the model inputs and parameters can cause large deviation in the intermediate calculation results (e.g. air change rate) and in the final numerical outputs of the model (annual heating and cooling energy demand). The uncertainty in the main construction (window air permeability, opening aperture, etc.), environmental factors (pressure coefficients), and the internal heat gains can all cause significant deviations in the predicted energy demand.

Additionally, the simulation method considering conductive and convective, and radiative models can provide more accurate results of window surface temperatures. Filling the void of information regarding energy flows within windows and temperature distributions in individual glazing and frame are reasons enough to justify the importance of this study. The primary aim of this research was to solve numerically the natural convection of fill gas simultaneously with the radiative exchange and the conduction in the solid portion glazing in the fenestration. These models enable the software to estimate localized heat-transfer effects and interactions, which cannot be addressed in the basic conductive models. The prediction of heat transfer in building details is beyond the simple task, and it requires a more detailed approach. The approach adopted in this project was employing Computational Fluid Dynamics (CFD) methods to predict the thermal behavior of the building element.

At the first step, the thermal behavior of a casement window, and its retrofitting options were evaluated for winter and summer boundary conditions. According to the result, externally retrofitting this type of window can improve significantly their thermal performance. The study also highlights the difference in results due to different modeling approaches. Specifically, purely conductive simulations of the thermal behavior of the casement window lead to results

different from those obtained via coupled conductive and convective heat transfer simulation. As such, a more reliable modeling approach requires the consideration of convective processes associated with airflow within the cavity space of a casement window.

In the next section, the thermal performance of these models and the effect of solar radiation was evaluated numerically under winter and summer boundary conditions. The study covered a thermal analysis of several ventilated window configurations. This research has achieved the goals that were set out at the onset. The question of the viability of naturally ventilated supply air ventilated window in a cold winter continental climate has been answered. In this unique type of supply air ventilated window, there was no mixing of intake and exhausted air.

CFD as a feasible tool has been used to test the uncertainty in window design and the possibility of solutions for a particular problem. To gain confidence concerning the model's reliability, its performance was first compared with laboratory and field measurements before its deployment toward the aforementioned parametric analysis. The results point to the supply air windows' potential to deliver preheated fresh air to indoor spaces. A temperature rise in the order of 3 to 18 K was computationally observed in the windows' cavity under the winter boundary conditions. Amongst the simulated alternatives, analyzing the geometry of the cavity shows that taller cavities and smaller cavity depth can provide higher incoming air temperature. In addition, two different types of ventilated window were analyzed for summer condition. Analyzing the summer performance of two type of ventilated window (exhaust and outdoor curtain mode), revealed that the application of low-emissivity glazing as the exterior glass pane can improve the cooling effect in both cases. In addition, the outdoor curtain air mode of the ventilated window shows a better performance under summer boundary conditions.

Forth section concentrated on assessing the flow behavior in the room with double-layered faces. The concept of age of air and flow behavior was analyzed for different configurations of double-layered facades. According to the simulation results, the size and position of the opening on each leaf can significantly influence the induced airflow and indoor air quality. The last section, covers the effect of local cooling panel on the flow behavior inside the room. This study indicates that the CFD simulation accuracy mostly depends on the appropriate setting of boundary conditions and numerical simulation parameters. The effect of different turbulence method on flow behavior was evaluated and the results verified with the measurement data.

7. Reference

ASHRAE, *Thermal environmental conditions for human occupancy ANSI-ASHRAE*, , in Standard ASHRAE 55-1992. 1992.

ASHRAE Fundamentals Handbook. 2005, ASHRAE: Atlanta.

Ansys Fluent 19.0, 2018, User's Guide. fluent Inc., Lebanon.

Arasteh D., Reilly M.S., and Rubin M.D., *A Versatile Procedure for Calculating Heat Transfer through Windows.* ASHRAE Transactions, 1989. 95.

Al-Sanea S.A. and Zedan M.F., *Effect of thermal bridges on transmission loads and thermal resistance of building walls under dynamic conditions.* Applied Energy, 2012. 98: p. 584-593.

Awbi H.B., *Calculation of convective heat transfer coefficients of room surfaces for natural convection.* Energy and Buildings, 1998. 28(2): p. 219-227.

Appelfeld D. and Svendsen S., *Experimental analysis of energy performance f a ventilated window for heat recovery under controlled conditions.* Energy and Buildings, 2011. 43(11): p. 3200-3207.

Austria, M.R.f.f.-V.i., *OENORM B8110-2*. 2003.

Artmann, N., H. Manz, and P. Heiselberg, *Climatic potential for passive cooling of buildings by night-time ventilation in Europe.* Applied Energy, 2007. 84(2): p. 187-201.

Bajraktari E., Lechleitner J., and Mahdavi A., *Estimating the Sound Insulation of Double Facades with Openings for Natural Ventilation.* Energy Procedia, 2015. 78: p. 140-145.

Baldinelli, G. and Bianchi F., *Windows thermal resistance: Infrared thermography aided comparative analysis among finite volumes simulations and experimental methods.* Applied Energy, 2014. 136: p. 250258.

Bakonyi D., *The Thermal Modeling of Traditional Double-skin Box Type Windows, in Department of Building Constructions*. 2016, Budapesti University Of Technology And Economics.

Bakonyi D. and Becker D., *Possibilities of Simulations in the Planning of the Retrofit of Historical Double Skin Windows* Advanced Materials Research, 2014. 899: p. 155–160.

Baker, P.H. and McEvoy M., *Test cell analysis of the use of a supply air window as a passive solar component.* Solar Energy, 2000. 69(2): p. 113-130.

Bakonyi D. and Dobszay G., *Thermal Models for Box Type Windows: Part 1.* Periodica Polytechnica Architecture, 2016. 47(1): p. 14-29.

Berglund L.G. and Fobelets A., *A Subjective Human Response to Low Level Air Currents and Asymmetric Radiation.* ASHRAE Transactions, 1987. 93(1): p. 497-523.

Betts P.L. and Bokhari I.H., *Experiments on turbulent natural convection in an enclosed tall cavity.* International Journal of Heat and Fluid Flow, 2000. 21: p. 675-683.

Blocken B., *50 years of Computational Wind Engineering: Past, present and future.* Journal of Wind Engineering and Industrial Aerodynamics, 2014. 129: p. 69-102.

Buratti C. and Moretti E., *Glazing systems with silica aerogel for energy savings in buildings.* Applied Energy, 2012. 98: p. 396-403.

Blocken B., Carmeliet J., and Stathopoulos T., *CFD evaluation of wind speed conditions in passages between parallel buildings—effect of wall-function roughness modifications for the atmospheric boundary layer flow.* Journal of Wind Engineering and Industrial Aerodynamics, 2007. 95(9): p. 941-962.

Bianchi F., Laura Pisello A., Baldinelli G., Asdrubali F., *Infrared Thermography Assessment of Thermal Bridges in Building Envelope: Experimental Validation in a Test Room Setup.* Sustainability, 2014. 6(10): p. 1-14.

Bhamjee M., Nurick A., and Madyira D.M., *An experimentally validated mathematical and CFD model of a supply air window: Forced and natural flow.* Energy and Buildings, 2013. 57: p. 289-301.

Bhamjee M., *A computational fluid dynamics and experimental investigation of an airflow window*. 2011, University of Johannesburg: Johannesburg, South Africa.

Blocken B. and Carmeliet J., *Pedestrian Wind Environment around Buildings: Literature Review and Practical Examples.* Journal of Thermal Envelope and Building Science, 2004. 28(2): p. 107-159.

Buratti C., *Indoor noise reduction index with open window.* Applied Acoustics, 2002. 63(4): p. 431-451.

Carlos J., Corvacho H., Pedro S., João C., *Real climate experimental study of two double window systems with preheating of ventilation air.* Energy and Buildings, 2010. 42(6): p. 928-934.

Carlos J.S., *Assessment of pre-heating air through a double window system on different building location and weather condition.* Building Simulation, 2014. 7(3): p. 247-261.

Carlos J.S. and Corvacho H., *Ventilated Double Window for the Preheating of the Ventilation Air Comparison of Its Performance in a Northern and a Southern European Climate.* Journal of Renewable Energy, 2013: p. 290865.

Capozzoli A., Gorrino A., and Corrado V., *A building thermal bridges sensitivity analysis.* Applied Energy, 2013. 107: p. 229-243.

Chan A.L.S., Chow T.T., Fong K.F., Lin Z., *Investigation on energy performance of double skin façade in Hong Kong.* Energy and Buildings, 2009. 41(11): p. 1135-1142.

Cappelletti F., Gasparella A.,Romagnoni P., Baggio P., *Analysis of the influence of installation thermal bridges on windows performance: The case of clay block walls.* Energy and Buildings, 2011. 43(6): p. 14351442

Clarke J.A. and Hensen J.L.M., *Integrated building performance simulation: Progress, prospects and requirements.* Building and Environment, 2015. 91: p. 294-306.

Carlos J.S., and Corvacho H., *Evaluation of the performance indices of a ventilated double window through experimental and analytical procedures: SHGC-values.* Energy and Buildings, 2015. 86: p. 886-897.

Chen Q., Lee K., Mazumdar S., Poussou S., Wang L., Wang M., Zhang Z., *Ventilation performance prediction for buildings: Model assessment.* Building and Environment, 2010. 45(2): p. 295-303.

Cheong D.K.W. and Huang S., *Performance evaluation of personalized ventilation system with two types of air terminal devices coupled with displacement ventilation in a mock-up office*. HVAC&R Research, 2013. 19(8): p. 974-985.

Chen Q. and Xu W., *A zero-equation turbulence model for indoor airflow simulation.* Energy Build, 1998, 28: p. 137–144.

Chen Q., *Ventilation performance prediction for buildings: A method overview and recent applications.* Building and Environment, 2009. 44(4): p. 848-858.

Cuce E., *Development of innovative window and fabric technologies for low- carbon buildings* 2014, University of Nottingham.

Cuce E. and Riffat S.B., *A state-of-the-art review on innovative glazing technologies.* Renewable and Sustainable Energy Reviews, 2015. 41: p. 695-714.

Cuce, E. and Cuce P.M., *Vacuum glazing for highly insulating windows: Recent developments and future prospects.* Renewable and Sustainable Energy Reviews, 2016. 54: p. 1345-1357.

Curcija W.P.G., *Two-Dimensional Natural Convection Over the Isothermal Indoor Fenestration Surface Finite Element Numerical Solution* ASHRAE Trans 1993. 99(1): p. 274–287.

Cuce, E., S.B. Riffat, and C.-H. Young, *Thermal insulation, power generation, lighting and energy saving performance of heat insulation solar glass as a curtain wall application in Taiwan: A comparative experimental study.* Energy Conversion and Management, 2015. p. 31-38.

Choi W., Joe J., Kwak Y., Huh J., *Operation and control strategies for multi-storey double skin facades during the heating season.* Energy and Buildings, 2012. 49: p. 454-465.

Choi H., Kang K., An Y., Kim E., Lee,Y., Kim T, *Analysis of Heat Transfer in a Slim Double Skin Façade using CFD Simulation*, in *16th International IBPSA Conference (Building Simulation 2019)*. 2019: Italy, Rome.

Cho K.-j. and Cho D.-w., *Solar Heat Gain Coefficient Analysis of a Slim-Type Double Skin Window System: Using an Experimental and a Simulation Method.* Energies, 2018. 11: p. 115.

Choudhary R. and Malkawi A., *A methodology for micro-level building thermal analysis: combining CFD and experimental set-ups.* Seventh International IBPSA Conference, 2001: p. 1275-1282.

Chiang W.-H., Wang C.-Y., and Huang J.-S., Evaluation of cooling ceiling and mechanical ventilation systems on thermal comfort using CFD study in an office for subtropical region. Building and Environment, 2012. 48: p. 113-127.

Dama A., Angeli D., and Larsen O.K., *Naturally ventilated double-skin façade in modeling and experiments.* Energy and Buildings, 2017. 144: p. 17-29.

Danza L., Barozzi B., Belussi L., Meroni I., Salamone F., *Assessment of the Performance of a Ventilated Window Coupled with a Heat Recovery Unit through the Co-Heating Test.* Buildings, 2016. 6(3).

Demirdžić I. and Muzaferija S., *Numerical method for coupled fluid flow, heat transfer and stress analysis using unstructured moving meshes with cells of arbitrary topology.* Computer Methods in Applied Mechanics and Engineering, 1995. 125(1): p. 235-255.

De Salis M.H.F., Oldham D.J., and Sharples S., *Noise control strategies for naturally ventilated buildings.* Building and Environment, 2002. 37(5): p. 471-484.

Demanega I., De Michele G., Avesani S., Pernigotto G., Babich F., Gasparella A., *CFD and ray tracing to evaluate the thermal performance of Complex Fenestration Systems*. 2018.

DIN2012a. . 2012, DIN EN ISO 10077-1:2010 Thermal Performance of Windows, Doors and Shutters – calculation of Thermal Transmittance.

El Ahmar S., Battista F., and Fioravanti A., *Simulation of the thermal performance of a geometrically complex Double-Skin Facade for hot climates: EnergyPlus vs. OpenFOAM.* Building Simulation, 2019. 12(5): p. 781-795.

EN ISO 10211-1. , in *Thermal bridges in building construction – heat flows and surface temperatures – general calculation methods.* . 1995, European Standard.

EN ISO 10077-2. , in *Thermal performance of windows, doors and shutters – calculation of thermal transmittance – numerical method for frames.* 2003, European Standard.

E 673, *Glass in building. Determination of thermal transmittance (U value). Calculation method*. 2011.

Fang Y., Eames P., Norton B., Hyde T., Zhao J., Wang J., Huang Y., *Low emittance coatings and the thermal performance of vacuum glazing.* Solar Energy, 2007. 81(1): p. 8-12.

Feist W., Schnieders J., Dorer V., Haas A., *Re-inventing air heating: Convenient and comfortable within the frame of the Passive House concept.* Energy and Buildings, 2005. 37(11): p. 1186-1203.

Fürbringer J.-M., Roulet C.-A., and Borchiellini R., *An overview of the evaluation activities of IEA ECBCS Annex 23.* Energy and Buildings, 1999. 30(1): p. 19-33.

Franke J. and Baklanov A., *Best Practice Guideline for the CFD Simulation of Flows in the Urban Environment: COST Action 732 Quality Assurance and Improvement of Microscale Meteorological Models*. 2007.

Fuliotto R., Cambuli F., Mandas N., Bacchin N., Manara G., Chen Q., *Experimental and numerical analysis of heat transfer and airflow on an interactive building facade.* Energy and Buildings, 2010. 42(1): p. 23-28.

Finlayson E., Mitchell R., Arasteh D., Huizenga C., Curcija D., *THERM 2.0: Program description, A PC program for analyzing the two-dimensional heat transfer through building products.* . 1998, Lawrence Berkeley National Laboratory: Berkeley, California.

Gao N. and Niu J., *CFD study on micro-environment around human body and personalized ventilation.* Building and Environment, 2004. 39: p. 795-805.

Gao N. and J. Niu, *Modeling the Performance of Personalized Ventilation under Different Conditions of Room Air and Personalized Air*. HVAC&R Research, 2005. 11(4): p. 587-602.

Gan G., Towards a better indoor thermal environment "CFD analysis of the performance of chilled ceiling systems", in 4th International Symposium on Ventilation for Contaminant Control, . 1994: Stockholm, Sweden. p. 551-556.

Garay R., Uriarte A., and Apraiz I., *Performance assessment of thermal bridge elements into a full scale experimental study of a building façade.* Energy and Buildings, 2014. 85: p. 579-591.

Garrison J.D. and Collins R.E., *Manufacture and cost of vacuum glazing.* Solar Energy, 1995. 55(3): p. 151161.

Gan G., *Thermal transmittance of multiple glazing: computational fluid dynamics prediction.* Applied Thermal Engineering, 2001. 21(15): p. 1583-1592.

Gavan V., *Full scale experimental evaluation and modeling of a double-skin façade. Optimal control of thermal and visual comfort.* , in *Institut National des Sciences Appliquees de Lyon*. 2009, Lyon, France.

Gustavsson L.,Dodoo A., and Sathre R., Climate change effects over the lifecycle of a building Report on methodological issues in determining the climate change effects over the lifecycle of a building. 2015, Sustainable Built Environment Research Group Linnaeus University: Sweden.

Gratia, E. and De Herde A., *Natural ventilation in a double-skin facade.* Energy and Buildings, 2004. 36(2): p. 137-146.

Griffith D., Turler D., and Arasteh D., *Improving computer simulations of heat transfer for projecting fenestration products: Using radiation viewfactor models.* ASHRAE Transactions, 1998. 104(1).

Gloriant F., Tittelein P., Joulin A., Lassue S., *Modeling a triple-glazed supply-air window.* Building and Environment, 2015. 84: p. 1-9.

Gosselin J.R. and Chen Q., *A computational method for calculating heat transfer and airflow through a dualairflow window.* Energy and Buildings, 2008. 40(4): p. 452-458.

Gosselin J. and Chen Q. *Dual Airflow Window for Indoor Air Quality Improvement and Energy Conservation in Buildings.* HVAC&R Research, 2008. 14(3): p. 359-372.

Ghadimi M., Ghadamian H., Hamidi A., Fazelpour F., Behghadam M., *Analysis of free and forced convection in airflow windows using numerical simulation of heat transfer.* International Journal of Energy and Environmental Engineering, 2012. 3(1): p. 14.

Gustavsen A., Arasteh D., Jelle P., Curcija C., Kohler C., *Developing Low-Conductance Window Frames: Capabilities and Limitations of Current Window Heat-Transfer Design Tools.* Journal of Building Physics, 2008. 32: p. 131-153.

Gustavsen, A. and Thue J.V., *Numerical Simulation of Natural Convection in Three-dimensional Cavities with a High Vertical Aspect Ratio and a Low Horizontal Aspect Ratio.* Journal of Building Physics, 2007. 30(3): p. 217-240.

Gustavsen A., Arasteh D., Kohler C., Curcija D.,*Two-Dimension Conduction and CFD Simulations for Heat Transfer in Horizontal Window Frame Cavities* ASHRAE 2005. 111 p. 1–13.

Gilani S., Montazeri H., and Blocken B., *CFD simulation of stratified indoor environment in displacement ventilation: Validation and sensitivity analysis.* Building and Environment, 2016. 95: p. 299-313.

Greffet R., Salagnac P., Michaux G., Ridoret J., *Airflow Window: Numeical Study and Sensibility Analysis of Thermal Performances*, in *13th Conference of International Building Performance Simulation Association*. 2013: Chambéry, France.

Haase M., Wigenstad T., Condensation Issues in Ventilated Façades. In *Materials with Complex Behaviour II. Advanced Structured Materials*, A. Öchsner, L.F.M.d. Silva, and H. Altenbach; Publisher: Springer Berlin, Germany, 2012.

Haase M. and Amato A., *An investigation of the potential for natural ventilation and building orientation to achieve thermal comfort in warm and humid climates.* Solar Energy, 2009. 83(3): p. 389-399.

Hayashi T., Ishizu Y., Kato S., Murakami S., *CFD analysis on characteristics of contaminated indoor air ventilation and its application in the evaluation of the effects of contaminant inhalation by a human occupant*. Building and Environment, 2002. 37(3): p. 219-230.

Hamza N., *Double versus single skin facades in hot arid areas.* Energy and Buildings, 2008. 40(3): p. 240248.

Hensen J., Barták M., and Frantisek D., *Modeling and simulation of a double-skin facade system.* Research in Architectural Engineering Series, 2007. 1.

He G., Shu L., Zhang S., *Double Skin Facades In The Hot Summer And Cold Winter Zone In China: Cavity Open Or Closed?,* Building Simulation, 2011.4:p. 283-291.

Hooff T., Blocken B., and Van Heijst G., *On the suitability of steady RANS CFD for forced mixing ventilation at transitional slot Reynolds numbers.* Indoor air, 2012. 23.

Howell S.A. and Potts I., *On the natural displacement flow through a full-scale enclosure, and the importance of the radiative participation of the water vapour content of the ambient air.* Building and Environment, 2002. 37(8): p. 817-823.

Hoogendoorn C.J. *Natural Convection in Enclosures*. in *Proceedings of the Eighth International Heat Transfer Conference*. 1986. Hemisphere, Washington D.C.

Høseggen R., Wachenfeldt B.J., and Hanssen S.O., *Building simulation as an assisting tool in decision making: Case study: With or without a double-skin façade?* Energy and Buildings, 2008. 40(5): p. 821-827.

Huifen Z., Yingchao F., Fuhua Y., Hao T., Ying Z., Sheng Y., *Mathematical Modeling of Double-Skin Facade in Northern Area of China.* Mathematical Problems in Engineering. 2013: p. 712878.

Ibrahim M., Biwole P., Wurtz E., Achard P., *Limiting windows offset thermal bridge losses using a new insulating coating.* Applied Energy, 2014. 123: p. 220-231.

(ISO)., I.O.f.S., *Thermal Bridges in Building Construction—Linear Thermal Transmittance—Simplified Methods and Default Values*, in *EN ISO 14683: 2008; ISO*. 2008: Geneva, Switzerland.

ISO 15099., in *Thermal performance of windows, doors and shading devices – detailed calculations.* . 2003, International Standard.

ISO 2007 ISO 10211, in *Thermal bridges in building construction – heat flows and surface temperatures*. 2007.

Iyi D., Hasan R., Penlington R., Underwood, C., *Double skin façade: Modelling technique and influence of venetian blinds on the airflow and heat transfer.* Applied Thermal Engineering, 2014. 71(1): p. 219-229.

Imanari T., Omori T., and Bogaki K., Thermal comfort and energy consumption of the radiant ceiling panel system.: Comparison with the conventional all-air system. Energy and Buildings, 1999. 30(2): p. 167-175.

Jaluria Y., *Challenges in the accurate numerical simulation of practical thermal processes and systems.* International Journal of Numerical Methods for Heat & Fluid Flow, 2013. 23: p. 158-175.

Jim C.Y., *Air-conditioning energy consumption due to green roofs with different building thermal insulation.* Applied Energy, 2014. 128: p. 49-59.

Ji Y., Cook M. J., Hanby V., Infield D. G., Loveday D. L., Mei L., *CFD modelling of naturally ventilated double-skin facades with Venetian blinds.* Journal of Building Performance Simulation, 2008. 1(3): p. 185196.

Jiru T.E. and Haghighat F., *Modeling ventilated double skin façade—A zonal approach.* Energy and Buildings, 2008. 40(8): p. 1567-1576.

Joe J., Choi W., Kwon H., Huh J., *Load characteristics and operation strategies of building integrated with multi-story double skin facade.* Energy and Buildings, 2013. 60: p. 185-198.

Jones W.P. and Launder B.E., *The prediction of laminarization with a two-equation model of turbulence.* International Journal of Heat and Mass Transfer, 1972. 15(2): p. 301-314.

Karava P., Stathopoulos T., and Athienitis A.K., *Airflow assessment in cross-ventilated buildings with operable façade elements.* Building and Environment, 2011. 46(1): p. 266-279.

Karava P., Stathopoulos T., and Athienitis A.K., *Wind-induced natural ventilation analysis.* Solar Energy, 2007. 81(1): p. 20-30.

Khalegi A, Hodgson M., *Relationship between ventilation, air quality and acoustics in 'green' and 'brown' buildings.* , in *19th International Congress of Acoustics*. 2007: Madrid, Spain.

Kull T.M., Mauring T., and Tkaczyk A.H., *Energy balance calculation of window glazings in the northern latitudes using long-term measured climatic data.* Energy Conversion and Management, 2015. 89: p. 896906.

Kohler C., Arasteh D., and Mitchell R., *THERM Simulations of Window Indoor Surface Temperatures for Predicting Condensation.* ASHRAE Transactions, 2001. 109, Part 1: p. 593-599.

Khoukhi M. and Maruyama S., *Temperature and Heat Flux Distributions through Single and Double Window Glazing Nongray Calculation.* Smart Grid and Renewable Energy, 2011. 2.

Kohler C., Arasteh D., Mitchell R., *THERM Simulations of Window Indoor Surface Temperatures for Predicting Condensation.* ASHRAE Transactions, 2001. 109, Part 1: p. 593-599.

Kong M., Dang T.Q., Zhang J., Khalifa H.E., *Micro-environmental control for efficient local cooling*. Build. Environ. 2017, 118, 300–312. Building and Environment, 2017. 118: p. 300-312

Kim T., Kato S., Murakami S., Rho J., *Study on indoor thermal environment of office space controlled by cooling panel system using field measurement and the numerical simulation*. Building and Environment, 2005. 40(3): p. 301-310.

La Rosa A.D., Recca A., Gagliano A., Summerscales J., Latteri A., Cozzo G., Cicala G. *Environmental impacts and thermal insulation performance of innovative composite solutions for building applications.* Construction and Building Materials, 2014. 55: p. 406-414.

Laverge, J., et al. *Condensation in a closed cavity double skin facade: a model for risk assessment*. 2010.

Launder, B. and D.B. Spalding, *The Numerical Computation of Turbulent Flow Computer Methods.* Computer Methods in Applied Mechanics and Engineering, 1974. **3**: p. 269-289.

Li Y., Darkwa J., and Kokogiannakis G., *Heat transfer analysis of an integrated double skin façade and phase change material blind system.* Building and Environment, 2017. 125: p. 111-121.

Lomas K.J., *Architectural design of an advanced naturally ventilated building form.* Energy and Buildings, 2007. 39(2): p. 166-181.

Liu J., Zhu S., Keun Kim M., Srebric J., A Review of CFD Analysis Methods for Personalized Ventilation (PV) in Indoor Built Environments. Sustainability, 2019. 11(15).

Liu J., Srebric J., and Yu N., *Numerical simulation of convective heat transfer coefficients at the external surfaces of building arrays immersed in a turbulent boundary layer*. International Journal of Heat and Mass Transfer, 2013. 61: p. 209-225.

Li Y. and Nielsen P., *CFD and ventilation research.* Indoor air, 2011. 21: p. 442-53.

Liu J., Heidarinejad M., Gracik S., Srebric J., Yu N., *An indirect validation of convective heat transfer coefficients (CHTCs) for external building surfaces in an actual urban environment.* Building Simulation, 2015. 8(3): p. 337-352.

Mahdavi A., *Thermal and Acoustical Performance of "Buffer Rooms". .* ASHRAE Transactions, 1993. 99(1): p. 1092 – 1105.

Mahdavi A. and Khosravi S.N., *Acoustical and airflow considerations concerning double-layered façades with openings for natural ventilation*, in *12th Nordic Symposium on Building Physics NSB*. 2020: Estonia.

Mahdavi A., Schober P., Pont U., Proskurnina O., *Vakuumglas in der Anwendung – Forschungsergebnisse und Ausblick*, in FENSTER-TÜREN-TREFF 2016: Saalfelden, Austria.

Mahdavi A., *Computational building models: theme and four variations*. in Building Simulation 03, 2003. Eindhoven.

Ma P., Wang L.-S., and Guo N., *Maximum window-to-wall ratio of a thermally autonomous building as a function of envelope U-value and ambient temperature amplitude*. Applied Energy, 2015. 146: p. 84-91.

Malvoni M., Baglivo C., Congedo P., Laforgia D., *CFD modeling to evaluate the thermal performances of window frames in accordance with the ISO 10077*. Energy, 2016. 111: p. 430-438.

Martin K., Erkoreka A., Flores-Abascal I., Odriozola-Maritorena M., Sala J.M., *Problems in the calculation of thermal bridges in dynamic conditions*. Energy and Buildings, 2011. 43(2): p. 529-535.

Mehta P.N.C., Gondaliya M.V.B., and Gundaniya M.J.V., *Applications of Different Numerical Methods in Heat Transfer-A Review*. International Journal of Emerging Technology and Advanced Engineering, 2013.

Marjanovic L., Cook M., Hanby V., Rees, S., *CFD modelling of convective heat transfer from a window with adjacent Venetian blinds*. Building Simulation, 2005.

Manz H. and Frank T., *Thermal simulation of buildings with double-skin façades*. Energy and Buildings, 2005. 37(11): p. 1114-1121.

Manz H., *Total solar energy transmittance of glass double façades with free convection.* Energy and Buildings, 2004. 36(2): p. 127-136.

Menter F.R., *Two-equation eddy-viscosity turbulence models* engineering application, AIAA Journal, 1994. 32(8): p. 1598–1605

Myhren J.A. and Holmberg S., *Flow patterns and thermal comfort in a room with panel, floor and wall heating.* Energy and Buildings, 2008. 40(4): p. 524-536.

Murakami S., Kato S., and Nakagawa H., *Numerical prediction of horizontal non-isothermal 3-D jet in room based on the k-model,.* ASHRAE Transactions, , 1991. 97 (1): p. 38-48.

Mundt E., Mathisen H.M., Nielsen P.V., Moser A. *Ventilation Effectiveness, rehva Federation of European Heating and Air-conditioning Association GUIDEBOOK NO 2.* . 2004.

Mochida A., Yoshino H., Takeda T., Kakegawa T., Miyauchi S., *Methods for controlling airflow in and around a building under cross-ventilation to improve indoor thermal comfort.* Journal of Wind Engineering and Industrial Aerodynamics, 2005. 93(6): p. 437-449.

Migneron J. and Potvin A., *Noise reduction of a double-skin façade considering opening for natural ventilation.* The Journal of the Acoustical Society of America, 2012. 131: p. 3320.

Montazeri H., Montazeri F., Azizian R., Mostafavi S.,, *Two-sided wind catcher performance evaluation using experimental, numerical and analytical modeling.* Renewable Energy, 2010. 35(7): p. 1424-1435.

Mundt E., Mathisen H.M., Nielsen P.V., Moser A., Ventilation Effectiveness, . REHVA Guidebook. Rehva Federation of European Heating and Air-conditioning Association, GUIDEBOOK NO 2. 2004.

McEvoy M.E., Southall R.G., and Baker P.H., *Test cell evaluation of supply air windows to characterise their optimum performance and its verification by the use of modelling techniques*. Energy and Buildings, 2003. 35(10): p. 1009-1020.

Minimum – Requirements for fRsi-Values in Austrian 2020, ÖNORM B 8110-2:2020.

Miroshnichenko I.V. and Sheremet M.A., *Turbulent natural convection heat transfer in rectangular enclosures using experimental and numerical approaches: A review*. Renewable and Sustainable Energy Reviews, 2018. 82: p. 40-59.

Montazeri H. and Montazeri F., *CFD simulation of cross-ventilation in buildings using rooftop windcatchers: Impact of outlet openings.* Renewable Energy, 2018. 118: p. 502-520.

Nagano K. and Mochida T., *Experiments on thermal environmental design of ceiling radiant cooling for supine human subjects.* Building and Environment, 2004. 39(3): p. 267-275.

Najaf Khosravi S., Saadatjoo P., Mahdavinejad M., *The effect of roof details on natural ventilation efficiency in isolated single buildings*. In PLEA. 2016. Los Angeles, USA.

Najaf Khosravi S., Mahdavi A., *Simulation support for the design of ventilated windows: a case study*. in 17th International IBPSA Conference (Building Simulation 2021),Bruges, Belgium.

Najaf Khosravi S., Mahdavi A., *A CFD-based parametric thermal performance analysis of supply-air ventilated windows, Energies* **2021**, *14*(9), 2420

Najaf Khosravi S., Pont U., Sikula O., Mahdavi A., *Numeric Simulation of Heat Transfer Phenomena in*

Existing and Retrofitted Casement Windows. In 16th International IBPSA Conference (Building Simulation 2019), Rome. Italy

Najaf Khosravi S., Sikula O., Pont U., Mahdavi A., *Implications of Model Complexity for the Simulated Thermal Behavior of a Casement Window*, IOP Conference Series: Earth and Environmental Science, CESB 2019.

Nusser B., Bachinger J., Schober K.P., *Untersuchungen zur hygrothermischen Funktionsweise des low-tech Window Air Verbundfensters*. 2016, Holz Forschung Austria: Vienna.

Nunes Z., Wilson B., and Rickard M., *An assessment of the acoustic performance of open windows, in line with ventilation requirements for natural ventilation*. 39th International Congress on Noise Control Engineering 2010, INTER-NOISE 2010, 2010. 1: p. 782-797.

Niu J., Kooi J.v.d., and Rhee H.v.d., *Energy saving possibilities with cooled-ceiling systems.* Energy and Buildings, 1995. 23(2): p. 147-158.

Nilsson H.O., *Thermal comfort evaluation with virtual manikin methods.* Building and Environment, 2007. 42(12): p. 4000-4005.

Niu, J. and Kooi J.V.D., *Grid optimization of k - E turbulence model simulation of natural convection in rooms.* In Proc. of Roomvent 1992. Aalborg, Denmark.

Oberkampf W.L. and Trucano T.G., *Verification and validation in computational fluid dynamics*. Progress in Aerospace Sciences, 2002. 38(3): p. 209-272.

Olonscheck M., Holsten A., and Kropp J.P., *Heating and cooling energy demand and related emissions of the German residential building stock under climate change.* Energy Policy, 2011. 39(9): p. 4795-4806.

Oldham D., Salis M., and Sharples S., *Reducing the ingress of urban noise through natural ventilation openings*. Indoor air, 2004. 14 Suppl 8: p. 118-26.

Omri, M. and N. Galanis, *Numerical analysis of turbulent buoyant flows in enclosures: Influence of grid and boundary conditions.* International Journal of Thermal Sciences, 2007. 46(8): p. 727-738.

Ostrach, S., *Natural Convection in Enclosures*. Journal of Heat Transfer Transactions of the ASME, 1988. 110(4): p. 1175–1190.

Pasut W. and De Carli M., *Evaluation of various CFD modelling strategies in predicting airflow and temperature in a naturally ventilated double skin façade*. Applied Thermal Engineering, 2012. 37: p. 267274.

Pappas A. and Zhai Z., *Numerical investigation on thermal performance and correlations of double skin façade with buoyancy-driven airflow*. Energy and Buildings, 2008. 40(4): p. 466-475.

Parra J., Guardo A., Egusquiza E., Alavedra P., *Thermal Performance of Ventilated Double Skin Façades with Venetian Blinds.* Energies 2015. 8(6): p. 4882-4898.

Pont U., Heiduk E., Schober P., Romirer H., Dolezal F., Proskurnina O., Schuss M., Sustr C., Hohenstein H., Mahdavi A., *VIG-SYS-reno Sondierung von Fenstersystemen mit innovativen Gläsern, speziell VakuumIsoliergläsern, zur Gebäudesanierung - Berichte auf Energie- und Umweltforschung*. 2018, Berichte aus Energie und Umweltforschung Final-Report for FFG - Programm Stadt der Zukunft / BMVIT.

Pont U., Woelzl M., Schober P., Khosravi S., Schuss M., Mahdavi A. *Recent progress in the development of windows with vacuum glass*. In CESBP. 2019. Prague, Czech Republic.

Proskurnina, O., U. Pont, and A. Mahdavi. *The Performance of Vacuum Glazing in Exsiting Window Constructions: a Case Study.* in BauSIM 2016. Dresden, Germany.

Poirazis H., *Double skin facades: A literature review. , in A Report of IEA SHC Task 34*, ECBCS Annex 43. . 2006, Lund University: Sweden.

Practical Handbook on Energy Conservation in Buildings Indian Building Congress. first ed. 2008, New Delhi: Nabhi Publications.

Popa C., Ospir D., Fohanno S., Chereche C., *Numerical simulation of dynamical aspects of natural convection flow in a double-skin façade*. Energy and Buildings, 2012. 50: p. 229-233.

Rabhi M., Bouali H., and Mezrhab A., *Radiation–natural convection heat transfer in inclined rectangular enclosures with multiple partitions.* Energy Convers Management, 2008. 49: p. 1228–1236.

Raithby G.D. and Hollands K.G.T., Natural Convection, In: Rosenhow, W.M., Hartnett, J.P. and Cho, Y.I. (eds), Handbook of Heat Transfer, 3rd edn, Chap. 4, McGraw-Hill, New York. Handbook of Heat Transfer, ed. W.M. Rosenhow, J.P. Hartnett, and Y.I. Cho. Vol. 4. 1998, McGraw-Hill: New York.

Roache P.J., *Quantification Of Uncertainty In Computational Fluid Dynamics.* Annual Review of Fluid Mechanics, 1997. 29(1): p. 123-160.

Rhee K.-N., Olesen B.W., and Kim K.W., *Ten questions about radiant heating and cooling systems*. Building and Environment, 2017. 112: p. 367-381.

Saelens D., Roels S., and Hens H., *The inlet temperature as a boundary condition for multiple-skin facade modelling*. Energy and Buildings, 2004. 36(8): p. 825-835.

Safer N., Woloszyn M., and Roux J.J., *Three-dimensional simulation with a CFD tool of the airflow phenomena in single floor double-skin facade equipped with a venetian blind*. Solar Energy. 2005. 79(2): p. 193-203.

Southall R. and McEvoy M., *Investigations into the functioning of a supply air window in relation to solar energy as determined by experiment and simulation*. Solar Energy - Solar Energ, 2006. 80: p. 512-523.

Souza C. O., Souza H. A., and Rodrigues E. F., *Experimental and numerical analysis of a naturally ventilated double-skin façade*. Energy and Buildings, 2018. 165: p. 328-339.

Skaff, M.C. and L. Gosselin, *summer performance of ventilated windows with absorbing or smart glazings.* Solar Energy, 2014. 105: p. 2-13

Strachan P.A. and Vandaele L., *Case studies of outdoor testing and analysis of building components*. Building and Environment, 2008. 43(2): p. 129-142.

Southall R. and McEvoy M., *Results From a Validated CFD Simulation of a Supply Air 'Ventilated Window'*. Air Distribution in Rooms (ROOMVENT), 2000. 2: p. 1049-1054.

Selçuk N. and Kayakol N., *Evaluation of discrete ordinates method for radiative transfer in rectangular furnaces*. International Journal of Heat and Mass Transfer, 1997. 40(2): p. 213-222.

Siegel R. and Howell J.R., *Thermal radiation heat transfer*. 2002, London: Taylor & Francis.

Synergy, B. Vacuum Glazing Technology. 2016.

Stetiu C., *Energy and peak power savings potential of radiant cooling systems in US commercial buildings.* Energy and Buildings, 1999. 30(2): p. 127-138.

Stamou A. and Katsiris I., *Verification of a CFD model for indoor airflow and heat transfer*. Building and Environment, 2006. 41(9): p. 1171-1181.

Srebric J., Heidarinejad M., and Liu J., *Building neighborhood emerging properties and their impacts on multi-scale modeling of building energy and airflows*. Building and Environment, 2015. 91: p. 246-262.

Tablada de la Torre A., Saelens D., Carmeliet J., Baelmans M., *Investigation on airflow and heat transfer of a glazing facade with external louvers,* in 4th International Building Physics Conference. 2009: Istanbul.

Tao G., Bjørn J.,Takeshi I., Arild G. , *Insulating glazing units with silica aerogel granules: The impact of particle size*. Applied Energy, 2014. 128: p. 27-34.

Tanimoto J. and Kimura K., *Simulation study on an air flow window system with an integrated roll screen.* Energy and Buildings, 1997. 26(3): p. 317-325.

Tanaka H., Okumiya M., Tanaka H., YoungYoon G., Watanabe K., *Thermal characteristics of a doubleglazed external wall system with roll screen in cooling season*. Building and Environment, 2009. 44(7): p. 1509-1516.

Teufl H., Schuss M., and Mahdavi A., *Potential and challenges of a user-centric radiant cooling approach.* Energy and Buildings, 2021. 246: p. 111104.

Tominaga Y., Mochida A., Yoshie R., Kataoka H., Nozu T., Yoshikawa M., Shirasawa T., *AIJ guidelines for practical applications of CFD to pedestrian wind environment around buildings.* Journal of Wind Engineering and Industrial Aerodynamics, 2008. 96(10): p. 1749-1761.

Tsan-Hsing S., Liou W., Shabbir A., Yang Z., Zhu J., *A new k-ϵ eddy viscosity model for high reynolds number turbulent flows.* Computers & Fluids, 1995. 24(3): p. 227-238.

Van Hooff T. and Blocken B., *CFD evaluation of natural ventilation of indoor environments by the concentration decay method: CO2 gas dispersion from a semi-enclosed stadium*. Building and Environment, 2013. 61: p. 1-17.

Van Hooff T. and Blocken B., *Coupled urban wind flow and indoor natural ventilation modelling on a highresolution grid: A case study for the Amsterdam ArenA stadium*. Environmental Modelling & Software, 2010. 25(1): p. 51-65.

Wang E., Wang H., Deng M., Wang K., Wang Y., *Simulation of the ventilation and energy performance of a PV-integrated breathing window.* Procedia Engineering, 2017. 205: p. 2779-2784.

Wilcox D.C., *Turbulence modelling for CFD.* 2nd ed. 1998: DCW Industries.

Wilson C.F., Simko T.M., and Collins R.E., *Heat Conduction through the Support Pillars in Vacuum Glazing.* Solar Energy, 1998. 63(6): p. 393-406.

Wright J.L. and Sullivan H.E., *Natural convection in sealed glazing units: A review*. ASHRAE Transactions 1989. 95(1).

Wright J.L. and McGowan A.G., *A Comparison of Calculated and Measured Indoor-Side Window Temperature Profiles,* ASHRAE Transactions, 2003. 109(2): p. 857-861.

Wright J.L. and McGowan A.G., *A Comparison of Calculated and Measured Indoor-Side Window Temperature Profiles*, American Society of Heating, Refrigerating and Air-Conditioning Engineers ASHRAE Transactions, 2003. 109(2).

Wilkins C., and Kosonen R., *Cool ceiling system a European air-conditioning alternative*, ASHRAE Journal, 1992. 34: p. 41-45.

Xu X.-l. and Yang Z., *Natural ventilation in the double skin facade with venetian blind*. Energy and Buildings, 2008. 40(8): p. 1498-1504.

Yang C., Demokritou P., Chen Q., Spengler J., *Experimental validation of a computational fluid dynamics model for IAQ applications in ice rink arenas*. Indoor air, 2001. 11: p. 120-6.

Yang B. and Sekhar C., *Interaction of dynamic indoor environment with moving person and performance of ceiling mounted personalized ventilation system*. Indoor and Built Environment, 2013. 23 (7): p. 920-932.

Yakhot V. and Orszag S.A., *Renormalization group analysis of turbulence*. I. Basic theory. Journal of Scientific Computing, 1986. 1(1): p. 3-51.

Yılmaz Z. and Çetintaş F., *Double skin façade's effects on heat losses of office buildings in Istanbul*. Energy and Buildings, 2005. 37(7): p. 691-697.

Yingdong H., Nianping L., *Meiling H., De H., Using radiant cooling desk for maintaining comfort in hot environment*. Energy and Buildings, 2017. 145: p. 144-154.

Zanghirella, F., Perino M., and Serra V., *A numerical model to evaluate the thermal behaviour of active transparent façades*. Energy and Buildings, 2011. 43(5): p. 1123-1138.

Zeng Z., Li X., Li C., Zhu Y., *Modeling ventilation in naturally ventilated double-skin façade with a venetian blind*. Building and Environment, 2012. 57: p. 1-6.

Zhou, L., Liu J., and Huang Q., *Analysis of Combined Natural Convection and Radiation Heat Transfer in a Partitioned Rectangular Enclosure with Semitransparent Walls*. Trans. Tianjin Univ. , 2019. 25: p. 472–487.

Zhao Y., Curcija D., and Goss W.P., *Convective Heat Transfer Correlations for Fenestration Glazing Cavities: A Review*. ASHRAE Transactions, 1999. 105(2): p. 900–908.

7.1. Tables

7.2. Figures